RESEARCH ARTICLE

New species of parasitic nasal mites infesting birds in Manitoba, Canada (Mesostigmata, Rhinonyssidae)

Wayne Knee[1]

1 *Canadian National Collection of Insects, Arachnids, and Nematodes, Agriculture and Agri-Food Canada, 960 Carling Avenue, K.W. Neatby Building, Ottawa, Ontario, K1A 0C6, Canada*

Corresponding author: *Wayne Knee* (whknee@gmail.com)

Citation: Knee W (2018) New species of parasitic nasal mites infesting birds in Manitoba, Canada (Mesostigmata, Rhinonyssidae). ZooKeys 786: 1–17. https://doi.org/10.3897/zookeys.786.28767

Abstract

Mites (Acari, Acariformes, Parasitiformes) are one of the most diverse and abundant groups of arthropods associated with birds. Several families of mites have colonised the respiratory tract of birds, the Rhinonyssidae (Mesostigmata) being the most diverse. There are 66 species of rhinonyssids (59 named, seven undescribed species) reported from Canadian birds. Two new species of rhinonyssids were discovered while surveying nasal mites from birds in Manitoba, Canada, and are herein described as *Sternostoma gallowayi* **sp. n.** from the horned lark (*Eremophila alpestris*), and *Vitznyssus erici* **sp. n.** from the common nighthawk (*Chordeiles minor*).

Keywords

Introduction

Birds are hosts to a hyperdiverse assemblage of symbiotic animals, residing in all conceivable habitats. Mites are one of the most diverse and frequently encountered associates of birds, with at least 40 families and 2500 described species that live in close association with birds (Proctor and Owens 2000). The symbiotic relationships between birds and their associated mites are varied. Many species are relatively benign such as most feather mites (Astigmata: Analgoidea, Pterolichoidea), while other species are deleterious para-

sites, such as the northern fowl mite (*Ornithonyssus sylviarum* (Canestrini and Fanzago) Mesostigmata: Macronyssidae) or scaly-leg mites (*Knemidokoptes*, Prostigmata: Knemidokoptidae) (Fain and Elsen 1967, Proctor and Owens 2000, Mullens et al. 2009).

Mites inhabit all parts of the avian integument; they can be found on and in the skin of their hosts, on and in feathers, and in the respiratory tract. Five families of acariform (Cloacaridae, Ereynetidae, Turbinoptidae, Cytoditidae) and parasitiform (Rhinonyssidae) mites, have evolved independently to be parasitic in the nasal passages or lungs of birds. There are at least 500 described species of nasal mites worldwide (Fain 1994), of which the Rhinonyssidae are the most diverse and abundant, with 66 species (59 named, 7 undescribed species) occurring in Canada (Knee and Galloway 2017). Rhinonyssids are slow-moving, obligate haematophagous endoparasites that dwell primarily in the nasal cavity and turbinates, though occasionally these mites invade the trachea, lungs and body cavity (Porter and Strandtmann 1952, Bell 1996). Typically, rhinonyssids are not considered to cause significant damage to their hosts; however, the feeding activity may cause trauma to nasal tissues (de Rojas et al. 2002), and species that invade the lungs and air-sacs, such as *Sternostoma tracheacolum* Lawrence, can cause pneumonia and death of their hosts (Bell 1996).

Nasal mites have been surveyed in many geographic regions throughout the world (Fain 1957a, Maa and Kuo 1965, Domrow 1969, Pence 1975, Butenko 1984, Knee and Galloway 2017); however, despite these efforts, our understanding of this mite assemblage is largely incomplete. A recent survey of nasal mites (Rhinonyssidae, Turbinoptidae, Ereynetidae) infesting birds in Manitoba (Knee and Galloway 2017) uncovered two new species of rhinonyssids. Herein, I propose and describe *Sternostoma gallowayi* sp. n., and *Vitznyssus erici* sp. n.

Materials and methods

Injured and sick birds were submitted to the Wildlife Haven (Manitoba Wildlife Rehabilitation Organization) and the Prairie Wildlife Rehabilitation Centre, mostly by members of the public, and after death they were stored at -20 °C until processing in TD Galloway's lab at the University of Manitoba (Winnipeg, Manitoba, Canada). The nasal passages of thawed birds were flushed with a solution of warm water and mild soap using a 12 mL Monojet® 412 curved tip orthodontic plastic syringe. The solution was flushed through each nostril, through the opening in the palette and back out the mouth into a Petri dish. Occasionally nasal mites were collected from whole-body washing, where a thawed bird was placed in a container ranging in volume from 4–40 L, depending on the size of the bird, submerged in warm water containing a few drops of liquid dish detergent. Each bird was agitated vigorously three to 10 minutes, depending on the size of the bird. Each bird was then removed from the container and rinsed thoroughly; the washing solution was filtered through a 90 µm sieve. This process was repeated once again with warm, soapy water, and once finally with warm water. The filtrate from all three washes was preserved in 70 or 95% ethanol. Samples were examined

for mites using a dissecting microscope. All nasal mites were collected and preserved in 70 or 95% ethanol for later identification.

Mites were removed from ethanol and cleared in 85% lactic acid, mounted in polyvinyl alcohol medium (6371A, BioQuip Products, Rancho Dominguez, California, United States of America), and cured on a slide warmer at 40 °C for 3–4 days. Slide-mounted specimens were examined using a Leica DM2500 compound microscope and Leica ICC550 HD camera, with differential interference contrast illumination (DIC). Initial drawings of mites were made with pencil on paper using a camera lucida. Illustrations were later merged in Adobe Photoshop CS5 and redrawn in Adobe Illustrator CS5 using an Intuos 3 Graphics Tablet from WACOM Co., Ltd. (Saitama, Japan). Leg chaetotaxy is based on the system proposed by Evans (1963) and Evans and Till (1965). Idiosomal chaetotaxy follows the system of Lindquist and Evans (1965). All measurements are in micrometres (μm), and measurements presented with the mean followed by the range in parentheses. Rhinonyssids have a reduced setal compliment when compared to most free-living Mesostigmata, and they frequently have unpaired setae on the idiosoma and legs; therefore, the number of setae on the legs and idiosoma can be variable between specimens within a species.

Type specimens are deposited in the Canadian National Collection of Insects, Arachnids, and Nematodes (Agriculture and Agri-Food Canada, Ottawa, Ontario, Canada). Host taxonomy follows Chesser et al. (2018) *Checklist of North American birds*, 7th edition, plus supplements. Scientific permits were issued to TD Galloway for migratory birds by the Canadian Wildlife Service, Environment Canada.

Results and discussion

Family Rhinonyssidae Trouessart, 1895

Genus *Sternostoma* Berlese & Trouessart, 1889

Type species. *Sternostoma cryptorhynchum* Berlese & Trouessart, 1889.

Diagnosis. Stigmata dorsal or lateral, without peritreme. Gnathosoma ventral, only partially visible dorsally. Cheliceral digits small, less than one tenth the length of the chelicerae. One or two dorsal plates. Sternal and anal plates usually present.

Sternostoma gallowayi sp. n.

http://zoobank.org/09B2A5E1-AB6E-42DB-9302-12A731B55EEE
Figs 1–5

Material examined. *Type material.* Holotype: female (CNC535681) from horned lark (WK357), *Eremophila alpestris*, Winnipeg, Manitoba, Canada, 22.x.2011, coll: T.D. Galloway. Paratypes: female (CNC991940) same collection information as holo-
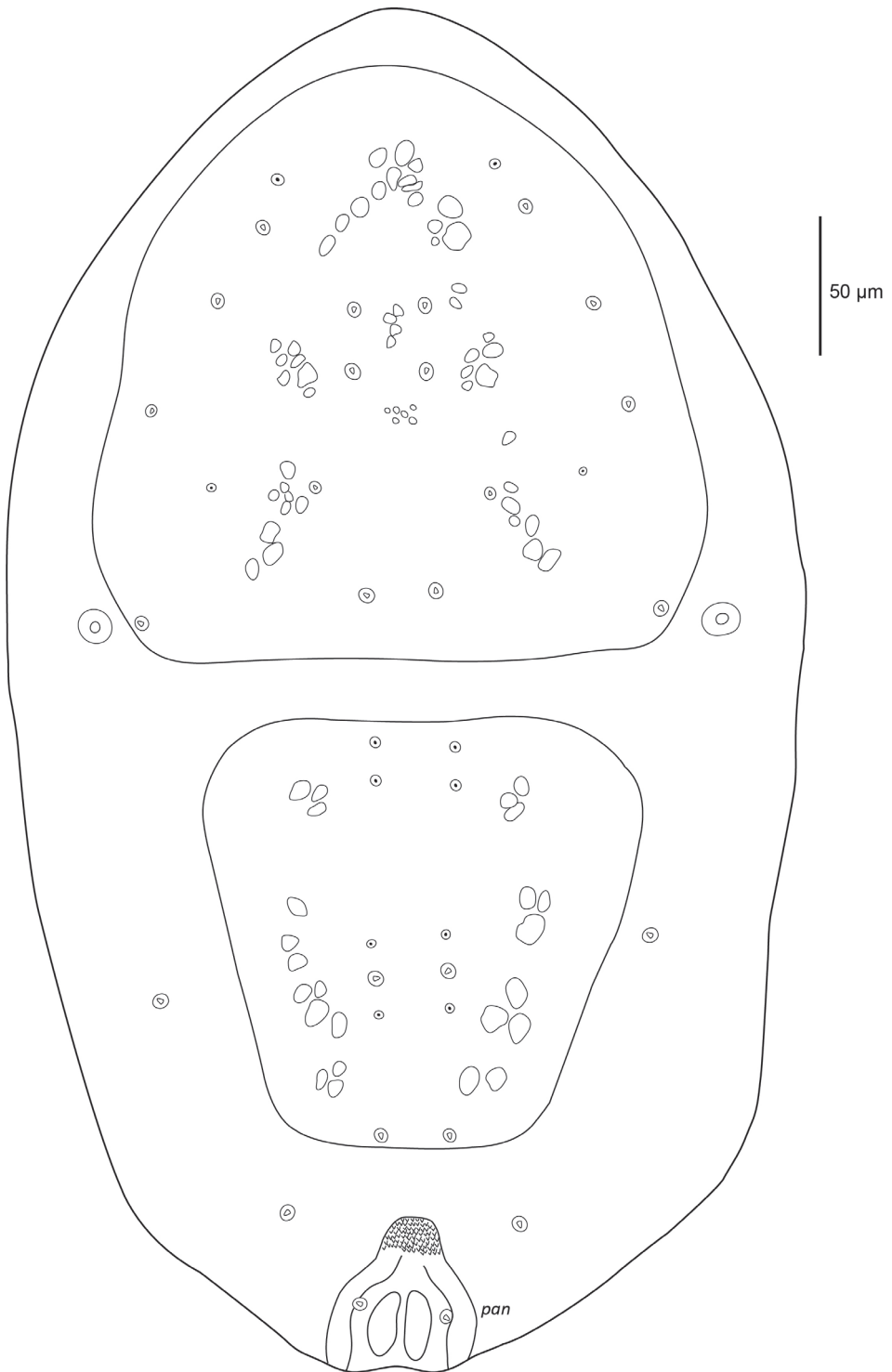
50 µm

pan

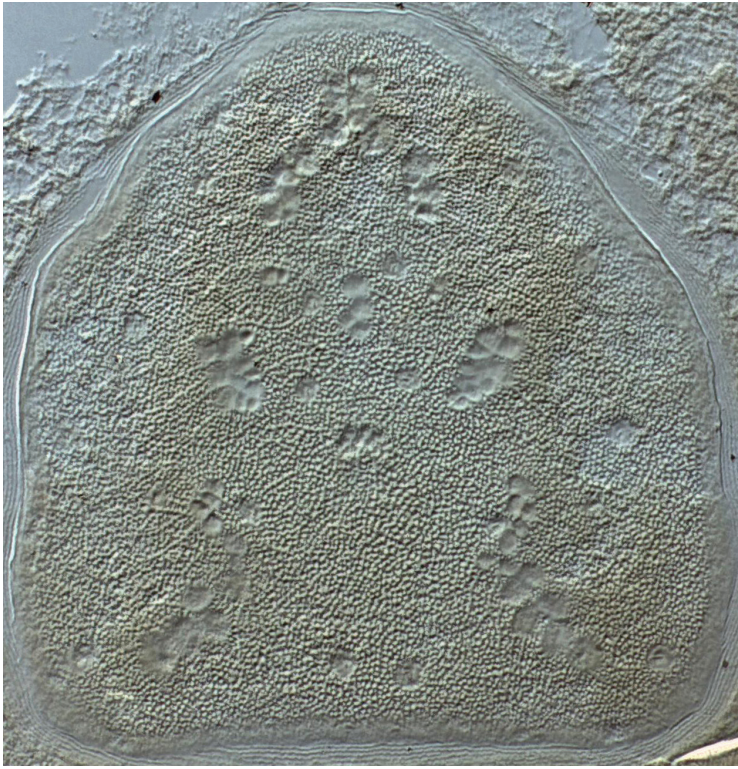**Figure 1.** Female *Sternostoma gallowayi* sp. n. dorsal idiosoma.

Figure 2. Female *Sternostoma gallowayi* sp. n. podosomal shield.

type. Two females (CNC991941, CNC991942) from horned lark (WK625), Winnipeg, Manitoba, Canada, 5.viii.2014, coll. TD Galloway.

Diagnosis female. Dorsum with two shields, podosomal shield large, covering most of podosoma with eight pairs of minute setae and two pairs of pore-like structures, opisthosomal shield medium-sized with two pairs of minute setae and four pairs of pore-like structures. Two pairs of minute setae in dorsal opisthosomal unsclerotised integument. Paranal setae on anal shield level with anus, postanal seta absent. Sternal shield longer than wide, three pairs of sternal setae (*st1–3*) on shield. Genital shield slightly reticulated lengthwise, broadly rounded posteriorly, seta *st5* on genital shield. Four pairs of minute setae in ventral opisthosomal unsclerotised integument. Ventral subcapitulum without setae. Ventrolateral and apical setae on tarsus II–IV thickened, baculiform and slightly curved distally.

Description female. *Dorsal idiosoma* (Figs 1–2). Idiosoma 427 (387–468) long excluding gnathosoma 267 (260–274) wide. Podosomal shield 205 (201–212) long, 202 (193–217) wide covering most of podosoma, with eight pairs of minute setae with rounded tips 1.9 (1.8–2) long in alveoli, and two pairs of pore-like structures in alveoli on shield. Podosomal shield rounded anteriorly, slightly convex lateral margins, posterior margin straight, plate with granular texture and vacuolate areas (Figure 2). Opisthosomal plate quadrangular 150 (148–153) long and 159 (155–161) wide at
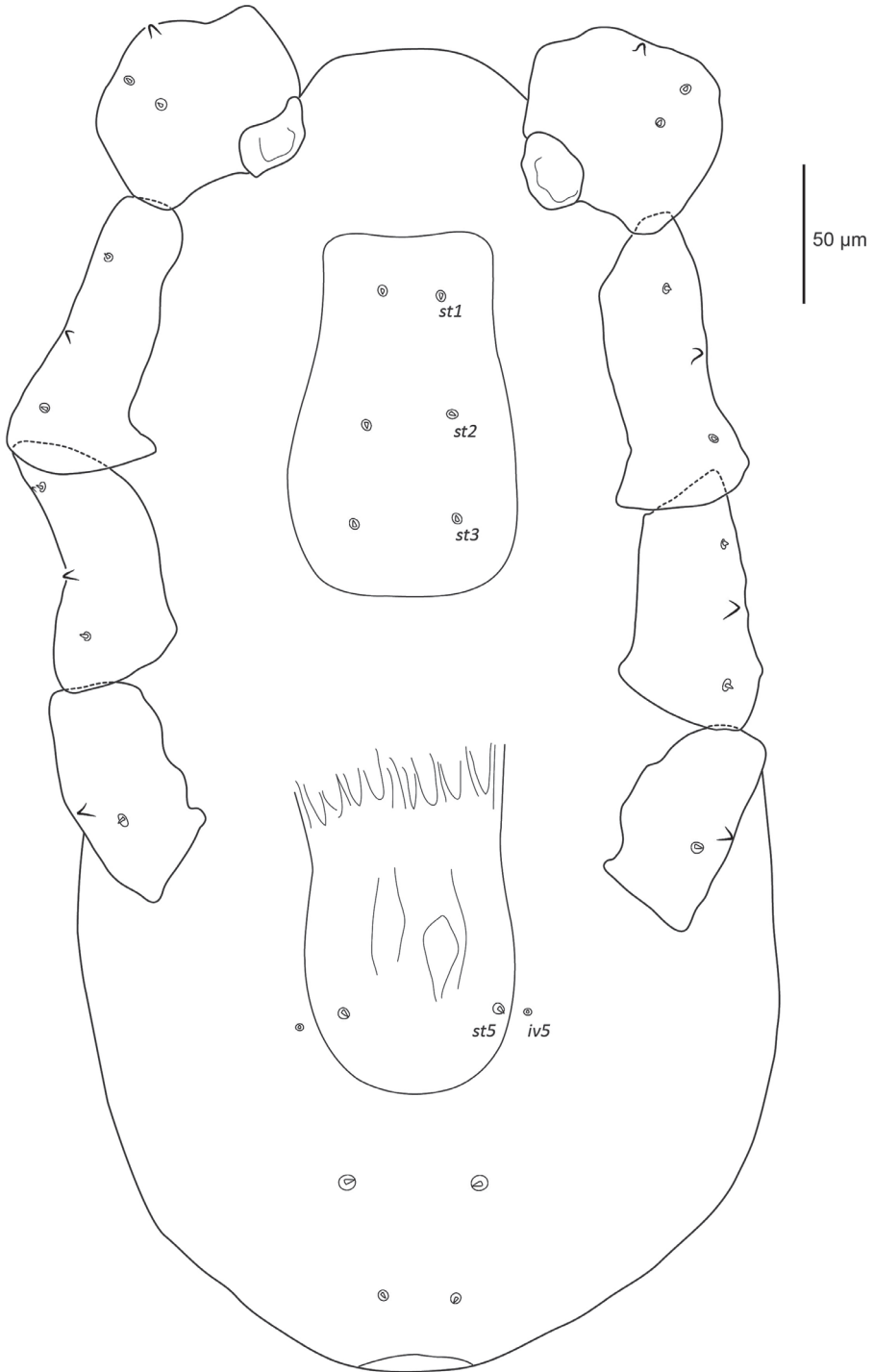
Figure 3. Female *Sternostoma gallowayi* sp. n. ventral idiosoma including coxae.

widest point, slightly wider than long, narrowing posteriorly. Plate with granular texture and vacuolate areas, two pairs of minute setae with rounded tip in alveoli, and four pairs of pore-like structures in alveoli. Dorsal integument finely striated, two pairs of minute setae with rounded tip in unsclerotised integument lateral and posterolateral of opisthosomal shield. Stigmata 11 (9–12) wide, without peritreme, situated near posterior corners of podosomal shield. Anal shield dorsoterminal 60 (56–65) long and 48 (45–51) wide, thickened well sclerotised lateral margins, cribrum present, paranal setae minute with rounded tip 1.8 (1.5–2.1) level with anus, postanal seta absent.

Ventral idiosoma (Figure 3). Sternal shield poorly sclerotised, with weak punctation, slightly wider towards posterior, longer than wide, 124 (120–128) long and 76 (73–79) at widest point, setae *st1* (1.6), *st2* (1.5), *st3* (1.5) in alveoli on shield. Genital shield large, 124 (121–126) long and 76 (73–82) wide level with *st5*, seta *st5* (2.1) on shield, slight reticulations lengthwise, and posterior broadly rounded, pair of lyrifissures *iv5* off genital shield. Cuticle finely striated, four pairs of minute setae with rounded tips in ventral opisthosomal unsclerotised integument.

Gnathosoma (Figure 4). Gnathosoma ventral in position, ventral length including palps 77 (69–82), maximum width 70 (68–73). Deutosternal groove present, deutosternal teeth absent, and subcapitulum without setae. Palps five-segmented, chaetotaxy
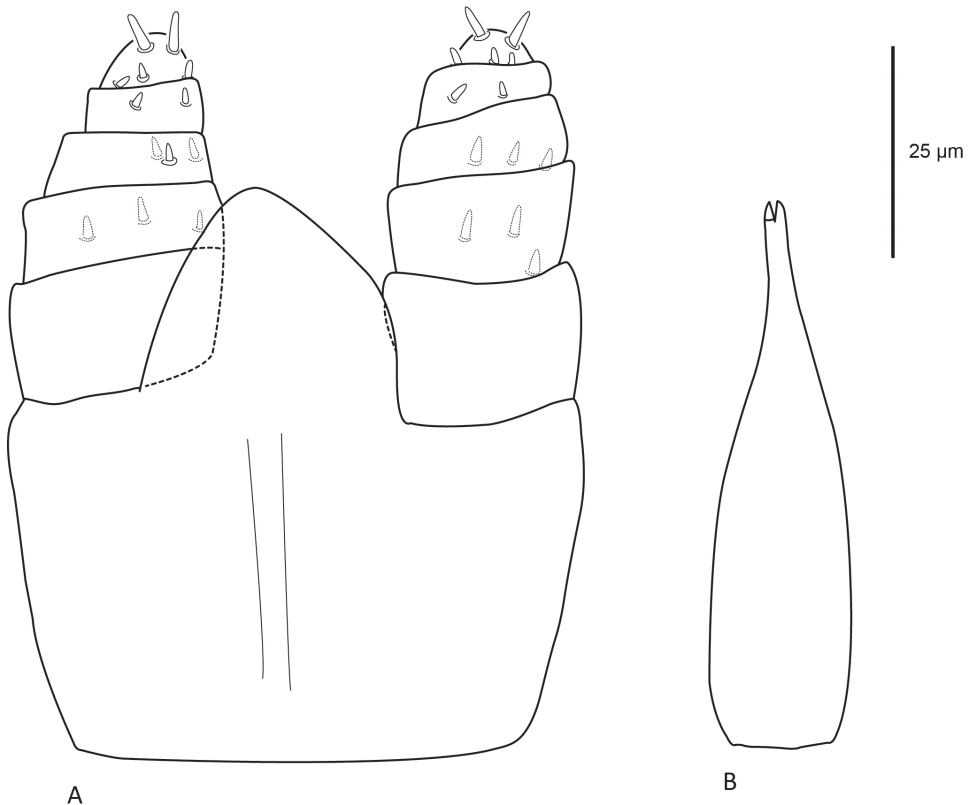

25 µm

A   B

Figure 4. Female *Sternostoma gallowayi* sp. n. (A) subcapitulum and palps, ventral aspect; (B) chelicerae.
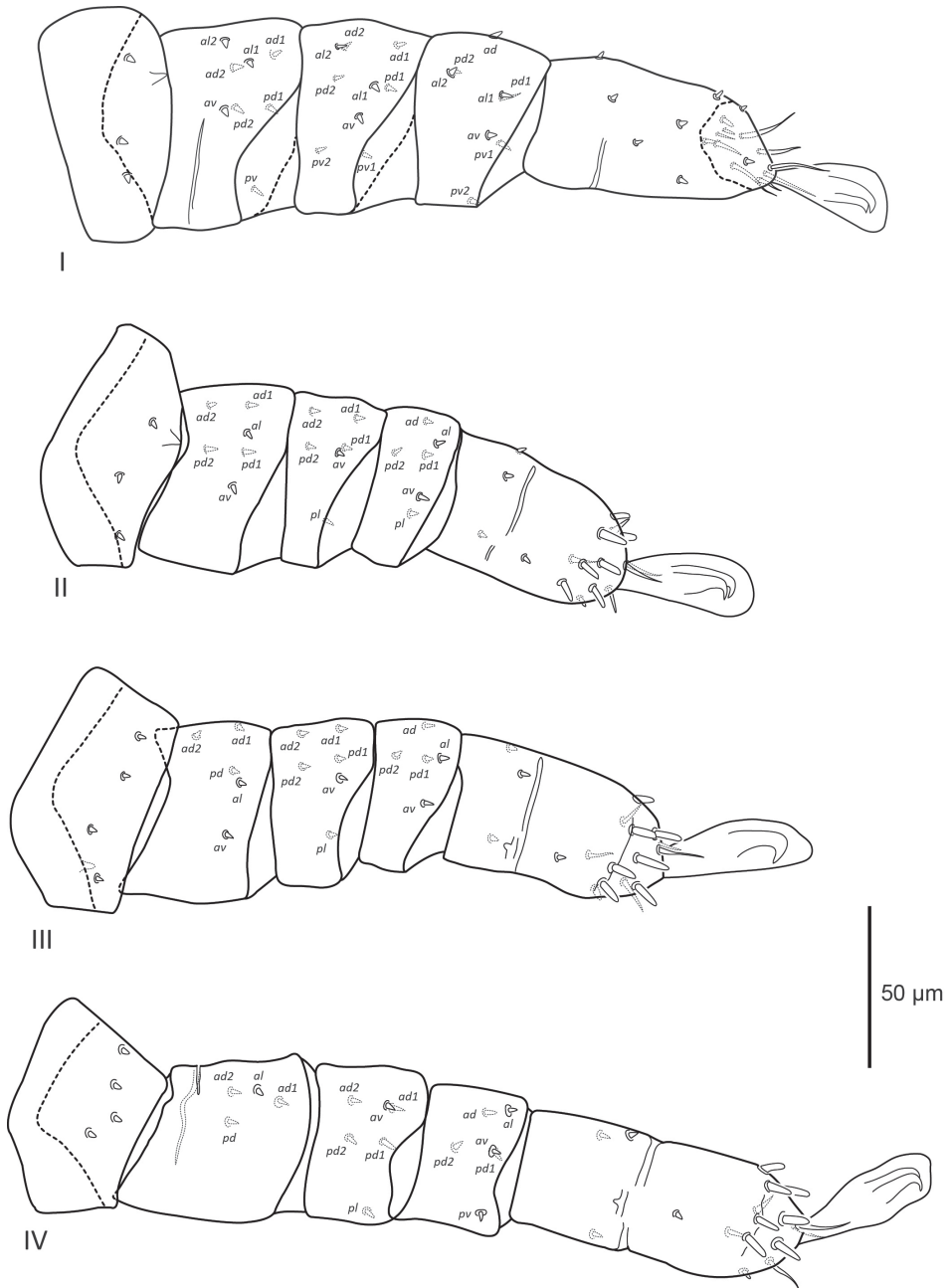
Figure 5. Female *Sternostoma gallowayi* sp. n. legs I–IV, coxae omitted.

of palps 0–3–3–2–5, all setae with rounded tips, palp apotele absent. Chelicerae widest proximally and tapering distally, 60 (57–63) long and 19 (18–20) at widest point, with small pointed fixed and moveable digits.

Legs (Figure 5). Excluding ambulacra, length of leg I 257 (226–283), leg II 206 (175–228), leg III 215 (196–243), and leg IV 263 (260–266). Setation of legs I–IV: coxae 2–2–2–1; trochanters 3–3–4–4; femora 8–6–5–4; genua 9–6–6–6; tibiae 8–6–5–6; tarsi 19–17–17–17. Most leg setae simple, minute, with rounded tip, a few apical tarsal setae filamentous. Ventrolateral and apical setae on tarsus II–IV (7.5) thickened, baculiform and slightly curved distally.

Male and immatures. unknown

Etymology. This species is named after Dr. Terry D Galloway, who has tirelessly collected nasal mites and other bird-associated arthropods for many years, and has given me the opportunity to continue my studies of these unique mites.

Remarks. The female of *Sternostoma gallowayi* sp. n. is most similar to those of *S. sialiphilus* Hyland and Ford, and *S. loxiae* Fain. These species each have two dorsal shields which are similar in extent and shape, enlarged and elongated ventrolateral and apical setae on tarsus II–IV, no setae in the unsclerotised dorsal podosomal integument, four pairs of setae in the ventral opisthosomal integument, two or less pairs of setae in the dorsal opisthosomal integument, and lack a postanal seta. *Sternostoma sialiphilus* has been collected from the bank swallow (*Riparia riparia*) in Canada, and the eastern bluebird (*Sialia sialis*) in the United States (Hyland and Ford 1961, Knee et al. 2008). *Sternostoma loxiae* has been collected from the red crossbill (*Loxia curvirostra*) in Canada and Belgium, from the American yellow warbler (*Dendroica petechia*), and mountain bluebird (*Sialia currucoides*) in Canada (Fain 1965, Knee et al. 2008, Knee and Galloway 2017).

Female *S. gallowayi* can be distinguished from that of *S. sialiphilus* and *S. loxiae* by having eight pairs of setae and two pairs of pores on the podosomal shield, *S. sialiphilus* has nine pairs of setae, *S. loxiae* has seven pairs of setae; two pairs of setae and four pairs of pores on the opisthosomal shield, *S. sialiphilus* has one pair of setae and three pairs of pores, *S. loxiae* has three pairs of setae and two pairs of pores on the shield; two pairs of setae in the dorsal opisthosomal unsclerotised integument, *S. sialiphilus* and *S. loxiae* have one pair; paranal setae level with anus, *S. sialiphilus* and *S. loxiae* the paranal setae are posterior to the anus; baculiform ventrolateral and apical setae on tarsus II–IV which are not distally inflated, *S. sialiphilus* and *S. loxiae* have distally inflated ventrolateral and apical setae on tarsus II–IV. *Sternostoma gallowayi* differs specifically from *S. sialiphilus* by the presence of seta *st5* on the genital shield, which is absent in *S. sialiphilus*, and the absence of contiguous alveoli between the podosomal and opisthosomal shields which are present in *S. sialiphilus*. *Sternostoma gallowayi* differs specifically from *S. loxiae* by having slight reticulation lengthwise on the genital shield, this reticulation is well-developed in *S. loxiae* (Fain 1966a). Comparisons were made using species descriptions from the literature and examining voucher material.

Horned larks are not commonly submitted to wildlife rehabilitation hospitals in Manitoba. Only six specimens have been submitted since 1994, five of which were examined for nasal mites. Of these, two were infested with *S. gallowayi*.

Genus *Vitznyssus* Castro, 1948

Type species: *Dermanyssus nitschi* Giebel, 1871 (=*Vitznyssus caprimulgi* (Fain, 1957))

Diagnosis. Female mites of *Vitznyssus* species are defined by Butenko (1984) as relatively long and slim, with long and thin legs, stigma with short peritreme level with coxa III, anal shield with well-defined cribrum, single podosomal shield on dorsal idiosoma, chelicerae long and thin distally with thickened bases, well-developed tritosternum and deutosternum with denticles.

Remarks. *Vitznyssus* is a small genus comprised of seven species collected from two disparate orders of birds: *V. afrotis* (Fain), *V. neotis* (Fain), *V. tetragis* Butenko, *V. vitzthumi* (Fain) from Otididae, Gruiformes; *V. caprimulgi* (Fain), *V. scotornis* (Fain), and *V. tsachevi* Dimov and Rojas from Caprimulgidae, Caprimulgiformes (Fain 1957b, 1966b, Butenko 1984, Dimov and de Rojas 2012). Butenko (1984) placed five *Astridiella* Fain, 1957 species described by Fain into *Vitznyssus*.

Vitznyssus erici sp. n.

http://zoobank.org/FF7BF246-7432-4B04-B887-0AFA708B1082
Figs 6–9

Material examined. *Type material.* Holotype: female (CNC535647) from common nighthawk (WK273), *Chordeiles minor*, Winnipeg, Manitoba, Canada, 4.ix.2010, coll: T.D. Galloway. Paratypes: two females (CNC991938, CNC991939) same collection information as holotype.

Diagnosis female. Large mite with one dorsal shield, podosomal shield longer than wide, rounded anteriorly, constricted posteriorly with irregular margins posterolaterally, six pairs of setiform setae, vacuolate areas and irregular transverse lines on podosomal shield. Subposterior setal pair on podosomal shield elongate, nearly twice as long as all other podosomal shield setae. Four pairs of setiform setae lateral and posterolateral of podosomal shield. Doral and ventral hysterosoma without small shieldlets. Sternal shield small, poorly sclerotised, constricted posteriorly, seta *st1* and lyrifissure *iv1* on sternal shield, setae *st2*, *st3,* and lyrifissure *iv2* off sternal shield. Genital shield elongate and narrow with parallel sides, seta *st5* off genital shield. Paranal setae setiform with filamentous tip anterior to anus, postanal seta setiform with filamentous tip slightly shorter than paranal setae. Well-developed tritosternum with paired laciniae. Palp apotele two-tined with bifid tips.

Description female. *Dorsal idiosoma* (Figure 6). Idiosoma 1016 (953–1168) long excluding gnathosoma, 493 (434–550) wide. Podosomal shield 387 (372–410) long, 261 (256–270) wide, rounded anteriorly, constricted posteriorly with irregular margins posterolaterally, six pairs of setiform setae, vacuolate areas and irregular transverse lines on podosomal shield. Subposterior setal pair on podosomal shield elongate 23 (21–27), almost twice as long as all other podosomal shield setae 12 (8–16). Dorsal integument finely striated, four pairs of setiform setae in unsclerotised integument lat-
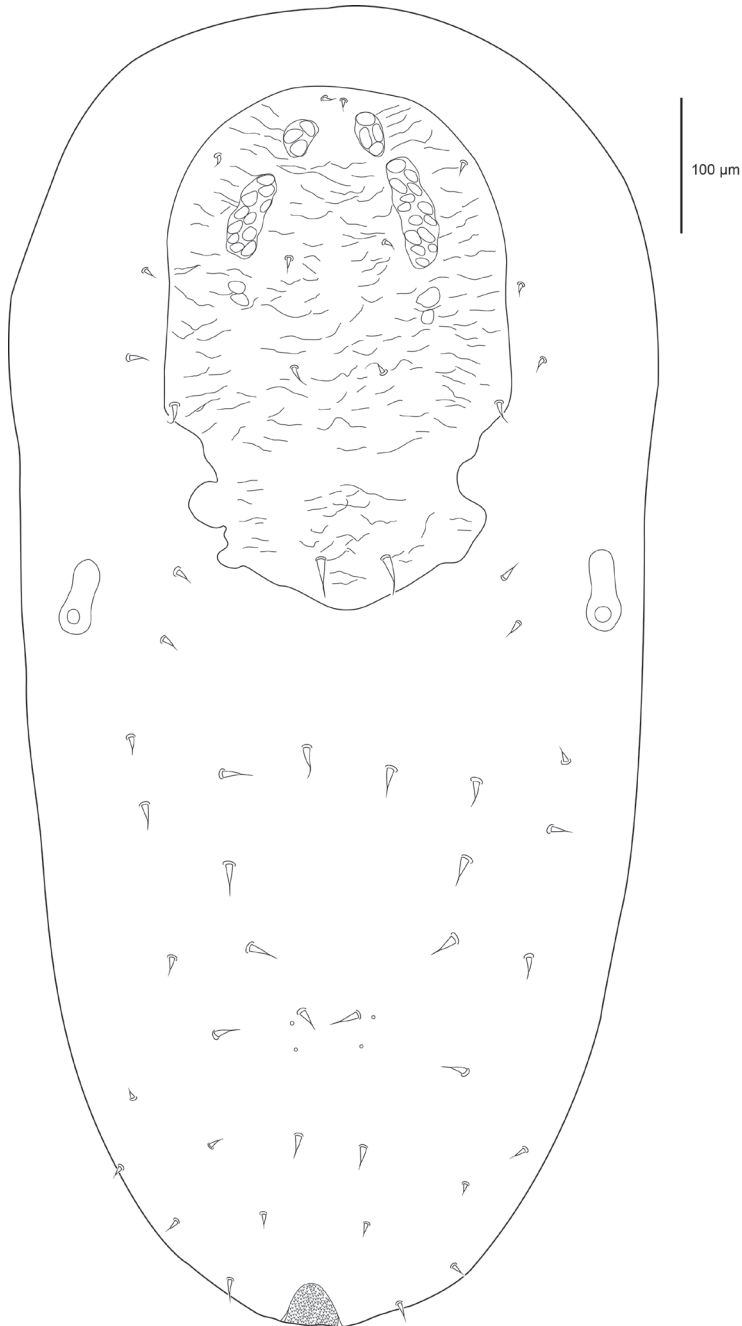
Figure 6. Female *Vitznyssus erici* sp. n. dorsal idiosoma.

eral and posterolateral of podosomal shield, 15–16 pairs of setiform setae 20 (15–22) and two pairs of pore-like structures in dorsal opisthosomal unsclerotised integument. Stigmata with short peritremes 54 (53–55).
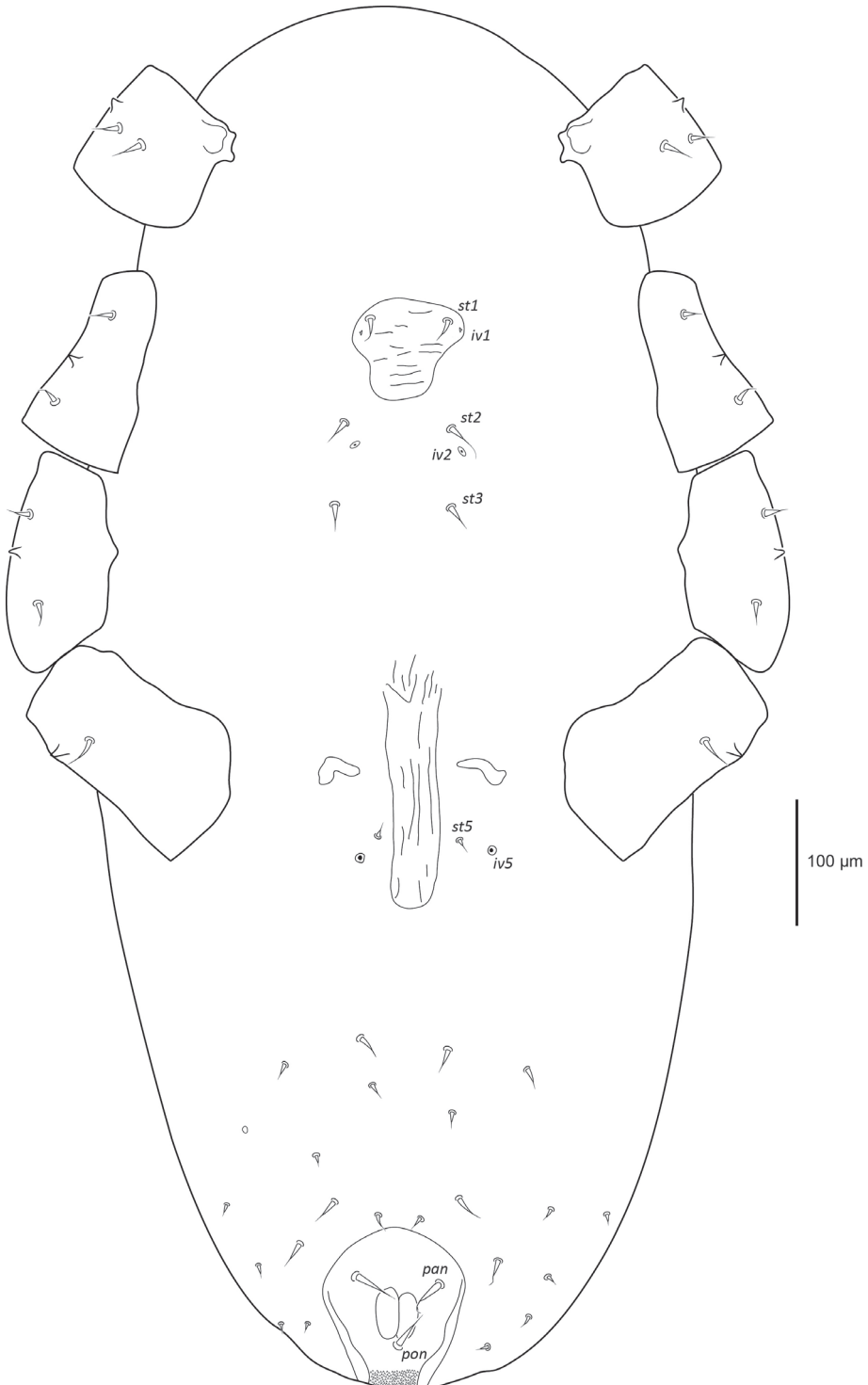
Figure 7. Female *Vitznyssus erici* sp. n. ventral idiosoma including coxae.

Ventral idiosoma (Figure 7). Sternal shield reduced and poorly sclerotised, 83 (80–87) long and 86 (86–87) maximum width anteriorly, constricted posteriorly, shield with irregular transverse lines, seta *st1* (18) and lyrifissure *iv1* on sternal shield. Setae *st2* (20), *st3* (19), and lyrifissure *iv2* in unsclerotised integument off sternal shield. Genital shield elongate and narrow, 196 (193–200) long and 40 (37–43) wide, parallel sides and reticulated lengthwise, seta *st5* (11) and pair of lyrifissures *iv5* off genital shield. Cuticle finely striated, 11 pairs of setiform setae in ventral opisthosomal unsclerotised integument. Anal shield 162 (155–169) long and 114 (112–115) wide, thickened lateral margins, cribrum present, paranal setae 46 (45–48) setiform with filamentous tip anterior to anus, postanal seta 32 (30–36) setiform with filamentous tip slightly shorter than paranal setae.

Gnathosoma (Figure 8). Gnathosoma terminal, ventral length including palps 236 (225–242), width 160 (152–166) posterior to *pc* seta. Subcapitulum with 10 rows of paired deutosternal denticles. Subcapitular setae setiform, *pc* 20 (15–23), *h1* 13 (12–14), *h2* 13 (11–15), and *h3* 33 (26–39). Well-developed tritosternum 233 long, with paired laciniae. Palps five-segmented, chaetotaxy of palps 0–4–4–8–9, palp apotele two-tined with bifid tips. Chelicerae elongate 242 (237–249), expanded proximally 50 (45–56), marked constriction distally with small pointed moveable and fixed digits.

Legs (Figure 9). Excluding ambulacra, length of leg I 541 (483–591), leg II 520 (487–541), leg III 518 (512–521), and leg IV 615 (596–627). Setation of legs I–

Figure 8. Female *Vitznyssus erici* sp. n. (A) subcapitulum and palp, ventral aspect; (B) tritosternum; (C) chelicerae.
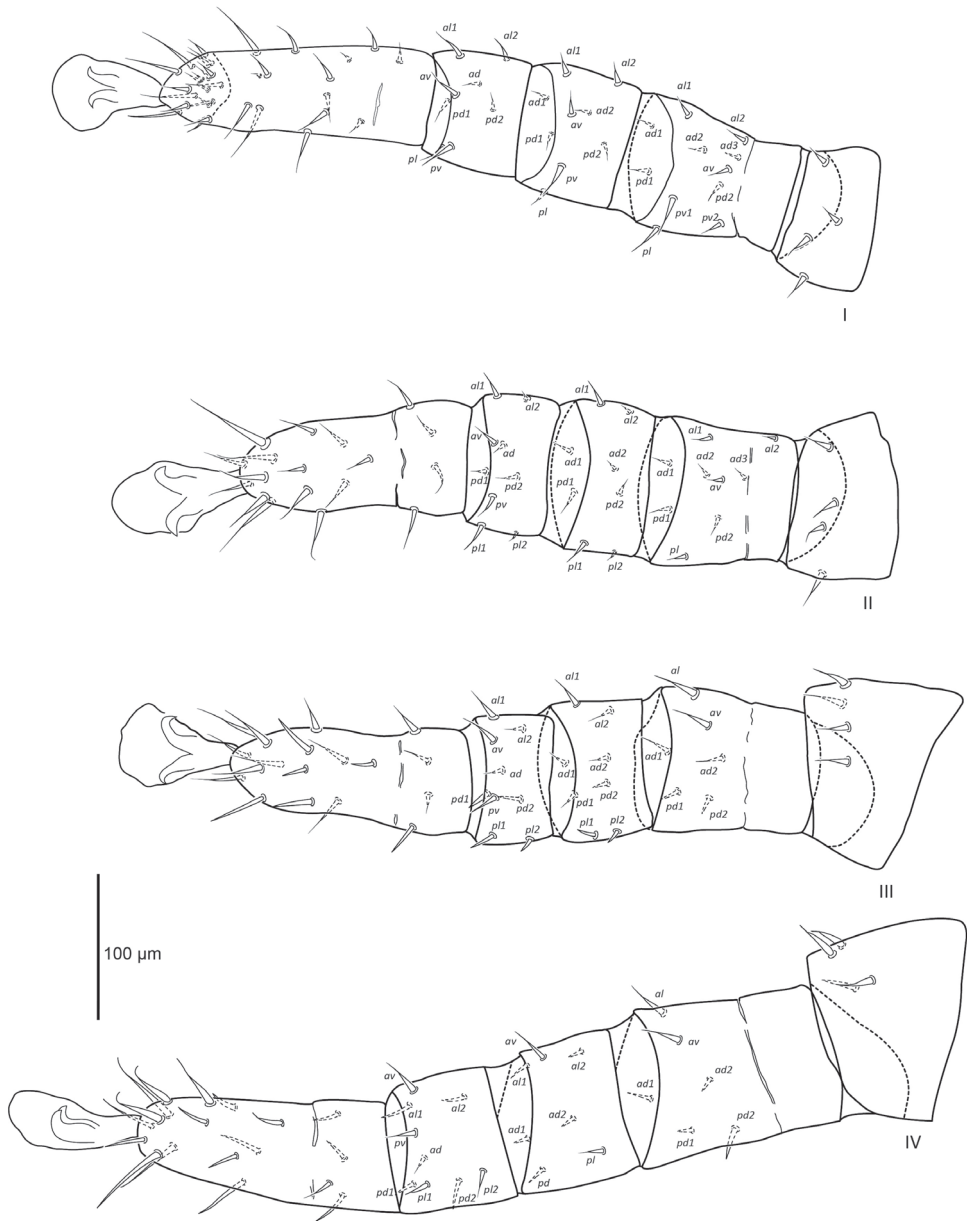
Figure 9. Female *Vitznyssus erici* sp. n. legs I–IV, coxae omitted.

IV: coxae 2–2–2–1; trochanters 4–4–4–4; femora I (2–3/1,2/2–1), II (2–3/1,2/0–1), III (1–2/1,2/0–0), IV (1–2/1,2/0–0); genua I (2–2/1,2/1–1), II (2–2/0,2/0–2), III (2–2/0,2/0–2), IV (2–2/1,1/0–1); tibiae I (2–1/1,2/1–1), II (2–1/1,2/1–2), III (2–1/1,2/1–2), IV (2–1/1,2/1–2); tarsi 33–18–18–18. Leg setae are setiform with filamentous tip.

Male and immatures. Unknown.

Etymology. This species is named after Eric Shewchuk, a close friend who has been beside me throughout the entirety of my studies on mites.

Remarks. The female of *Vitznyssus erici* sp. n. is most similar that of *V. afrotis* Fain, which was described from the southern black bustard (*Afrotis afra*) in South Africa (Fain 1966b). These two species are most similar in that they are large mites (at least 1000 μm long), and both have: one dorsal shield which is longer than wide and eroded along the margins, especially posterolaterally; sternal shield reduced, with seta *st1* on the shield; elongate and narrow genital shield; palp apotele two-tined with bifid tips; elongate tritosternum with two laciniae; elongate paranal setae anterior to anus, and elongate postanal setae present.

Female *V. erici* differ from that of *V. afrotis* by: the presence of irregular transverse lines on the podosomal shield, which are absent in *V. afrotis*; the posterolateral margins of the podosomal shield are more eroded, invaginated and irregular than that of *V. afrotis*; the anterior margin of the podosomal shield is broadly rounded with no setae in the integument anterior of the shield, the anterior margin is slightly eroded in *V. afrotis* and a pair of setae are off the shield anteriorly; the sternal shield is larger, with a posteromedial projection, and lyrifissure *iv1* is on the shield, *V. afrotis* sternal shield is smaller and without a posteromedial projection, *iv1* is off the shield; the genital shield margins are parallel and not flared posteriorly like they are in *V. afrotis*; and by the absence of small accessory shieldlets on the dorsal or ventral hysterosoma, which are present in *V. afrotis*. Fain (1966b) described *V. afrotis* as lacking a sternal shield; however, the holotype and paratype specimens examined have a small narrow sternal shield with seta *st1* on the shield. Comparisons were made using the species description for *V. afrotis* and examination of the holotype and paratype specimens loaned from the Royal Belgian Institute for Natural Sciences.

Including *V. erici* there are now four *Vitznyssus* species known from Otididae (bustards) and four species known from Caprimulgidae (nightjars) hosts. Bustards only occur in the Eastern Hemisphere, while nightjars are broadly distributed in both hemispheres. Considering the geographic distribution of these mites and the disparate host bird orders, the monophyly of the genus and species boundaries should be investigated using molecular markers and morphometric analyses.

The common nighthawk (*Chordeiles minor*) has been a focus for studies of ectoparasites in Manitoba (Galloway 2006, Galloway and Lamb 2015). Despite the apparent decline in populations of common nighthawk in the province (Taylor 1996), these birds are frequently submitted to rehabilitation hospitals. However, using the methods described here, nasal mites are either rare or rarely collected. Out of 138 common nighthawks examined for this study since 1999, nasal mites were collected from only one. The conservation status of this mite certainly deserves consideration.

Acknowledgements

References

Bell PJ (1996) The life history and transmission biology of *Sternostoma tracheacolum* Lawrence (Acari: Rhinonyssidae) associated with the Gouldian finch *Erythrura gouldiae*. Experimental and Applied Acarology 20: 323–341. https://doi.org/10.1007/BF00052962

Butenko OM (1984) Non-passerine nasal mites of Russia. Zoological Institute, Russian Academy of Science, Saint Petersburg, Russia, 188 pp.

Chesser RT, Burns KJ, Cicero C, Dunn JL, Kratter AW, Lovette IJ, Rasmussen PC, Remsen Jr JV, Stotz DF, Winger BM, Winker K (2018) Check-list of North American Birds (online). American Ornithological Society. http://checklist.aou.org/taxa [accessed 1 August 2018]

de Rojas M, Mora MD, Ubeda JM, Cutillas C, Navajas M, Guevara DC (2002) Phylogenetic relationships in rhinonyssid mites (Acari: Rhinonyssidae) based on ribosomal DNA sequences: insights for the discrimination of closely related species. Parasitology Research 88: 675–681. https://doi.org/10.1007/s00436-002-0647-y

Dimov I, de Rojas M (2012) One new species of nasal mites of the genus *Vitznyssus* (Rhinonyssidae) from the Leningrad province, Russia. Journal of the Acarological Society of Japan 21: 125–130.

Domrow R (1969) The nasal mites of Queensland birds (Acari: Dermanyssidae, Ereynetidae, and Epidermoptidae). Proceedings of the Linnaean Society of New South Wales 93: 297–426.

Evans GO (1963) Observations on the chaetotaxy of the legs in the free-living gamasina (Acari: Mestostigmata). Bulletin of the British Museum (Natural History) Zoology 10: 277–303.

Evans GO, Till WM (1965) Studies on the British Dermanyssidae (Acari: Mesostigmata). Part 1. External morphology. Bulletin of the British Museum (Natural History) Zoology 13: 249–294.

Fain A (1957a) Les acariens des familles Epidermoptidae et Rhinonyssidae parasites des fosses nasales d'oiseaux au Ruanda-Urundi et au Congo belge. Annales du Musee Royal du Congo Belge (Tervuren). Série in Octavo, Sciences Zoologiques 60: 1–176.

Fain A (1957b) Les acariens du genre *Astridiella* n.g. (Rhinonyssidae) parasites nasicoles de l'engoulevent et de l'outarde. Rivista di Parassitologia 18: 91–102.

Fain A (1965) Diagnoses d'acariens parasites nouveaux. Revue de Zoologie et de Botanique Africaines 72: 152–160.

Fain A (1966a) Les acariens parasites nasicoles des oiseaux de Belgique. V. Deux nouvelles especes de Rhinonyssidae. Bulletin et Annales de la Societe Entomologique de Belgique 102: 117–122.

Fain A (1966b) Notes sur quelques Rhinonyssidae (Acari: Mesostigmata). Revue de Zoologie et de Botanique Africaines 74: 83–96.

Fain A (1994) Adaptation, specificity and host-parasite coevolution in mites (Acari). International Journal for Parasitology 24: 1273–1283. https://doi.org/10.1016/0020-7519(94)90194-5

Fain A, Elsen P (1967) Les acariens de la famille Knemidokoptidae producteurs de gale chez les oiseaux. Acta Zoologica et Pathologica Antverpiensia 45: 3–142.

Galloway TD (2006) Ectoparasites (Phthiraptera: Philopteridae; Acari: Ixodidae) of common nighthawk, *Chordeiles minor*, and whip-poor-will, *Caprimulges vociferus* (Caprimulgi-formes: Caprimulgidae), in Manitoba. Journal of the Entomological Society of Manitoba 137: 5–11.

Galloway TD, Lamb RJ (2015) Abundance and stability of populations of a chewing louse, *Mulcticola macrocephalus* (Phthiraptera: Philopteridae), on common nighthawks, *Chordeiles minor* (Caprimulgiformes: Caprimulgidae) in Manitoba, Canada. The Canadian Entomologist 147: 723–731. https://doi.org/10.4039/tce.2014.85

Hyland KE, Ford HG (1961) *Sternostonia sialiphilus* n. sp. (Acarina : Rhinonyssidae) from the nasal cavities of the eastern bluebird, *Sialia sialis* (Linnaeus). Journal of Parasitology 47: 101–103.

Knee W, Galloway TD (2017) New host and locality records for endoparasitic nasal mites (Acari: Rhinonyssidae, Turbinoptidae, and Ereynetidae) infesting birds in Manitoba, Canada. The Canadian Entomologist 149: 89–103. https://doi.org/10.4039/tce.2016.47

Knee W, Proctor H, Galloway T (2008) Survey of nasal mites (Rhinonyssidae, Ereynetidae, and Turbinoptidae) associated with birds in Alberta and Manitoba, Canada. The Canadian Entomologist 140: 364–379. https://doi.org/10.4039/n08-017

Lindquist EE, Evans GO (1965) Taxonomic concepts in the Ascidae, with a modified setal nomenclature for the idiosoma of the Gamasina (Acarina: Mesostigmata). Memoirs of the Entomological Society of Canada 47: 1–64.

Maa TC, Kuo JS (1965) A field survey of arthropod parasites of birds in Taiwan. Journal of Medical Entomology 1: 395–401. https://doi.org/10.1093/jmedent/1.4.395

Mullens BA, Owen JP, Kuney DR, Szijj CE, Klingler KA (2009) Temporal changes in distribution, prevalence and intensity of northern fowl mite (*Ornithonyssus sylviarum*) parasitism in commercial caged laying hens, with a comprehensive economic analysis of parasite impact. Veterinary Parasitology 160: 116–133. https://doi.org/10.1016/j.vetpar.2008.10.076

Pence DB (1975) Keys, species and host list and bibliography for nasal mites of North American birds (Acarina: Rhinonyssinae, Turbinoptinae, Speleognathinae and Cytoditidae). Special Publications of the Museum of Texas Tech University No. 8: 1–148.

Porter JC, Strandtmann RW (1952) Nasal mites of the English sparrow. Texas Journal of Science 4: 393–399.

Proctor H, Owens I (2000) Mites and birds: diversity, parasitism and coevolution. Trends in Ecology & Evolution 15: 358–364. https://doi.org/10.1016/S0169-5347(00)01924-8

Taylor P (1996) Apparent decline of migrant common nighthawks near Pinawa, Manitoba. Blue Jay 54: 35–38.

RESEARCH ARTICLE

Cryptic diversity in *Andrognathus corticarius* Cope, 1869 and description of a new *Andrognathus* species from New Mexico (Diplopoda, Platydesmida, Andrognathidae)

Patricia L. Shorter[1,2], Derek A. Hennen[1], Paul E. Marek[1]

1 *Virginia Polytechnic Institute and State University, Department of Entomology, Price Hall, 170 Drillfield Drive, Blacksburg, Virginia, USA* **2** *Louisiana State University, Department of Entomology & School of Renewable Natural Resources, Life Sciences Building, Forestry Lane, Baton Rouge, Louisiana, USA*

Corresponding author: *Patricia L. Shorter* (pshort3@lsu.edu)

Citation: Shorter PL, Hennen DA, Marek PE (2018) Cryptic diversity in *Andrognathus corticarius* Cope, 1869 and description of a new *Andrognathus* species from New Mexico (Diplopoda, Platydesmida, Andrognathidae). ZooKeys 786: 19–41. https://doi.org/10.3897/zookeys.786.27631

Abstract

Andrognathus is a genus of small, thin-bodied millipedes found in deciduous forests of North America. Poorly understood, these organisms inhabit decaying wood and have morphologically conserved and difficult-to-identify sexual characters that have limited study historically. Recent use of scanning electron microscopy has uncovered variation in male genitalia that was previously unknown in the genus. The distribution of *Andrognathus* and the extent of this variability across the continent, however, were undocumented, and a wealth of natural history collections remained uncatalogued. Here a new species of *Andrognathus* is described from New Mexico, *Andrognathus grubbsi* **sp. n.**, natural history collections are utilized to create a comprehensive map of the genus, and a neotype established for the type species, *Andrognathus corticarius* Cope, 1869. Analysis of the cytochrome oxidase I gene (COI) for *A. corticarius* was completed for the type series and individuals across the species distribution, but little variation was found. *Andrognathus grubbsi* **sp. n.** joins *A. corticarius* and *A. hoffmani* Shear & Marek, 2009 as the only members of the genus.

Introduction

Andrognathus corticarius Cope, 1869 is a small-bodied platydesmidan millipede broadly distributed in mixed mesophytic deciduous forests in the eastern United States (Figure 1A). It is commonly found in aggregations of adults and juveniles beneath bark (Figure 1B, C) (hence the specific name *corticarius*). A diagnostic feature of the species is the shape of the paranota of the fifth body ring, which are bilobed with the ozopores elevated on stalks and directed anteriorly (Figure 2A) (Cook and Loomis 1928). The known range of *A. corticarius* extends from the panhandle of Florida, north into southern Indiana and Pennsylvania (Figure 3). The species is a member of the subterclass Colobognatha, a group that includes millipedes with mouthparts generally reduced in size, and eight leg-pairs anterior to the primitive leg-like gonopods (9 and 10) that have a plesiomorphic complement of six podomeres (Latzel 1884; Hoffman 1980). Colobognatha encompass taxa with superlative leg counts (e.g., *Illacme plenipes* Cook & Loomis, 1928 with 750 and *Siphonophora millepeda* Loomis, 1934 with 742), and are euanamorphic, meaning they add leg-pairs and segments throughout their lifespan for an indeterminate amount of time (Enghoff et al. 1993). Colobognatha includes four orders: Polyzoniida, Platydesmida, Siphonocryptida, and Siphonophorida (Golovatch et al. 2015), which are generally differentiated by the shape of the head and variable fusion of the pleura and terga (Hoffman 1980). The presence of ocelli and antennal shape are other primary characters that differentiate these orders. While colobognaths are often collected, and a considerable amount of material in natural history collections exists, they are poorly understood due to their small size and apparently invariant gonopods. As a result, the Colobognatha are notorious as a challenging group (Read and Enghoff 2009), and the taxon's last global taxonomic synthesis was by Attems (1951).

The order Platydesmida is differentiated from other Colobognatha by having chewing mouthparts, the trunk ring pleurites fused with the tergites, and a gnathochilarium composed of a plesiomorphic five sclerites (Enghoff et al. 2015). Members of the order possess chemical defenses containing heterocyclic nitrogen-containing alkaloids and some members display paternal care (Gardner 1975; Shear 2015). Some species of platydesmidans, such as the andrognathid genera *Brachycybe* Wood, 1864 (Gardner 1975) and *Pseudodesmus* Pocock, 1887 (Lewis 1984), aggregate in a stellate pattern, where the cephalic ends of multiple individuals point inward toward a central hub and telsons radiate outward in a star or spoke-like configuration (termed a pinwheel). *Andrognathus corticarius* has not been found in these formations. The families Andrognathidae and Platydesmidae are differentiated solely by the morphological trait of narrow sternites that make the coxae appear to be nearly contiguous in andrognathids (Cook and Loomis 1928; Enghoff et al. 2015). However, proximity of coxae may be a homoplasy, and based on a recent phylogenomic analysis of the Diplopoda, the genera *Platydesmus* and *Brachycybe* are more closely related to one another than either is to *Andrognathus* thereby indicating non-monophyly of the family Andrognathidae (Rodriguez et al. 2018). Andrognathidae currently has 12 genera with a primarily Holarctic distribution, but two genera are found in Southeast Asia: *Brachycybe* Wood, 1864 and *Pseudodesmus* Pocock, 1887 (Hoffman 1980; Enghoff et al. 2015). The family is

divided into three subfamilies: Dolisteninae Latzel, 1884; Bazillozoniinae Verhoeff, 1935; and Andrognathinae Cope, 1869 that contains *Andrognathus* as its sole genus (Hoffman 1980).

Andrognathus corticarius is the type species for the genus and was discovered by Edward Drinker Cope in Virginia more than a century ago. Cope's fieldwork was focused on cave species, primarily fossil vertebrates, but he also collected myriapods. Cope listed the type locality of *A. corticarius* only as "Montgomery County, Virginia" (Cope 1869: 182).

Unfortunately, the type material of *A. corticarius* has not been located and is presumed lost (Hoffman 1999; see also below Materials and Methods section). For 138 years, the genus contained only *A. corticarius*; however a series of andrognathids that possessed the characteristic lobed paranota of the fifth body ring were discovered in Nuevo Leon, Mexico by Casey Richart in 2007. These specimens were subsequently described as the species *Andrognathus hoffmani* Shear & Marek, 2009. In the same paper, the authors indicated that a cryptic species complex may exist in *A. corticarius*, stating that it deserves a more detailed examination (Shear and Marek 2009). However, the lack of type material of *A. corticarius* has meant that the identity of the species has remained uncertain.

The small body size of *A. corticarius* and its apparent uniformity at low optical magnification may underestimate the diversity of the species. Here we use high-magnification imaging to document the range of genitalic variation in *A. corticarius* and suggest that the species is a cryptic species complex. To stabilize the taxonomy of the group we designate a neotype for *A. corticarius* and describe a new *Andrognathus* species from New Mexico, United States.

Materials and methods

Material examined. Natural history collections and newly collected specimens of *Andrognathus* were used for this study. Material collected in the field (2005–2017) was brought back to the lab alive for DNA extraction and specimen preparation. Individuals were found by flipping and breaking apart decaying hardwood logs and examining the surfaces of large fallen branches in mesic forest habitats, such as areas where xystodesmid millipedes are found (Means et al. 2015). In contrast, some individuals were occasionally found in dry habitats under pine logs. *Andrognathus corticarius* individuals appear to burrow into dead organic matter and humus, and are often found inside decaying wood and beneath the bark. They are not typically beneath leaves as is commonly observed with xystodesmid millipedes (Means et al. 2015). Decaying logs that were just beginning to lose bark and soften due to decomposition were ideal habitats. Collected specimens were labelled with locally unique identification (LUID) codes beginning with the prefix "MPE-", and were deposited in Virginia Tech Insect Collection (abbreviation VTEC, https://www.collection.ento.vt.edu) These data are available for download from VTechData (https://data.lib.vt.edu/collections/44558d39p, https://doi.org/10.7294/kbtb-8v48, Suppl. material 1).

Other material for this study comprised specimens deposited in the North Carolina State Museum (NCSM) and the Virginia Museum of Natural History (VMNH) (Suppl. material 1). These collections were chosen as they are the largest repositories of *Andrognathus* specimens. These specimens were given labels with the LUID code, "AND-". The collection labels of these specimens were georeferenced with GEOLocate to recover the geographical coordinates of the occurrence (Rios and Bart 2010). Elevation was estimated using Google Earth (http://www.earth.google.com). As it documented the northernmost locality of the genus *Andrognathus*, we included an observation in Pennsylvania from the citizen science observation website BugGuide (BugGuide.net 2016) and confirmed the validity of the record with the observer; these specimens were not collected. A distribution map for the species utilizing specimens collected for this study, along with georeferenced localities from the literature (Gardner 1975, Shear and Marek 2009, Shelley 1978, Shelley 2000) (Suppl. material 2) was generated with the online GIS software Simplemappr (Shorthouse 2010) (Figure 3). These data are also available for download from VTechData (https://data.lib.vt.edu/collections/44558d39p, https://doi.org/10.7294/kbtb-8v48).

The Academy of Natural Sciences of Drexel University (ANSP) in Philadelphia, where Cope traditionally deposited his material, was contacted to determine if any type material was present in their holdings. The type database of the Museum of Comparative Zoology at Harvard (MCZ), a second repository of Cope material, was searched online to determine if the material was deposited there (MCZBase 2017). No andrognathid specimens assignable to the original types of Cope were present in either of the collections. Hoffman (1999) speculated that the type locality of *A. corticarius* is Yellow Sulfur Springs (Montgomery County, Virginia), a popular resort in the late 19th century. Fourteen male and seven female specimens of *A. corticarius* were collected at Yellow Sulfur Springs in 2016.

Morphological analysis and imaging. Seventeen well-preserved males of *A. corticarius* (Table 1) were selected for SEM imaging including individuals from: Liberty County, Florida (southernmost known point); Dekalb County, Alabama (westernmost); Kanawha County, West Virginia (northernmost); and Campbell County, Virginia (easternmost). Only females were available from other peripheral portions of the species range.

For morphological analysis, the gonopod-bearing body ring was mounted ventral side up on a 12.7 mm aluminum SEM stub using carbon tape (Pellco, California). The stubs were coated with 20 nm of platinum and palladium with a Leica EM ACE 600 high vacuum coater, and imaged on a FEI Quanta 600 FEG environmental SEM. Micrographs were taken of the gonopod-bearing ring as a whole and of the sixth podomere process of the anterior (A6) and posterior (P6) gonopods. For specimens collected in New Mexico, a male and a female were imaged.

DNA extraction and genetic analysis. Fresh material of recently collected individuals was preserved for genetic analysis. The middle third of the millipede trunk was excised and stored in RNALater at -80 °C, and the head, anterior and posterior rings, and gonopods were retained as voucher specimens in 70% isopropanol. The DNA of three individuals from a locality, selected to examine within site nucleotide variation, was extracted and purified using a DNeasy Blood & Tissue Kit (Qiagen, Valencia, Califor-

nia). A region of the cytochrome oxidase I gene (COI) was amplified with polymerase chain reaction (PCR) using the primers LCO1490 and HCO2198 (Folmer et al 1994; Hebert et. al. 2003) according to the methods described in Marek et al. (2012). Amplified DNA was confirmed with electrophoresis on a 10% agarose gel, and raw PCR amplicons were cleaned, quantified, and Sanger-sequenced at the University of Arizona Genomics Core on an ABI 3100 capillary DNA sequencer. Raw chromatograms were analyzed in the Mesquite module Chromaseq version 1.2 using phred and phrap for nucleotide base-calling, trimming, and quality control (Maddison and Maddison 2010; Ewing et al. 1998). The COI sequences were translated into amino acids, and aligned by eye. Mean uncorrected pairwise distances were calculated using Mesquite. A pairwise distance matrix for these data are available for download from VTechData (https://data.lib.vt.edu/collections/44558d39p, https://doi.org/10.7294/kbtb-8v48, Suppl. material 3).

Results

Specimens included in this study provided 55 localities for *Andrognathus* (including 36 from previously undocumented localities) and resulted in the first comprehensive distribution map of the genus (Figure 3). A total of 274 specimens was examined: 185 individuals (64 males, 83 females, 38 juveniles) were from the NCSM and VMNH, and 89 (45 males, 30 females, 14 juveniles) were newly collected specimens with genomic DNA preserved in the VTEC.

Due to the loss of the holotype and type material of *A. corticarius*, a male individual collected at the presumed type locality in Yellow Sulfur Springs was designated as a neotype. This is listed below in the material examined section. Analysis of the somatic and gonopodal morphology resulted in the delimitation of *A. grubbsi* sp. n. as its own species, and revision of the genus is presented below in the Taxonomy section.

Andrognathus taxonomy

Order Platydesmida Cook, 1895
Family Andrognathidae Cope, 1869
Subfamily Andrognathinae Cope, 1869

Genus *Andrognathus* Cope, 1869

Type species. *Andrognathus corticarius* Cope, 1869: 182; Gardner 1975: 15, figs 1, 5–7; Hoffman 1999: 180; Shear and Marek 2009: 157, figs 1–10.

Other species included. *Andrognathus corticarius* Cope, 1869, *Andrognathus hoffmani* Shear & Marek, 2009, *Andrognathus grubbsi* sp. n.

Genus diagnosis. Adult *Andrognathus* differ from other andrognathid genera based on the following:

Exoskeleton: Adults with 45–70 rings. Individuals long (11 to 27 mm) and thin, less than one mm wide, with short paranota, not covering legs (as in *Brachycybe*). Color varies from cream to dark brown (Figure 1), with paranota lighter, not pink as in *Gosodesmus* Chamberlin, 1922, *Ischnocybe* Cook & Loomis, 1928, *Brachycybe*. Entire body pilose, particularly head and antennae. Head rounded, pear-shaped, nearly truncate, eyeless (Figure 4). Antennae enlarged apically, slightly elbowed at fourth antennomere (Figure 4). Gnathochilarium and labrum tightly appressed, mandibles not visible externally. Anterior margin of labrum smooth, with small depressed triangular area (Figs 4, 5A, B); without ramified cuticular papillae (as in *Brachycybe*). Paranota of ring five swept forward (anteriorly); distinctly bilobed in *corticarius* (Figure 2A). Paranotal caudolateral margins posterior to ring five sharply projecting caudally, unlike *Gosodesmus* where the paranotal margins are quadrate. Porosteles clearly differentiated, ozopores rimmed with peritrema, directed anteriorly on ring five (Figs 2, 5C), laterally on remaining rings. Telson: Hypoproct absent, preanal ring barrel-shaped (Figure 5D). Gonopods: Anterior gonopods rounded and robust; A6 spatulate (Figs 6–9) not with a distal series of thin ribbon-like styli, as in *Brachycybe*. Posterior gonopod long with P6 extended beyond A6, ending in a variable crown, which may be elongated, spatulate, or bifurcate (Figs 6–9) but never composed of a bundle of styli as in *Brachycybe*. P6 with medial spur-like process (possibly claw/tarsungulum). See also diagnosis of *Andrognathus* in Shear and Marek (2009).

Note. *Andrognathus* was placed in Andrognathinae (a monotypic subfamily) due to the lobed condition of the fifth pair of paranota (Hoffman, 1980).

Andrognathus corticarius Cope, 1869

Figs 1–4, 6–9, Tables 1, 2
Vernacular name: Cope's noodle millipede

Andrognathus corticarius Cope, 1869: 182; Gardner 1975: 15, figs 1, 5–7; Shear and Marek 2009: 157, figs 1–10. (There are no synonyms for *A. corticarius*.)

Type species. Original type material lost. Collected by Cope "from Montgomery County, Virginia".

Material examined. Neotype: Male neotype (VTEC, MPE01942); 1 male from Virginia, Montgomery County, Christiansburg, Yellow Sulfur Springs Spa (37.1796, -80.3979, Elev. 607m), 30 June 2016 (Colls: P. Shorter, J. Means, V. Wong). Head and posterior body rings preserved as voucher. Collected on a hardwood log on a footpath between the old hotel gardens and an abandoned bowling alley.

Other material examined: 3 males, 3 females, details as for neotype; 109 males, 113 females, and 52 juveniles were examined from Virginia and nine other states (West Virginia, Tennessee, North Carolina, Florida, South Carolina, Alabama, Georgia, Ohio, and Kentucky), details in Suppl. material 1.
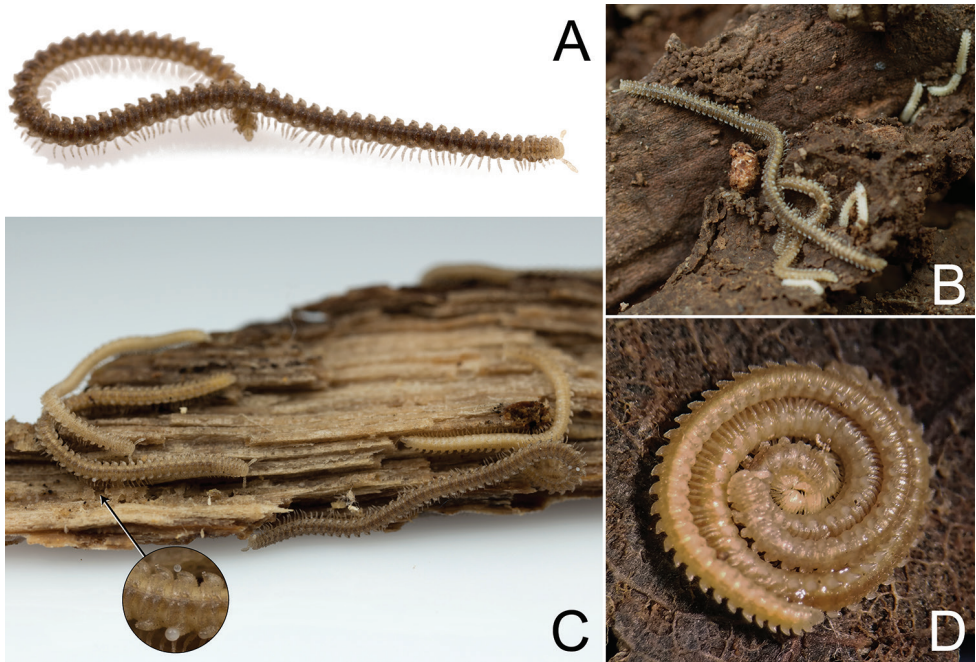
Figure 1. *Andrognathus corticarius* Cope, 1869 from Stadium Woods, Montgomery County, Virginia (**A–C**) Pulaski County, Virginia (**D**). **A** Adult male, dorsolateral view, approximate length 24 mm (VTEC catalog #MPE01962) **B** Adults and juveniles *in situ*. Aggregated individuals were found inside a decaying hardwood log **C** Adult aggregation. Inset shows the chemical secretions on the ozopores on the bottom left and bottom right individuals **D** Male and female coiled around eggs.

We here designate a neotype for *A. corticarius* because the holotype or syntypes have not been located and are presumed lost (see Material and methods section), and because our morphological studies indicate that "*A. corticarius*" may represent more than one species. To provide a basis for taxonomy of the group we have selected a specimen from the type locality which agrees in all details with the description given by Cope (1869).

Diagnosis. Adult males of *A. corticarius* are distinct from other *Andrognathus* species based on the following combination of characters: Exoskeleton. Ring five with pleuroterga distinctly bilobed, papilioform (Figure 2A); lobe of anterior corner flared anteriorly, lobe of posterior corner bulging laterally, contrasting with the reduced lobes of *A. hoffmani* and *A. grubbsi* sp. n. Ring VI with metaterga singly lobed, with angulate paranota bearing a posterolaterally oriented ozopore, separating *A. corticarius* from *A. hoffmani* and *A. grubbsi* sp. n. in which the paranota are rounded and bear a laterally oriented ozopore (Figure 2). Paranota becoming progressively more directed posteriorly along subsequent body rings. Posterior gonopod with P6 terminating in a distally flared calyx, tip with many small serrations (Figs 6–8, Figure 9A), not spatulate as in *A. hoffmani* (Figure 9B) and *A. grubbsi* sp. n. (Figure 9C). Claw (ungulum) of P6 present, thorn-shaped, varying in size; claw not perpendicular to the shaft of the gonopod as in *A. grubbsi* sp. n.
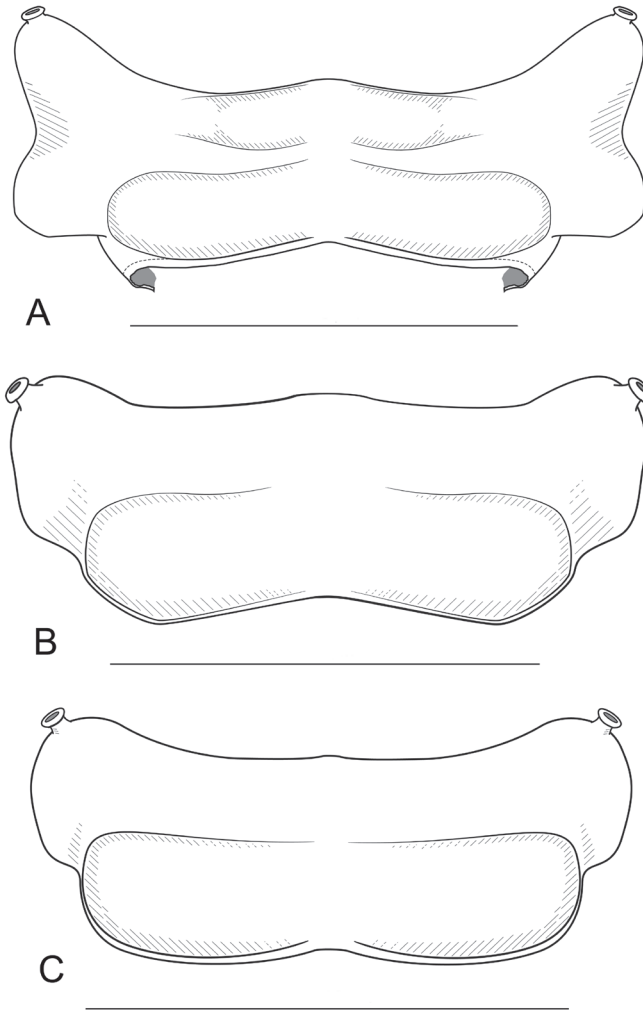
Figure 2. *Andrognathus* ring 5, dorsal view. **A** *Andrognathus corticarius* **B** *Andrognathus hoffmani* **C** *Andrognathus grubbsi* sp. n. Scale bars: 0.5 mm (**A, C**); 0.4 mm (**B**).

Neotype details. Body length (BL) = 17.9 mm, head width (HW) = 0.46 mm, collum width (CW) = 0.61 mm, metazonite width at 1/4 length of body (W1) = 0.81 mm, number of podous tergites (p) = 57, number of legs (l) = 210. NCBI accession # MH282831.

Variation. *Andrognathus corticarius* is known from the panhandle of Florida, north into southern Indiana and Pennsylvania (Figure 3). Variation in somatic characters of males and females is given in Table 1, and variation in gonopodal characters in Table 2. The morphology of the A6 and P6 podomeres and the claw of the P6 of the male gonopods of *A. corticarius* differed most across the distribution of the species (Table 2).

Table 1. Measurements (in mm) Anatomical details for *A. corticarius* individuals from the edges of the geographic distribution, and for the neotype (*). Cells with a hyphen (-) indicate specimens lacking the feature due to destruction for genetic analysis. ([†]) Ring count does not include the two apodous rings (a) and the telson (T).

Code	State	Sex	Ring Count[†]	Leg Count	BL	HW	CW	W1
MPE01991	OH	M	–	–	–	0.4	0.5	0.6
MPE01942*	VA	M	57	210	17.9	0.5	0.6	0.8
AND0024	VA	M	34	118	8.2	0.4	0.5	0.8
AND0001	NC	M	45	162	13	0.4	0.6	0.8
AND0031	AL	M	34	118	6.3	0.4	0.5	0.7
AND0038	FL	M	35	122	8.2	0.4	0.6	0.7
MPE01986	OH	F	–	–	–	0.4	0.6	0.8
AND0049	VA	F	41	146	9.5	0.4	0.6	0.8
AND0006	NC	F	43	154	9.8	0.4	0.6	0.8
AND0028	AL	F	55	202	15.9	0.4	0.6	0.8
AND0003	FL	F	51	186	13.8	0.5	0.6	0.8

Table 2. Variable gonopodal characters in *A. corticarius*. Neotype (*).

	A6 Ribbed	A6 Spatulate smooth curve	A6 Ribbed, scalloped edges	A6 Medial bifurcate hook	P6 claw Toothlike hook	P6 claw Bulbous, Rounded	P6 claw Pinched	P6 claw Bulbous, Rounded tooth lacking	P6 claw Bifurcate	Apex of P6 Singular fringed crown	Apex of P6 Bifurcate	Apex of P6 Bifurcate branched
MPE01998	+				+					+		
MPE01804		+					+		+			
MPE01942*		+			+					+		
MPE02169		+			+					+		
MPE01431		+					+		+			
AND043		+					+			+		
MPE01966			+		+					+		
AND040		+						+	+			
AND041		+						+	+			
AND039				+				+				+
AND005		+			+					+		
AND038		+							+		+	

Four individuals from the subset of geographically widespread samples differed from the neotype in two of these three characters of the male gonopods (Figs 6B, 7A, 8A, 8D); a male from Chesterfield County, South Carolina, deviates from the neotype in all three of these characters (Figure 8B).
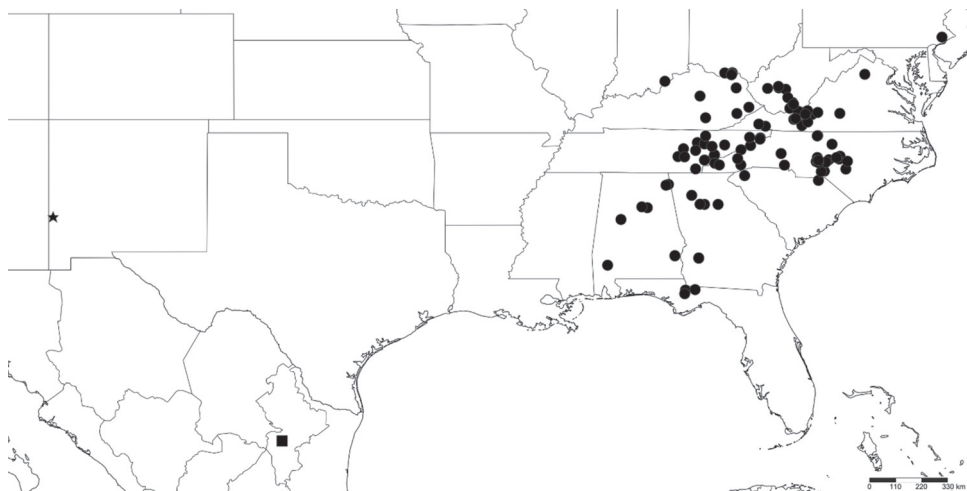
Figure 3. Distribution map of *Andrognathus*. Dots: *Andrognathus corticarius*, square: *Andrognathus hoffmani*, star: *Andrognathus grubbsi* sp. n. The species *A. corticarius* is reported from Ohio and Pennsylvania for the first time, and the genus is reported from New Mexico for the first time.

Figure 4. *Andrognathus corticarius* head and anterior body rings, ventral view. Scale bar: 0.3 mm.

Genetic analysis. Genetic analysis using the COI region showed relatively low variation within eastern *A. corticarius* (mean pairwise distance = 0.16%). The aligned COI sequences were length invariant, trivial to align, and resulted in a matrix of 605 DNA base-pairs for 14 individuals. Individuals from Boone County, West Virginia and Scioto County, Ohio had a maximum pairwise distance of 0.99% (605 bp). The maximum pairwise distances between individuals from the same locality in Montgomery Co., Virginia, was 0.17% (605 bp).

Distribution and ecology. *Andrognathus corticarius* is now known from Indiana, Ohio, Pennsylvania, Kentucky, West Virginia, Virginia, Tennessee, North Carolina, South Carolina, Georgia, Alabama, and Florida (Figure 3). The map assembled here extended the known range of *A. corticarius* northward into southwestern Ohio and southeastern Pennsylvania and synthesized and expanded distributions from the literature (Figure 3). Based on the collection dates of museum specimens, the activity period of the species appears to span March – November, with the greatest number of specimens encountered mid-summer. Individuals are often found clinging to the underside of logs in mesic deciduous forests in aggregations of millipedes, including juveniles (Figure 1B). *Andrognathus corticarius* is found from elevations of 51 m to 1160 m, and infrequently as lone adults in leaf litter and in drier habitats (Figure 10).

After some specimens of *A. corticarius* were collected in Pulaski Co., Virginia in 2016, a male and female were observed to be coiled together at the bottom of their container (Figure 1D). Upon closer inspection, the female was coiled around a cluster of eggs, with the male on top of her. The millipedes stayed in this configuration even when removed from their container and examined for approximately 20 minutes. This is a previously unobserved behavior in the genus, which was not known to demonstrate parental care.

Andrognathus grubbsi sp. n.
http://zoobank.org/DCD92723-2649-41F6-89EB-41868CF48B99
Figs 2, 5, 9, 11
Vernacular Name: The Spaghetti Western millipede

Material examined. Male holotype (VTEC, AND0044), 1 female paratype (VTEC, AND0051), 1 female paratype (VMNH, AND0045) from New Mexico, Catron Co., Gila National Forest, "near Glenwood", 33.3254, -108.8847, uncertainty: 5000 m, August 1980 (collector: A. G. Grubbs).

Diagnosis. Distinct from other members of the genus by the following: anterior lobe of pleurotergite V flared anteriorly (Figs 2C, 5C), but not distinctly bilobed, papilioform as in *A. corticarius* (Figure 2A). Apex of the P6 process bifurcate, each process flanged (Figure 9C), not a calyx as in *A. corticarius* (Figs 6–8, 9A). Distal process spatulate, bent at a 90° angle, covering the proximal process in a roof-like configuration (Figure 9C), contrasting with the upright, parallel processes of *A. hoffmani* (Figure 9B). Claw of the gonopod small, not large as in *A. corticarius* and *A. hoffmani*.
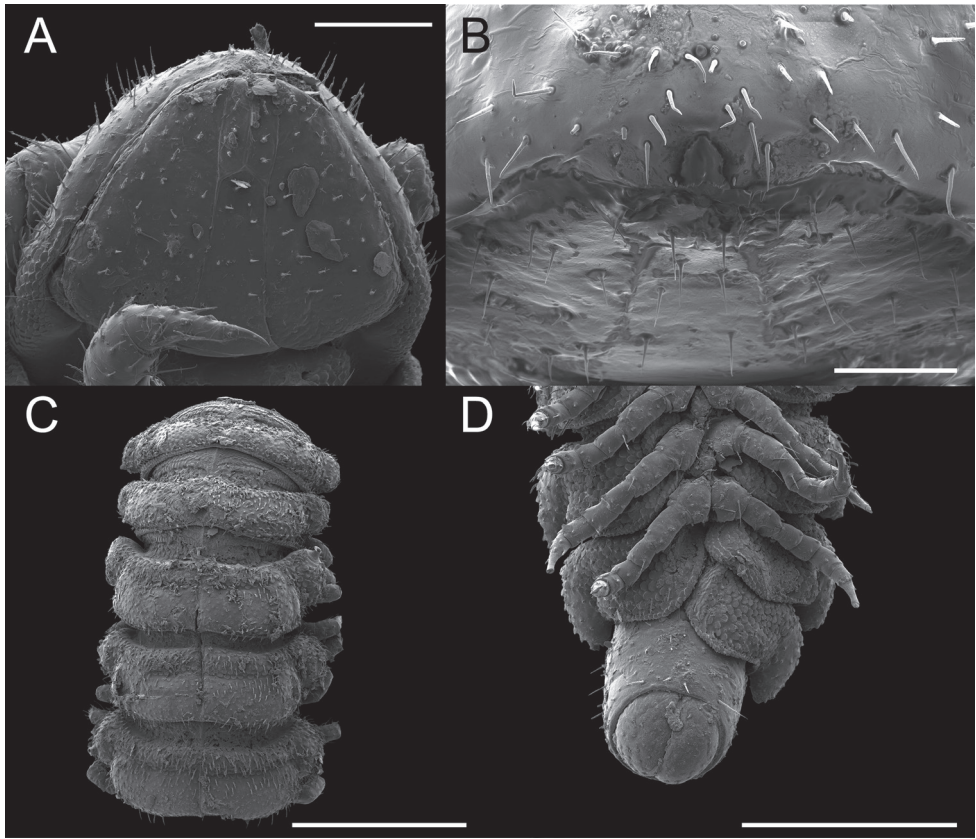
Figure 5. *Andrognathus grubbsi* sp. n., female paratype, (VTEC Catalog #AND0045). **A** Head, ventral view **B** Tip of labrum **C** Dorsal view of rings 3–7 **D** Posterior body rings, ventral view. Scale bars: 0.1 mm (**A**), 0.05 mm (**B**), 0.5 mm (**C**), 0.4 mm (**D**).

Description of male holotype. Counts and measurements: number of podous tergites (p) = 45. Number of apodous tergites (a) = 2. Number of legs (l) = 170. (45 + 2 + T). Body length (BL) = 12.8 mm. Head width (HW) = 0.39 mm. Interantennal socket width (ISW) = 0.19 mm. Antennomere 6 width (AW) = 0.10 mm. Collum width (CW) = 0.45 mm. Metazonite width at 1/4 length of body (W1) = 0.69 mm. Metazonite length at 1/4 length of body (L1) = 0.23 mm. Metazonite height at 1/4 length of body (H1) = 0.45 mm. **Body:** With characters from the genus diagnosis. Body with 47 rings, faded yellow in color due to long-term storage in ethanol. **Head:** Pilose, pear shaped, anteriorly narrowed toward mouth. Eyeless. Antennae extending back to second body ring, relative antennomere lengths 6>2>5>3>4>7>1. Antennomeres short and globular, with obvious ~90° bend at fourth antennomere (Figure 11B). Head evident viewed dorsally, collum not covering head, anterior and posterior margins slightly sinuate medially. **Exoskeleton:** Prozonites and metazonites of rings 2–4 distinct in appearance; paranota arising from anterior portion of ring and lacking ozopores (Figure 5C). Fifth ring noticeably elongated, metazonite bearing a distinct lateral and posterior ridge, and transverse groove (Figure 5C). Paranota of the fifth ring lobed, lacking bifurcation and posterior
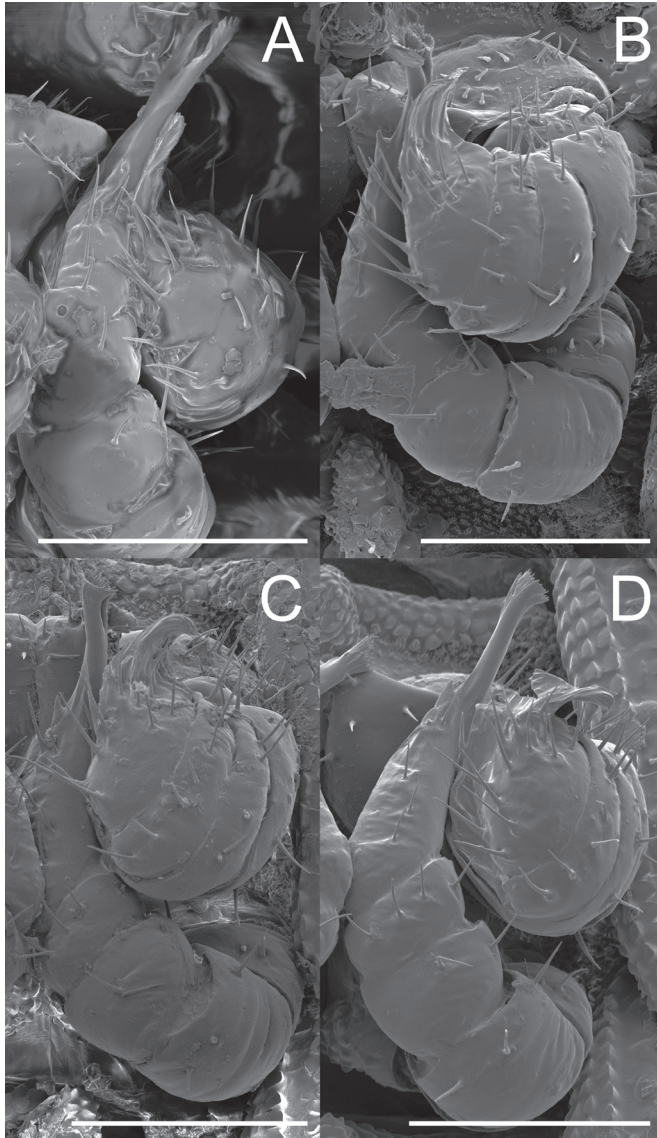
Figure 6. Gonopod variation within *Andrognathus corticarius*, ventral view, left gonopods. **A** Scioto Co., Ohio (view of the mirrored right gonopod, due to damage to the left gonopod) **B** Raleigh Co., West Virginia **C** Neotype, Montgomery Co., Virginia (Christiansburg) **D** Montgomery Co., Virginia (Blacksburg). Scale bars: 0.1 mm.

placement (Figs 2C, 5C). Ozopores beginning on the fifth ring, oriented anterolaterally; on following rings oriented posterolaterally. Porosteles elongated, (in contrast to short porosteles of other members of the genus), with a doughnut-like rim (Figure 11C). Ring VI and other ozoporiferous rings subequal in length, paranota directed laterally, peritremata directed posterolaterally. Posterior-most paranota and peritremata gradually shifting in orientation; directed posteriorly, with sharp caudolateral corners. Prozonites
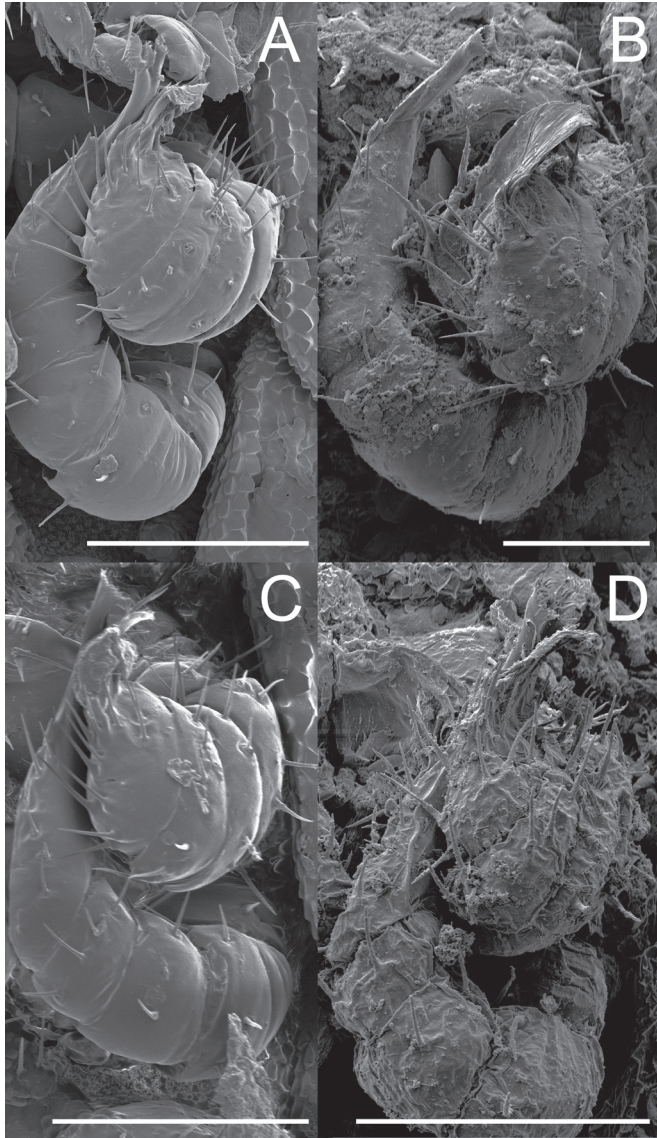
Figure 7. Gonopod variation within *Andrognathus corticarius*, ventral view, left gonopods. **A** Pulaski Co., Virginia **B** Campbell Co., Virginia **C** Carroll Co., Virginia **D** Madison Co., North Carolina. Scale bars: 0.1 mm (**A, C, D**), 0.05 mm (**B**).

lacking setae, covered with minute disc-like tubercles (Figs 5C, 11A). Metazonites se-tose, with fewer tubercles limited to median transverse groove and anterior portion of paranota. Metazonal limbus lined with uniform rectangular tabs (Figs 5C, 11A). Pleu-rites covered with disc-like tubercles and setae, pleurites of apodous rings overlapping (Figure 5D). Sternites with bulbous median knob with a few setae and raised tubercles (Figure 11A). *Legs:* Podomeres of walking legs bearing long setae. Coxa globular, with medial excavation, anterior face with raised tubercles. Coxae contiguous anteromedially
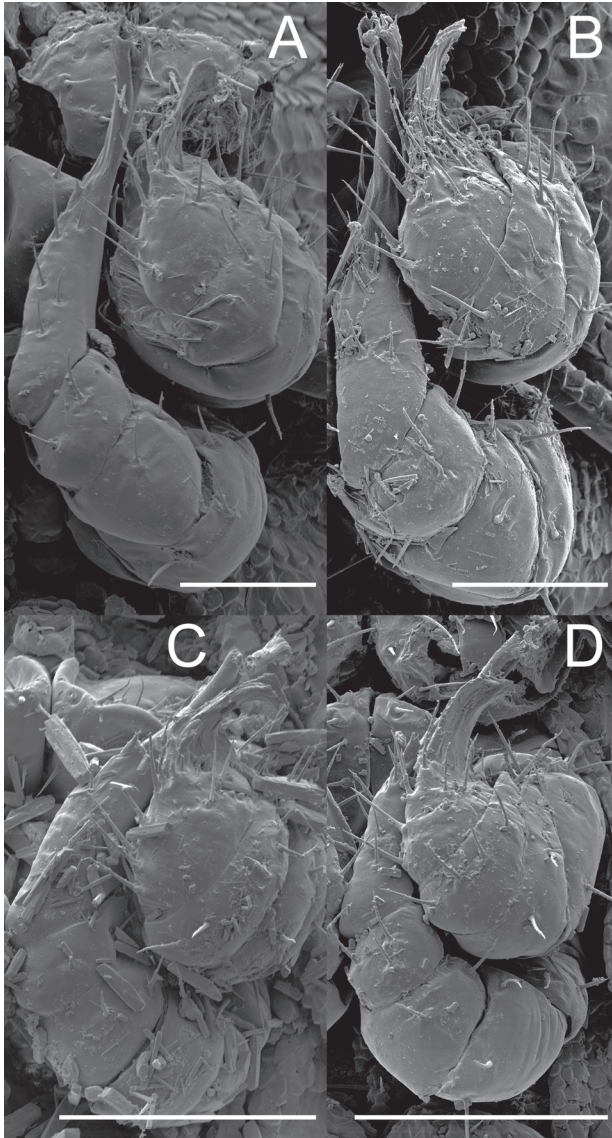
Figure 8. Gonopod variation within *Andrognathus corticarius*, ventral view, left gonopods. **A** Lee Co., North Carolina **B** Chesterfield Co., South Carolina **C** DeKalb Co., Alabama **D** Liberty Co., Florida. Scale bars: 0.05 mm (**A, B**), 0. 1 mm (**C, D**).

(Figure 11A). Trochanters thin, other podomeres rectangular with slight widening at apex. Prefemur longest podomere, following podomeres subequal. Tarsal claw simple, slightly curved (Figure 11A). Single comb row of stout setae on anteromedian edge of leg pairs one through three. ***Gonopods:*** Ninth and tenth leg pairs modified into simple leg-like gonopods (Figure 9C). Anterior gonopod with stout coxae (A1) bearing medium triangular coxal apophyses that project anteriorly (Figure 9C). Subsequent podomeres (A3 – A6) wider than long. Sixth podomere (A6) spade-shaped, medially
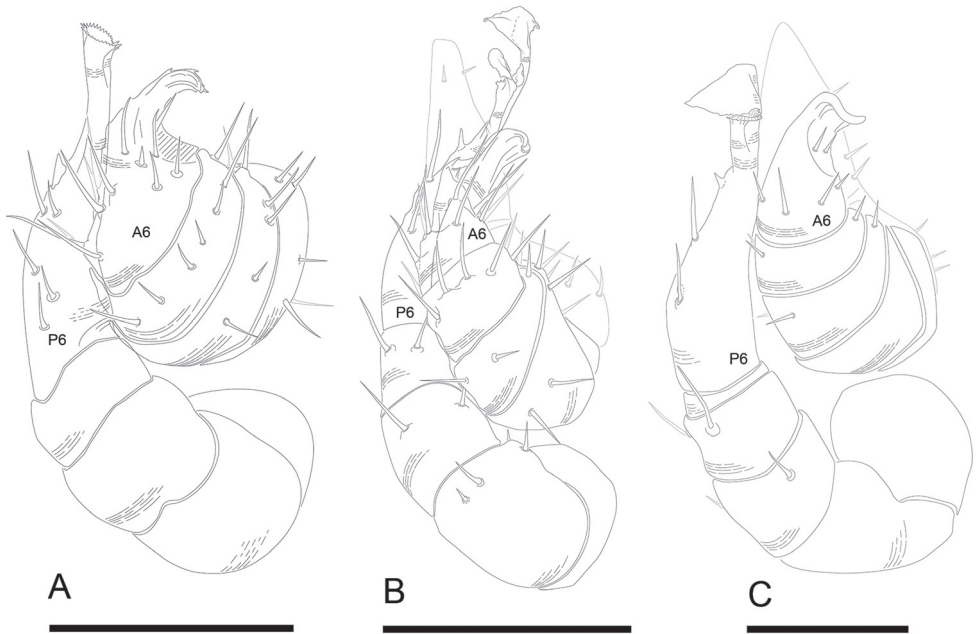
Figure 9. *Andrognathus* gonopods, ventral view of left gonopods. **A** *Andrognathus corticarius* (podomeres A1, A2 missing) **B** *Andrognathus hoffmani* **C** *Andrognathus grubbsi* sp. n. A6: anterior gonopod podomere 6. P6: posterior gonopod podomere 6. Scale bars: 0.1 mm(**A, B**), 0.05 mm (**C**).

spatulate, with setae (Figure 9C). Posterior gonopod narrower than anterior (Figure 6C). Coxae and second podomeres (P1, P2) stout, slightly wider than long. Subsequent podomeres (P3 – P5) tapering to an elongated P6 that meets the apex of the anterior gonopods. Claw (ungulus) of P6 a stout isosceles triangle on medial side (Figure 9C). P6 bifurcate distally, with two processes (Figure 9C). Proximal process flange-like, projecting upward. Distal process spatulate, twisting over the proximal process at a 90° angle (Figure 9C). Color: Faded yellow after being stored in alcohol for 37 years.

Paratypes. (female) AND051 and AND0045. Counts and measurements: p = 53 and 57, a = 2, l = 194 and 210, BL = 19.40 mm and 17.00 mm, CW = missing and 0.46 mm, W1 = 0.83 mm and 0.90 mm. Somatic characters similar to holotype.

Etymology. This species is named for its collector, cave biologist Andy Grubbs. While not a myriapodologist, his collecting philosophy was that someday there would be someone interested in the specimens that he collected. Now, almost 40 years later, that philosophy has been vindicated. The specific name is a genitive noun derived from his surname.

Distribution and ecology. *Andrognathus grubbsi* sp. n. is known only from the type locality in "Glenwood, New Mexico". The exact location is unknown; however, proximity of Glenwood to the U.S. Forest Service Bighorn Campground in Gila National Forest suggests that the specimens may have been collected there. The campground site is situated in the Arizona/New Mexico Mountains ecoregion (Level III), likely in the Madrean Lower Montane Woodlands (Level IV) (Omernik 1987). The
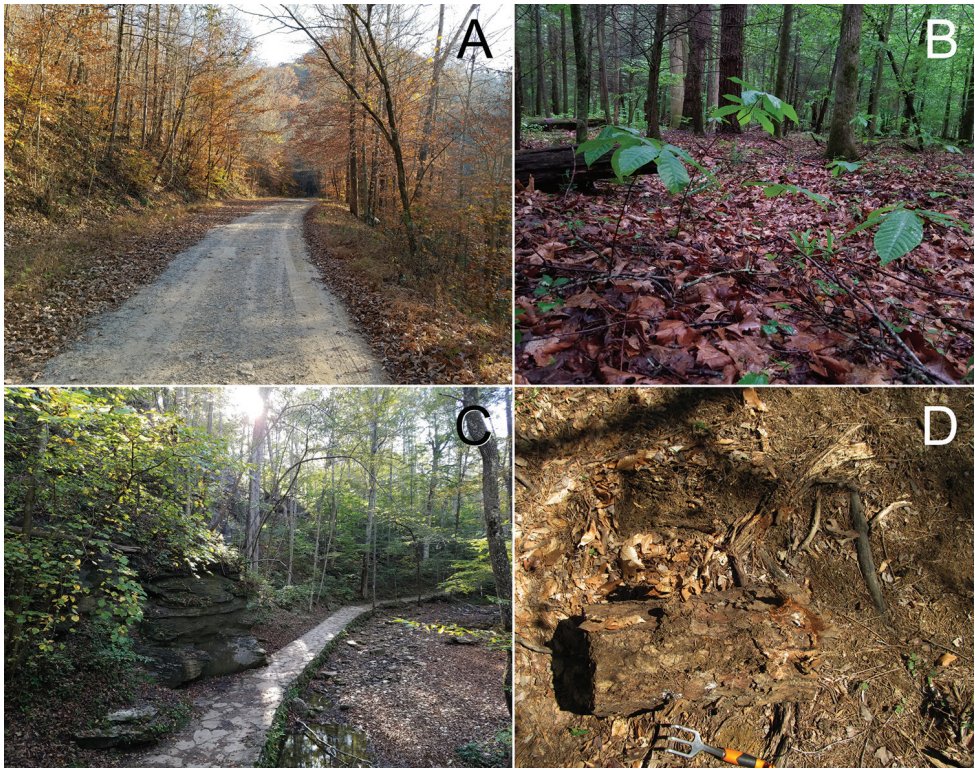
Figure 10. *Andrognathus corticarius* habitat. **A** Boone County, West Virginia **B** Morgan County, Tennessee **C** Carter County, Kentucky **D** Montgomery County, Virginia.
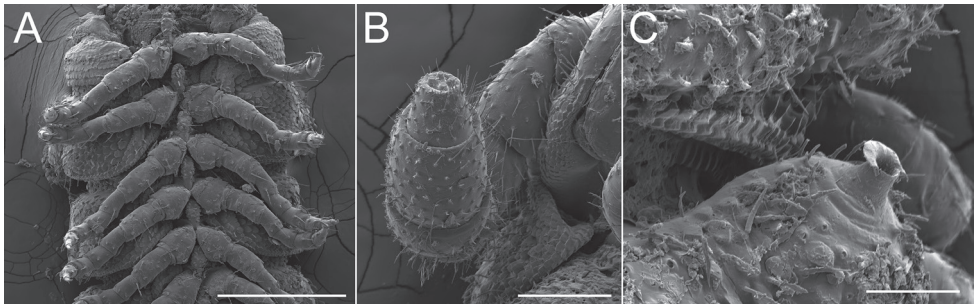

Figure 11. Somatic characters of *Andrognathus grubbsi* sp. n. (catalog # AND0045). **A** Mid-body rings, ventral view **B** Distal antennomeres, ventral view **C** Ozopore of ring five, dorsal view. Scale bars: 0.3 mm (**A**), 0.1 mm (**B**), 0.05 mm (**C**).

dominant vegetation in the area is composed of pinyon pines and juniper trees (Gila National Forest 2018). This type locality is considerably separated from other known *Andrognathus* localities. *Andrognathus hoffmani* in Mexico is ca. 1270 km southeast of the specimens from New Mexico, and *A. corticarius* in Alabama, the westernmost record for the species, is ca. 1990 km southeast.

Discussion

The genus *Andrognathus* currently comprises three species: *A. corticarius*, *A. hoffmani*, and *A. grubbsi* sp. n. *Andrognathus grubbsi* sp. n. falls unambiguously within the genus (based on the modified fifth ring), but is geographically and morphologically distinct from its congeners. The possibility that there are cryptic species within *A. corticarius* was first suggested based on a limited sample of individuals, and without molecular phylogenetic data (Shear and Marek 2009). Our investigation with scanning electron microscopy within a geographical context inferred with a larger sample of natural history specimens has provided evidence that *A. corticarius* may encompass several distinct species. We base this hypothesis on our observations of gonopod variation across the distribution of *A. corticarius* (Figs 6–8). Northern and eastern individuals tend to vary little from the type, and differentiation appears to be more substantial further south. The claw of P6 tends to become more complex in the southern part of the range: appearing either bifurcate or bulbous. The apex is also bifurcate in many of the southern individuals. The exception to this trend is an individual (AND0039) from South Carolina (Figure 8B), which is an outlier to distributional trends and is highly divergent morphologically from the type. This anatomical variation in *A. corticarius* gonopods across its wide distribution in the eastern U.S. is noteworthy when compared to the many millipede species with large distributions and conserved gonopod shape. For example, *Pleuroloma flavipes* Rafinesque, 1820 and *Gyalostethus monticolens* (Chamberlin, 1951) (Polydesmida: Xystodesmidae) both have gonopods that vary only slightly across their > 3 million km^2 and > 300,000 km^2 geographical distributions (Hoffman 1960, 1965, Shelley 1980). The confamilial species *Brachycybe lecontii* (Wood, 1864) possesses no readily apparent gonopodal differences across its distribution (> 450,000 km^2) in the eastern U.S. (Brewer et al. 2012), a distribution which is largely congruent with that of *A. corticarius*. However, in *B. lecontii* distinct genetic differences are observed in nuclear (192fin gene region) and mitochondrial (COI) DNA that indicates that at least four geographically separated and non-overlapping clades exist (Brewer et al. 2012). In contrast, in *A. corticarius*, we found the opposite and observed noticeable gonopodal differences between geographically widespread populations and yet a paucity of genetic differences in our COI data. Due to a lack of congruence between our morphological and genetic datasets, and lack of geographical consistency in gonopodal shape variation, we refrain from formally naming these distinct populations as species. In future investigations of species boundaries in *A. corticarius*, an integrative approach implementing additional genetic loci, ecological niche data, and a detailed analysis of gonopod morphology should be used.

It is uncertain if populations of *A. corticarius* vary in other gene loci along its distribution. Though it is uncommon for the COI gene region to be nearly invariant, similar results have been seen in other dispersal-limited invertebrate taxa. This low genetic variation across geographically separated populations is surprising given expectations of rapid evolution in animal mitochondrial loci due to the haploid nature of COI and its maternal mode of inheritance (Ladoukakis and Zouros 2017). In a study of the har-

vestman genus *Acuclavella* Shear, 1986, sampling of five widely-separated species in the Pacific Northwest and COI sequencing indicated a lower than expected within-species nucleotide variation (Richart and Hedin 2013) similar to our COI variation in *A. corticarius*. In future work, other genes should be targeted and utilized in analyzing *A. corticarius* evolution to investigate genetic differences between localities and to reconcile differing gene histories that may be more informative than just a single genealogy.

By assembling an updated distribution map of *Andrognathus*, we have shown that the genus occurs in the eastern U.S. (in the Appalachian Mountains and Coastal Plain), and in two isolated locations in Glenwood, New Mexico and Cerro el Potosi, Mexico. Other millipede taxa with a similar distribution are *Rhysodesmus* Cook, 1895, which has two species in the eastern U.S. and nearly 70 known in Texas and Mexico (Marek et al. 2014). Similar distributions occur in the fern species *Pellaea wrightiana* Hooker, 1858 (http://efloras.org/object_page.aspx?object_id=5145&flora_id=1; accessed July 30, 2018) and *Asplenium septentrionale* (Linneaus, 1758) (http://efloras.org/object_page.aspx?object_id=5187&flora_id=1; accessed July 30, 2018) The mountains of southern New Mexico and Texas, and the Sierra Madre in Mexico likely hold additional millipede taxa. Searching these locations for additional species of *Andrognathus* would be fruitful in understanding diversity of the genus and evolution of the taxon.

Andrognathus species occur in mesic forested habitats at mid-elevations (51–1523 m a.s.l.). As global warming affects the distribution of species and causes aridification of habitats, *Andrognathus* millipedes may face a limited set of options. These invertebrates may shift to higher elevations or north facing slopes to avoid desiccation. By understanding the alpha-taxonomy and distribution of these dispersal limited mesic-adapted species today, conservation specialists will have the baseline data relevant to the conservation needs of these arthropods, and relatives.

References

Attems C (1951) Revision systématique des Colobognatha (Myriapodes Diplopodes) et description d'espèces nouvelles. Mémoires du Muséum national d'Histoire naturelle, Paris (n.s. A) 3: 193–231.

Brewer MS, Spruill CL, Rao NS, Bond JE (2012) Phylogenetics of the millipede genus *Brachycybe* Wood, 1864 (Diplopoda: Platydesmida: Andrognathidae): Patterns of deep evolutionary history and recent speciation. Molecular Phylogenetics and Evolution 64: 232–242. https://doi.org/10.1016/j.ympev.2012.04.003

BugGuide.net (2016) BugGuide.net: Identification, Images, & Information for Insects, Spiders & their Kin for the United States & Canada. http://bugguide.net/node/view/1136695

Cook OF, Loomis HF (1928) Millipeds of the order Colobognatha with descriptions of six new genera and type species, from Arizona and California. Proceedings of the U.S. National Museum 72(18): 1–28. https://doi.org/10.5479/si.00963801.72-2714.1

Cope ED (1869) Synopsis of the extinct Mammalia of the cave formations in the United States, with observations on some Myriapoda found in and near the same, and on some extinct mammals of the caves of Anguilla, WI, and of other localities. Proceedings of the American Philosophical Society 11(81): 147–192. http://biodiversitylibrary.org/page/31205032

Enghoff H, Dohle W, Blower JG (1993) Anamorphosis in millipedes (Diplopoda)– the present state of knowledge with some developmental and phylogenetic considerations. Zoological Journal of the Linnean Society 109(2): 103–234. https://doi.org/10.1111/j.1096-3642.1993.tb00305.x

Enghoff H, Golovatch S, Short M, Stoev P, Wesener T (2015) Diplopoda–taxonomic overview. In: Minelli A (Ed.) Treatise on Zoology – Anatomy, Taxonomy, Biology. The Myriapoda 2. Brill, Leiden, 363–454. https://doi.org/10.1163/9789004188273_017

Ewing B, Hillier L, Wendl MC, Green P (1998) Base-calling of automated sequencer traces using Phred. I. Accuracy assessment. Genome Research 8: 175-185. http://doi.org/10.1101/gr.8.3.175

Folmer O, Black M, Hoeh W, Lutz R, Vrijenhoek R (1994) DNA primers for amplification of mitochondrial cytochrome c oxidase subunit I from diverse metazoan invertebrates. Molecular Marine Biology and Biotechnology 3(5): 294–299. http://www.mbari.org/wp-content/uploads/2016/01/Folmer_94MMBB.pdf

Gardner MR (1975) Revision of the millipede family Andrognathidae in the Nearctic region. Memoirs of the Pacific Coast Entomological Society 5: 1–61.

Gila National Forest (2018) Gila National Forest, United States Department of Agriculture, Forest Service. https://www.fs.usda.gov/recarea/gila/recarea/?recid=1969 [29 April 2018]

Golovatch S, Evsyukov A, Reip HS (2015) Colobognatha millipedes in the Caucasus (Diplopoda: Polyzoniida, Platydesmida, Siphonocryptida). Zootaxa 3972(2): 250–266. https://doi.org/10.11646/zootaxa.3972.2.6.

Hebert PD, Cywinska A, Ball SL (2003) Biological identifications through DNA barcodes. Proceedings of the Royal Society of London B: Biological Sciences 270: 313–321. https://doi.org/10.1098/rspb.2002.2218

Hoffman RL (1960) Revision of the milliped genus *Cherokia* (Polydesmida: Xystodesmidae). Proceedings of the United States National Museum 112(3436): 227–264 https://doi.org/10.5479/si.00963801.112-3436.227

Hoffman RL (1965) Revision of the milliped genera *Boraria* and *Gyalostethus.* Proceedings of the United States National Museum 117: 305–347. https://doi.org/10.5479/si.00963801.117-3514.305

Hoffman RL (1980 [1979]) Classification of the Diplopoda. Muséum d'Histoire naturelle, Genève, 237 pp. [date of publication 3 June 1980]

Hoffman RL (1999) Checklist of millipeds of North and Middle America. Virginia Museum of Natural History Special Publications, Martinsville, 584 pp. https://www.fieldmuseum.org/sites/default/files/hoffman_checklist_1999.pdf

Ladoukakis ED, Zouros E (2017) Evolution and inheritance of animal mitochondrial DNA: rules and exceptions. Journal of Biological Research-Thessaloniki 24: 2. https://doi.org/10.1186/s40709-017-0060-4

Latzel R (1884) Note sur les Julides de la Belgique, suivie da la description d'une espèce nouvelle. Extrait des Comptes rendus de la Société Entomologique de Belgique. https://babel.hathitrust.org/cgi/pt?id=hvd.32044107192346.

Lewis JGE (1984) Notes on the biology of some common millipedes of the Gunung Mulu National Park, Sarawak, Borneo. Sarawak Museum Journal 33 (54): 179-185.

Maddison WP, Maddison DR (2010) Mesquite: a molecular system for evolutionary analysis. Version 2.74. http://mesquiteproject.org/

Marek PE, Shear WA, Bond JE (2012) A redescription of the leggiest animal, the millipede *Illacme plenipes* with notes on its natural history and biogeography (Diplopoda, Siphonophorida, Siphonorhinidae). ZooKeys 241: 77–112. https://doi.org/10.3897/zookeys.241.3831

Marek PE, Tanabe T, Sierwald P (2014) A species catalog of the millipede family Xystodesmidae (Diplopoda: Polydesmida). Virginia Museum of Natural History Publications 17: 1–117. ttp://www.vmnh.net/content/File/Research_and_Collections/VMNHSpecialPub17.pdf

MCZBase (2017) MCZBase: The Database of Zoological Collections, Museum of Comparative Biology-Harvard University. http://mczbase.mcz.harvard.edu/SpecimenSearch.cfm.

Means JC, Francis EA, Lane AA, Marek PE (2015) A general methodology for collecting and preserving xystodesmid and other large millipedes for biodiversity research. Biodiversity Data Journal 3(3): e5665. https://doi.org/10.3897/BDJ.3.e5665

Omernik JM (1987) Ecoregions of the conterminous United States. Annals of the Association of American Geographers 77: 118-125. https://doi.org/10.1111/j.1467-8306.1987.tb00149.x

Read HJ, Enghoff H (2009) The order Siphonophorida – A taxonomist's nightmare? Lessons from a Brazilian collection. Soil Organisms 81(3): 543–556. http://www.senckenberg.de/files/content/forschung/publikationen/soilorganisms/volume_81_3/22_read.pdf

Richart CH, Hedin M (2013) Three new species in the harvestmen genus *Acuclavella* (Opil-
    iones, Dyspnoi, Ischyropsalidoidea), including description of male *Acuclavella quattuor*
    Shear, 1986. ZooKeys 311: 19–68. https://doi.org/10.3897/zookeys.311.2920

Rios NE, Bart HL (2010) GEOLocate (Version 3.22)[computer software]. Tulane University
    Museum of Natural History, Belle Chasse, LA.

Rodriguez J, Jones TH, Sierwald P, Marek PE, Shear WA, Brewer MS, Kocot KM, Bond JE
    (2018) Step-wise evolution of complex chemical defenses in millipedes: a phylogenomic
    approach. Scientific Reports 8(1): 3209.

Shear WA, Marek PE (2009) *Andrognathus hoffmani*, n. sp., a second species in the genus
    and the first species of Andrognathidae from México (Diplopoda, Platydesmida, An-
    drognathidae). Festschrift in honor of Richard Hoffman, Memoirs of the Virginia Mu-
    seum of Natural History 16: 149–158. https://www.fieldmuseum.org/sites/default/files/
    shear%26marek_festschrift_2009.pdf

Shear WA (2015) The chemical defenses of millipedes (Diplopoda): biochemistry, physiology
    and ecology. Biochemical Systematics and Ecology 61: 78–117. https://doi.org/10.1016/j.
    bse.2015.04.033

Shelley RM (1978) Millipeds of the eastern Piedmont region of North Carolina, U.S.A. (Diplopo-
    da). Journal of Natural History 12: 27–79. https://doi.org/10.1080/00222937800770051a

Shelley RM (1980) Revision of the milliped genus *Pleuroloma* (Polydesmida: Xystodesmidae).
    Canadian Journal of Zoology 58: 129–168. https://doi.org/10.1139/z80-017

Shelley RM (2000) Annotated checklist of the millipeds of North Carolina (Arthropoda: Di-
    plopoda), with remarks on the genus *Sigmoria* Chamberlin (Polydesmida: Xystodesmidae).
    The Journal of the Elisha Mitchell Scientific Society 116(3): 177–205. https://dc.lib.unc.
    edu/cdm/singleitem/collection/jncas/id/3612/rec/2

Shorthouse DP (2010) SimpleMappr, an online tool to produce publication-quality point
    maps. http://www.simplemappr.net.

Supplementary material 1

Specimen catalog
Authors: Patricia L. Shorter, Derek A. Hennen, Paul E. Marek
Data type: specimens data

Link: https://doi.org/10.3897/zookeys.786.27631.suppl1

Supplementary material 2

Locality data

Authors: Patricia L. Shorter, Derek A. Hennen, Paul E. Marek

Data type: occurence

Copyright notice: This dataset is made available under the Open Database License (http://opendatacommons.org/licenses/odbl/1.0/). The Open Database License (ODbL) is a license agreement intended to allow users to freely share, modify, and use this Dataset while maintaining this same freedom for others, provided that the original source and author(s) are credited.

Link: https://doi.org/10.3897/zookeys.786.27631.suppl2

Supplementary material 3

Mean uncorrected pairwise distance matrix

Authors: Patricia L. Shorter, Derek A. Hennen, Paul E. Marek

Data type: statistical data

Copyright notice: This dataset is made available under the Open Database License (http://opendatacommons.org/licenses/odbl/1.0/). The Open Database License (ODbL) is a license agreement intended to allow users to freely share, modify, and use this Dataset while maintaining this same freedom for others, provided that the original source and author(s) are credited.

Link: https://doi.org/10.3897/zookeys.786.27631.suppl3

RESEARCH ARTICLE

A peer-reviewed open-access journal

ZooKeys

Launched to accelerate biodiversity research

Two new species of the millipede genus *Metonomastus* Attems, 1937 from the Balkan Peninsula (Diplopoda, Polydesmida, Paradoxosomatidae)

Dragan Antić[1,2], Boyan Vagalinski[3], Pavel Stoev[4,5], Sergei Golovatch[6]

1 *Institute of Zoology, University of Belgrade-Faculty of Biology, Studentski Trg 16, 11000 Belgrade, Serbia* **2** *Serbian Biospeleological Society, Trg Dositeja Obradovića 2, 21000 Novi Sad, Serbia* **3** *Institute of Biodiversity and Ecosystem Research at the Bulgarian Academy of Sciences, 2 Yurii Gagarin Street, 1113, Sofia, Bulgaria* **4** *National Museum of Natural History, Sofia, Tsar Osvoboditel Blvd. 1, Sofia 1000, Bulgaria* **5** *Pensoft Publishers, Sofia, Bulgaria* **6** *Institute for Problems of Ecology and Evolution, Russian Academy of Sciences, Leninsky pr. 33, Moscow 119071, Russia*

Corresponding author: *Dragan Antić* (dragan.antic@bio.bg.ac.rs)

Citation: Antić D, Vagalinski B, Stoev P, Golovatch S (2018) Two new species of the millipede genus *Metonomastus* Attems, 1937 from the Balkan Peninsula (Diplopoda, Polydesmida, Paradoxosomatidae). ZooKeys 786: 43–57. https://doi.org/10.3897/zookeys.786.28386

Abstract

In addition to the eleven previously known species of the Mediterranean genus *Metonomastus*, two more species are described: *M. petrovi* **sp. n.**, from the Rhodopi Mts. and Bunardzhik Hill in Bulgaria, and *M. radjai* **sp. n.**, from the island of Mljet in Croatia. The relationships between the congeners and their distributions are briefly discussed. All 13 species of the genus are keyed.

Keywords

Bulgaria, cave, Croatia, Dinarides, island, millipede, Rhodopes, taxonomy

Introduction

In the latest taxonomic survey of the genus *Metonomastus* Attems, 1937, Golovatch and Stoev (2004) recognized eleven species. Among these, only one species, *M. bosniensis* (Verhoeff, 1901), was considered dubious as it had been described from a single female (holo-

type) coming from within the distribution area of *M. albus* (Verhoeff, 1901), a fairly common and abundant congener. This Mediterranean genus includes only small-sized forms (< 10 mm long) ranging from the Apennine and Balkan peninsulas in the west to northwestern Anatolia in the east (Hoffman and Lohmander 1968; Golovatch and Stoev 2004).

The present paper is devoted to descriptions of two new species of *Metonomastus* found in the Rhodopi Mountains and Bunardzhik Hill in Bulgaria and the Dinaric island of Mljet in Croatia.

Material and methods

Preservation, dissecting, imaging, and terminology

Specimens preserved in 70% ethanol were examined with Nikon SMZ 745T and Zeiss Stemi 2000-C binocular stereo microscopes. All taxonomically important structures were dissected and mounted in glycerine as temporary microscopic preparations and observed with a Carl Zeiss Axioscope 40 and an Olympus BX51 light microscope. Pictures of legs were taken with a Canon PowerShot A80 digital camera connected to the Axioscope 40 microscope, and with an Olympus XC30 digital camera connected to the Olympus BX51 microscope. Line drawings of gonopods were made using tracing paper placed on a computer monitor showing pictures of those structures. Pictures of habitus structures were taken using a Nikon DS-Fi2 camera with a Nikon DS-L3 camera controller attached to a Nikon SMZ 1270 binocular stereo microscope, and with a Nikon Coolpix S3700 attached to one eyepiece of a Carl Zeiss Discovery.V8 binocular stereo microscope. Focal stacking was completed with Zerene Stacker software. Some relevant structures were investigated with JEOL JSM-6460LV (University Centre for Electron Microscopy, Department of Biology and Ecology, University of Novi Sad, Serbia) and JEOL JSM-5510 (Faculty of Chemistry, Sofia University) scanning electron microscopes.

Descriptions of the new taxa largely follow Golovatch and Stoev (2004), except for the gonopodal terms "tibiotarsus" and "prefemur" which are replaced by "solenophore" and "prefemorite", respectively.

The final images were processed with Adobe Photoshop CS6.

Abbreviations used to denote gonopodal structures are explained directly in figure captions.

Museum and collection acronyms

IZB   Institute of Zoology, University of Belgrade – Faculty of Biology, Belgrade, Serbia
NHMSC   Natural History Museum, Split, Croatia
NMNHS   National Museum of Natural History, Sofia, Bulgaria

Taxonomy

Genus *Metonomastus* Attems, 1937

Microdesmus Verhoeff, 1901: 223; preoccupied, replaced with *Metonomastus* by Attems (1937: 46)
Nannodesmus Chamberlin, 1943: 35; replacement name for *Microdesmus* Verhoeff, 1901; synonymized by Hoffman and Lohmander (1968: 72)
Microdesminus Strasser, 1960: 96; synonymized by Golovatch and Stoev (2004: 203)
Diagnosis. Small (< 10 mm long) moniliform polydesmoids with pale body and 19 segments in both sexes (Figs 1, 5). Metaterga mostly with 2–3 rows of setae; exceptions are *M. saetosus* (Strasser, 1960) and *M. bosniensis* (Verhoeff, 1901) (see below). Pleurosternal carinae poorly developed, present only on ring 2 or on rings 2–4. Antennae long, clavate; antennomeres 5 and 6 each with a group of bacilliform sensilla. In males, femora of pregonopodal legs enlarged, each usually with a small adenostyle. Gonopods directed anteriad, with a somewhat elongated and slender coxite (cx). Prefemorite (pf) densely setose, mostly elongated, at least equal in length to acropodite, the only exception is *M. albus* with a shorter prefemorite. Acropodite consisting of two or three, more or less well-developed branches. The two dominant branches are mostly solenomere (sl) and solenophore (sph); the exception is *M. petrovi* sp. n. with three acropodital branches, but with a completely reduced solenophore.

Included species

Metonomastus albus (Verhoeff, 1901)
M. bosniensis (Verhoeff, 1901)
M. capreae (Verhoeff, 1942)
M. hirtellus (Silvestri, 1903)
M. mariae (Strasser, 1965)
M. patrizii Manfredi, 1950
M. petrelensis Mauriès, Golovatch & Stoev, 1997

M. petrovi sp. n.
M. pomak Golovatch & Stoev, 2004
M. radjai sp. n.
M. romanus (Verhoeff, 1951)
M. saetosus (Strasser, 1960)
M. strasseri Hoffman & Lohmander, 1968

Metonomastus petrovi **sp. n.**
http://zoobank.org/ADAE2B3A-37D6-4EB0-B152-5CA394ED5518
Figs 1–4

Material examined. Holotype male (NMNHS), Bulgaria, Western Rhodopi Mts., Satovcha District, Cave Stapalkata, 650 m a.s.l., clay-guano, 17.VI.2006, B. Petrov & P. Stoev leg.

Paratypes. 2 males, 5 females (NMNHS), same data as holotype.

Additional material. 2 females, 1 juvenile (NMNHS), Bulgaria, Western Rhodopi Mts., Pazardzhik District, Peshtera town, Cave Snezhanka, 19.IV.2009, P. Beron leg.; 1 male, 1 female (NMNHS), Bulgaria, Plovdiv, Bunardzhik Hill, under decaying wood, 10.IV.2018, P. Mitov leg.

Etymology. The species is named after Boyan Petrov, a renowned Bulgarian mountaineer, a dear friend and colleague zoologist from the National Museum of Natural History, Sofia, who disappeared in Tibet in May 2018 during the ascent of his 11th eight-thousander, Shishapangma. Boyan was one of the collectors of this new species. Noun in genitive case.

Diagnosis. The new species belongs to the *Metonomastus* group of species with three acropodital branches, but clearly differs from both previously described species in this group, *M. strasseri* Hoffman & Lohmander, 1968, and *M. pomak* Golovatch & Stoev, 2004, by the presence of a strongly developed, beak-shaped solenomere, by the

Figure 1. *Metonomastus petrovi* sp. n., holotype ♂ **A** habitus, lateral view **B** anterior part of the body, lateral view **C** posterior part of the body, lateral view.
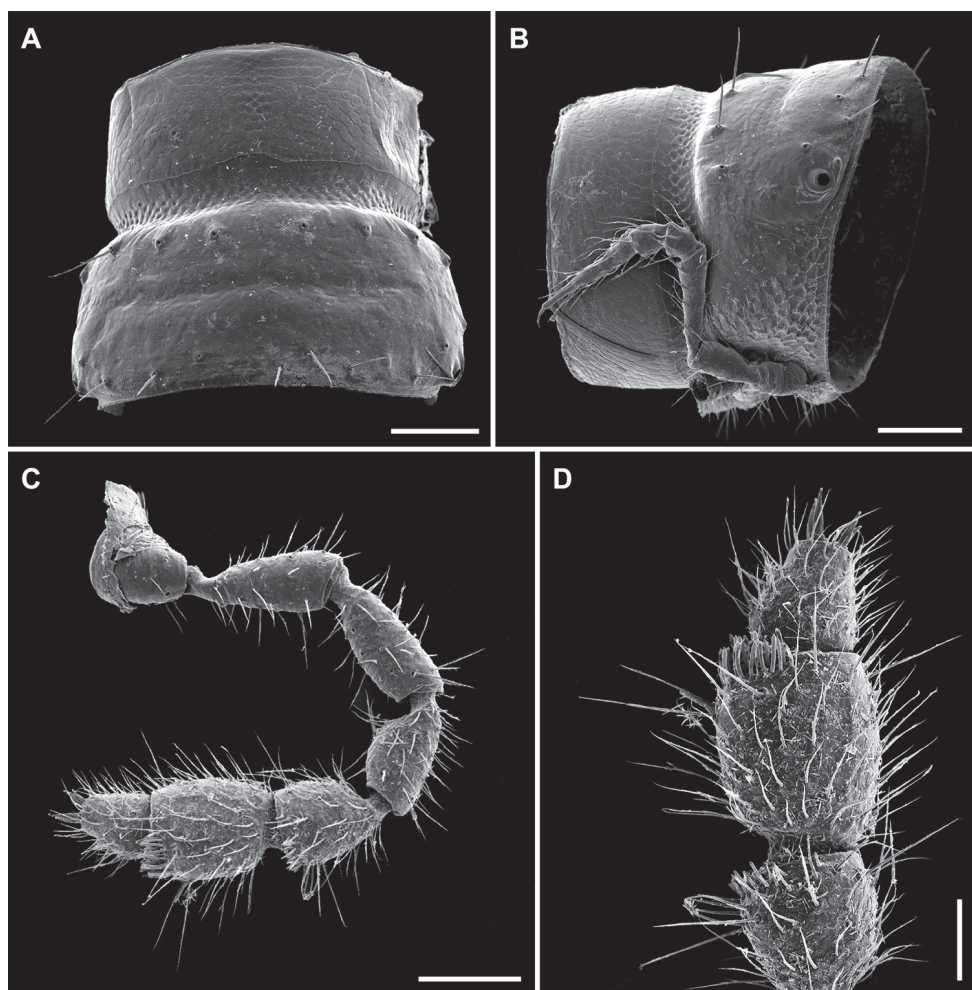
Figure 2. *Metonomastus petrovi* sp. n. **A** paratype ♀, ring 9, dorsal view **B** paratype ♀, ring 10, lateral view **C** paratype ♂, left antenna **D** paratype ♂, tip of left antenna. Scale bars: 0.1 mm (**A, B, C**), 0.05 mm (**D**).

completely reduced solenophore and by the development of a strongly arched, micro-spiculate, ventromesal, acropodital process.

Description. Length 4.4–4.8 mm (males), 4.2–5.5 mm (females). Width of mid-body rings 0.31–0.37 and 0.33–0.42 mm (males), 0.35–0.42 and 0.42–0.47 mm (females) on pro- and metazonae, respectively. Holotype male 4.8 mm long, 0.37 and 0.42 mm wide on midbody pro- and metazonae, respectively.

Body moniliform (Figure 1A), with 19 segments in both sexes. Colouration entirely pallid. Texture microreticulate throughout (Figure 2A, B).

Head densely pubescent throughout, clypeolabral region densely setose. In males, width of head (0.41–0.5 mm broad) >> collum ≤ ring 2 ≤ 3 ≥ 4 < 5 ≥ 6 = 17; thereafter
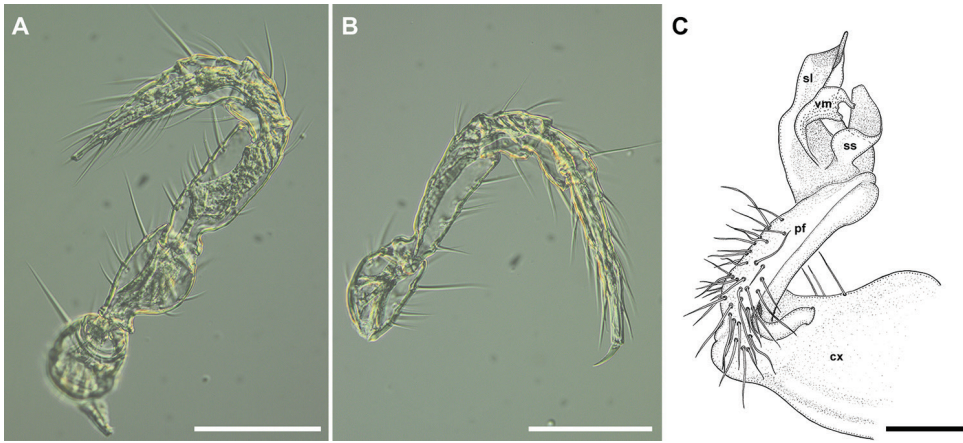
Figure 3. *Metonomastus petrovi* sp. n., paratype ♂ **A** leg 4 (claw fallen off) **B** leg 6 **C** right gonopod, mesal view. Abbreviations: **cx** coxite, **pf** prefemorite, **sl** solenomere, **ss** saddle-shaped process, **vm** ventromesal process. Scale bars: 0.1 mm (**A, B**), 0.05 mm (**C**).

body gradually, but significantly tapering. In females, width of head (0.42–0.5 mm broad) >> collum = ring 2 < 3 = 4 < 5 = 17; thereafter body rather rapidly tapering; in larger females, ring 5 = 14 < 15 = 17.

Antennae (Figure 2C, D) long, clavate, *in situ* reaching behind ring 2 when stretched dorsally. Antennomere length 2 = 3 = 6 > 4 = 5 = 7 > 1, 6th being the thickest, both 6th and 5th each with a compact group of bacilliform sensilla dorso-apically. Interantennal isthmus ca 0.7 times as broad as diameter of antennal socket.

Collum with 3 rows of setae; two rows of similar setae per postcollum metatergum: one frontally, the other caudally, setae long and simple. Metaterga (Figure 2A, B) with a weak, mid-dorsal, transverse sulcus on rings 5 to 17; sulcus absent from 18th. Paraterga (Figure 2A, B) laterally extremely poorly developed, being very faintly delimited by a shallow sulcus only dorsally. Certain midbody rings occasionally with visibly more or less strongly developed paranota compared to neighboring rings. Ozopores indistinct, located near posterior margin of paraterga; pore formula normal. Strictures between pro- and metazonae very faintly striolate, deep and narrow. Pleurosternal carinae present on ring 2 as small lobes, thereafter missing. Limbus faintly microcrenulate. Epiproct long, slender, nearly half as long as telson height. Hypoproct semi-circular, 1+1 strongly separated caudal setae borne on minute knobs. Sterna broad and weakly impressed.

Legs (Figure 2B) about 1.1–1.2 times as long as midbody height in males, 0.8–0.9 times in females, without modifications, only pregonopodal male prefemora slightly bulged dorsally (Figure 3A, B).

Gonopods (Figs 3C, 4): Coxite (cx) massive, moderately long, dorsolaterally very sparsely setose. Prefemorite (pf) somewhat longer than acropodite, densely setose ventrally. Postfemoral sulcus distinct, short, traceable on median and, partly,
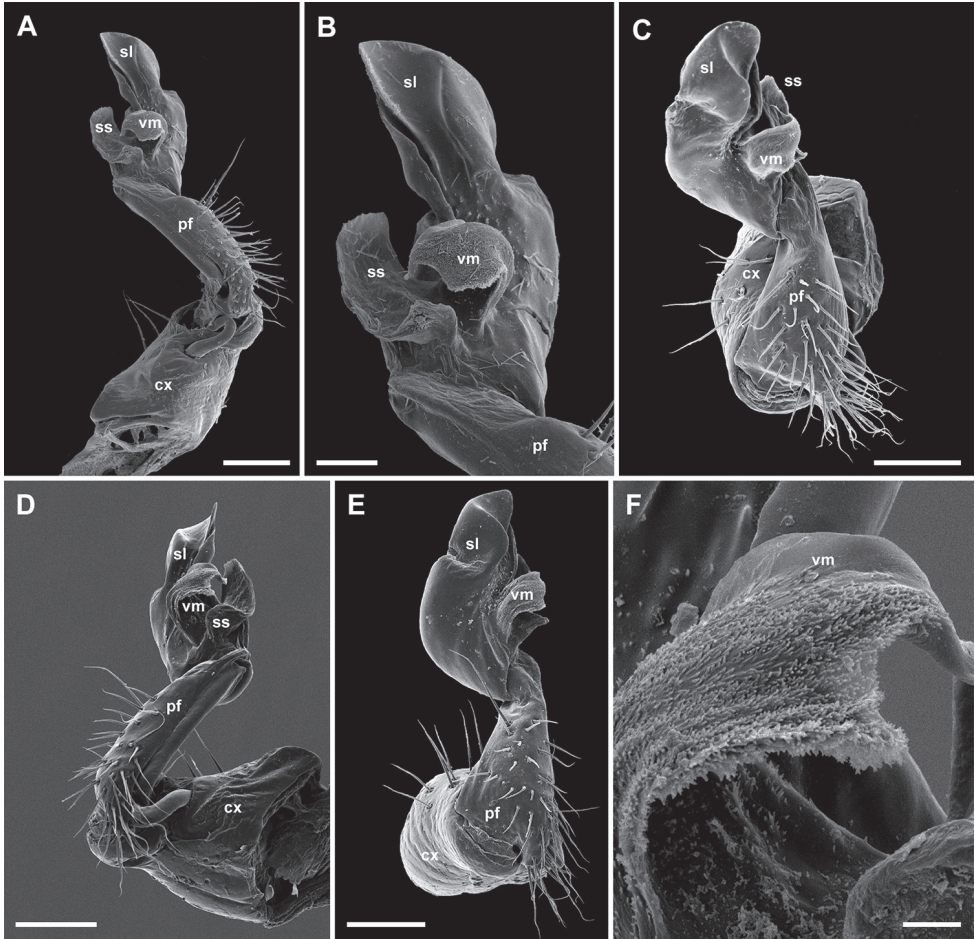
Figure 4. *Metonomastus petrovi* sp. n. **A** paratype ♂, left gonopod, ventromesal view **B** paratype ♂, distal part of left gonopod, ventromesal view **C** paratype ♂, right gonopod, ventral view **D** non-type ♂, right gonopod, mesal view **E** non-type ♂, right gonopod, ventral, slightly lateral view, **F** non-type ♂, right gonopod, ventromesal process, same view, enlarged. Abbreviations: **cx** coxite, **pf** prefemorite, **sl** solenomere, **ss** saddle-shaped process, **vm** ventromesal process. Scale bars: 0.2 mm (**B**), 0.05 mm (**A, C, D, E**), 0.005 mm (**F**).

ventral sides. Acropodite consisting of three branches: mesal process (ss) curved and saddle-shaped, ventromesal process (vm) more strongly arched, its outer surface microspiculate (Figure 4F), solenomere (sl) robust, blunt, somewhat beak-shaped, ventrolaterally with a deep and broad transverse groove. Seminal groove running on mesal side all along prefemorite, then shifting dorsally on acropodite, terminating ventromesally on solenomere.

Remarks. This species is known both from caves and from an epigean environment. Like some other representatives of the genus, this new species can be considered a troglophile.

Metonomastus radjai sp. n.

http://zoobank.org/C1C9931C-C20A-49F6-A91E-FD1E810385AD
Figs 5–9

Material examined. Holotype male (NHMSC), Croatia, Dalmatia, island of Mljet, Blato, near Kozarica, under stones, 23.XII.2015, T. Rađa leg.

Paratypes. 1 male (NHMSC), 2 males (IZB), 4 females (NHMSC), 7 females (IZB), 4 juveniles (IZB), same data as holotype.

Etymology. The new species is named after the collector, Tonći Rađa, a renowned Croatian biospeleologist who discovered numerous new or interesting arthropods. Noun in genitive case.

Figure 5. *Metonomastus radjai* sp. n., paratype ♀ (IZB) **A** habitus, lateral view **B** anterior part of the body, lateral view **C** posterior part of the body, lateral view. Scale bars: 1 mm (**A**), 0.5 mm (**B, C**).

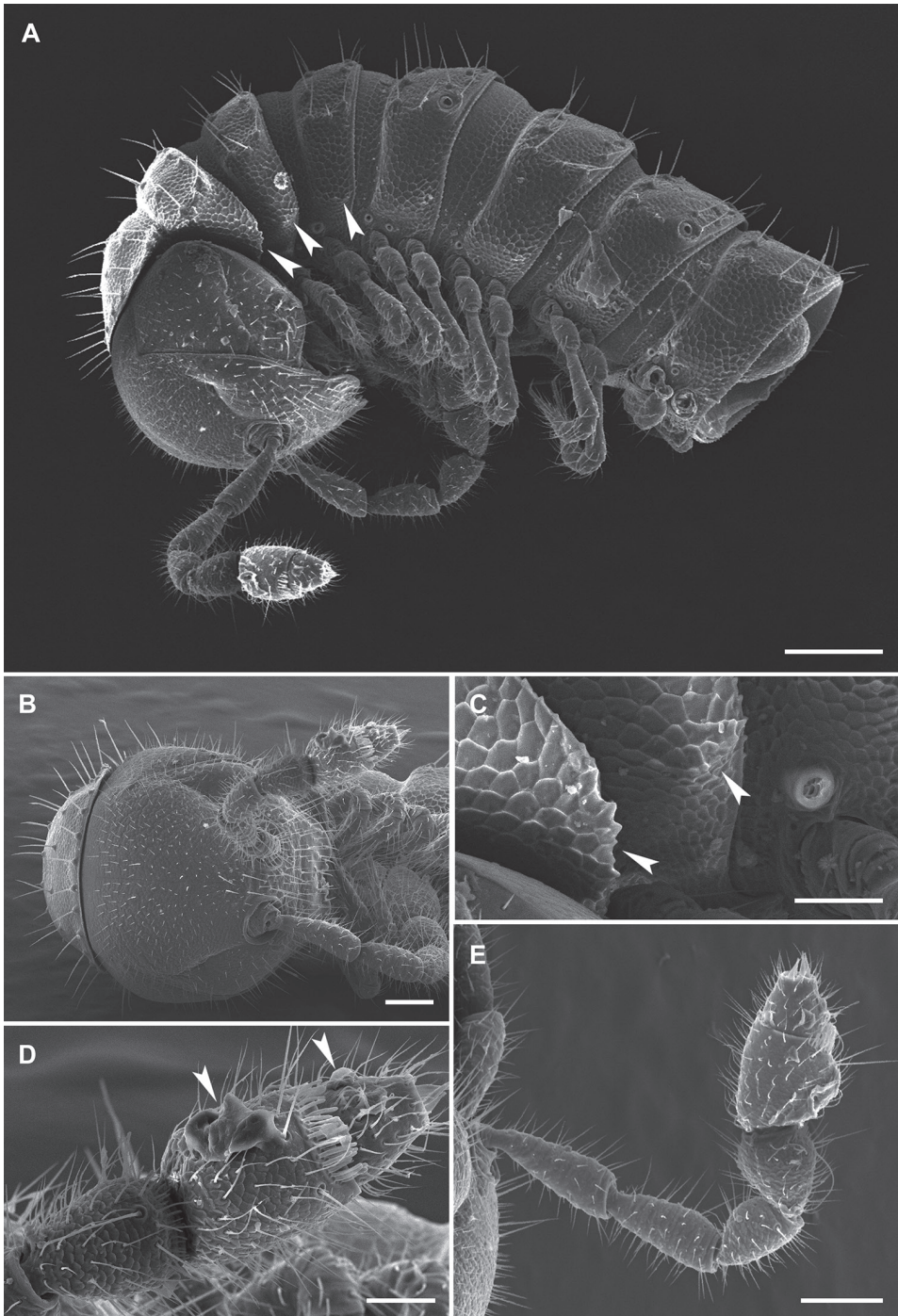**Figure 6.** *Metonomastus radjai* sp. n., paratype ♀ (IZB) **A** anterior part of the body, lateral view **B** head, frontal view **C** pleurosternal carinae of the body rings 2 and 3, lateral view **D** tip of left antenna (with artefacts) **E** left antenna. Arrows indicate pleurosternal carinae (**A, C**) or artefacts on antenna (**D**). Scale bars: 0.2 mm (**A**), 0.1 mm (**B, E**), 0.05 mm (**C, D**).
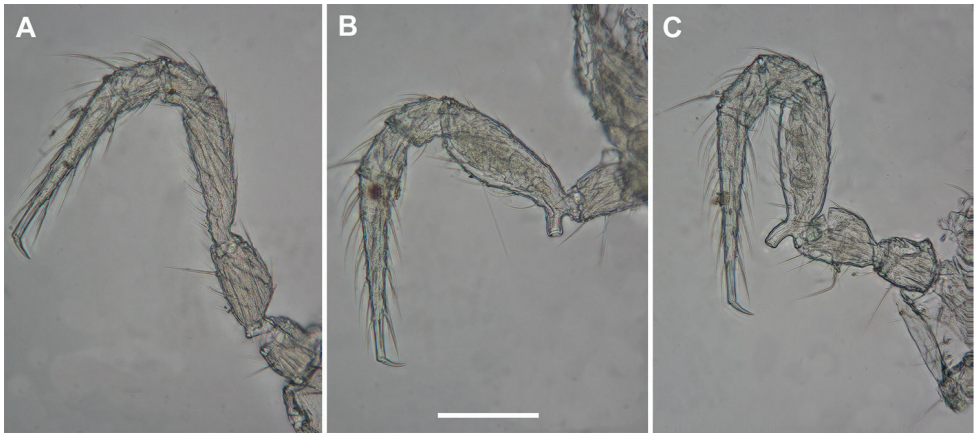
Figure 7. *Metonomastus radjai* sp. n., paratype ♂ (IZB) **A** leg 4 **B** leg 5 **C** leg 6. Scale bar: 0.1 mm.

Diagnosis. The new species belongs to the *Metonomastus* group of species with two postfemoral branches, but clearly differs from all of these by the presence of a well-developed, broad, lamellar solenophore (= tibiotarsus) directed strongly mesad, and proximally curved ventrad. The solenomere is without additional processes and is also directed strongly mesad.

Description. Length 3.7–3.9 mm (males), 4.3–5 mm (females). Width of midbody rings 0.30–0.33 and 0.37–0.4 mm (males), 0.42–0.44 and 0.47–0.5 mm (females) on pro- and metazonae, respectively. Holotype male 3.7 mm long, 0.3 and 0.37 mm wide on midbody pro- and metazonae, respectively.

All other characters as in *M. petrovi* sp. n., except as follows.

Microreticulated texure more obvious (Figs 6A, 8A, B). Width of head 0.42–0.44 mm (males), 0.5–0.55 mm (females). Antennomere length 2 = 3 = 6 > 4 = 5 > 7 > 1 (Figure 6E). Postcollum metaterga each with a barely visible, mid-dorsal, transverse sulcus (Figure 8A, B). Pleurosternal carinae present on rings 2–4 in the form of small denticles, more strongly developed on 2nd ring (Figure 6A, C). Legs about 1.5 times as long as midbody height in both sexes. In males, pregonopodal legs each with a distinct dorsobasal hump on prefemur; leg-pairs 5–7 each with a ventrobasal femoral adenostyle (Figure 7B, C).

Gonopods (Figs 8E-G, 9): Coxite (cx) massive, slightly elongated, laterally with three setae, one being particularly long. Prefemorite (pf) subquadrate in ventral and dorsal views, somewhat narrower in lateral and mesal views, about as long as acropodite, densely setose ventromesally. Acropodite represented by two processes: solenomere (sl) and solenophore (sph). Both solenomere and solenophore simple and directed mesad. Solenomere ventral in position, slender, acuminate, distally terminating in two small teeth. Solenophore strongly developed, dorsal in position, wide, lamellar, proximally curved ventrad. Seminal groove running through dorsomesal side of prefemorite, then shifting laterodistally through solenomere.

Remarks. This species was found under stones next to a dry stone wall close to the seashore.
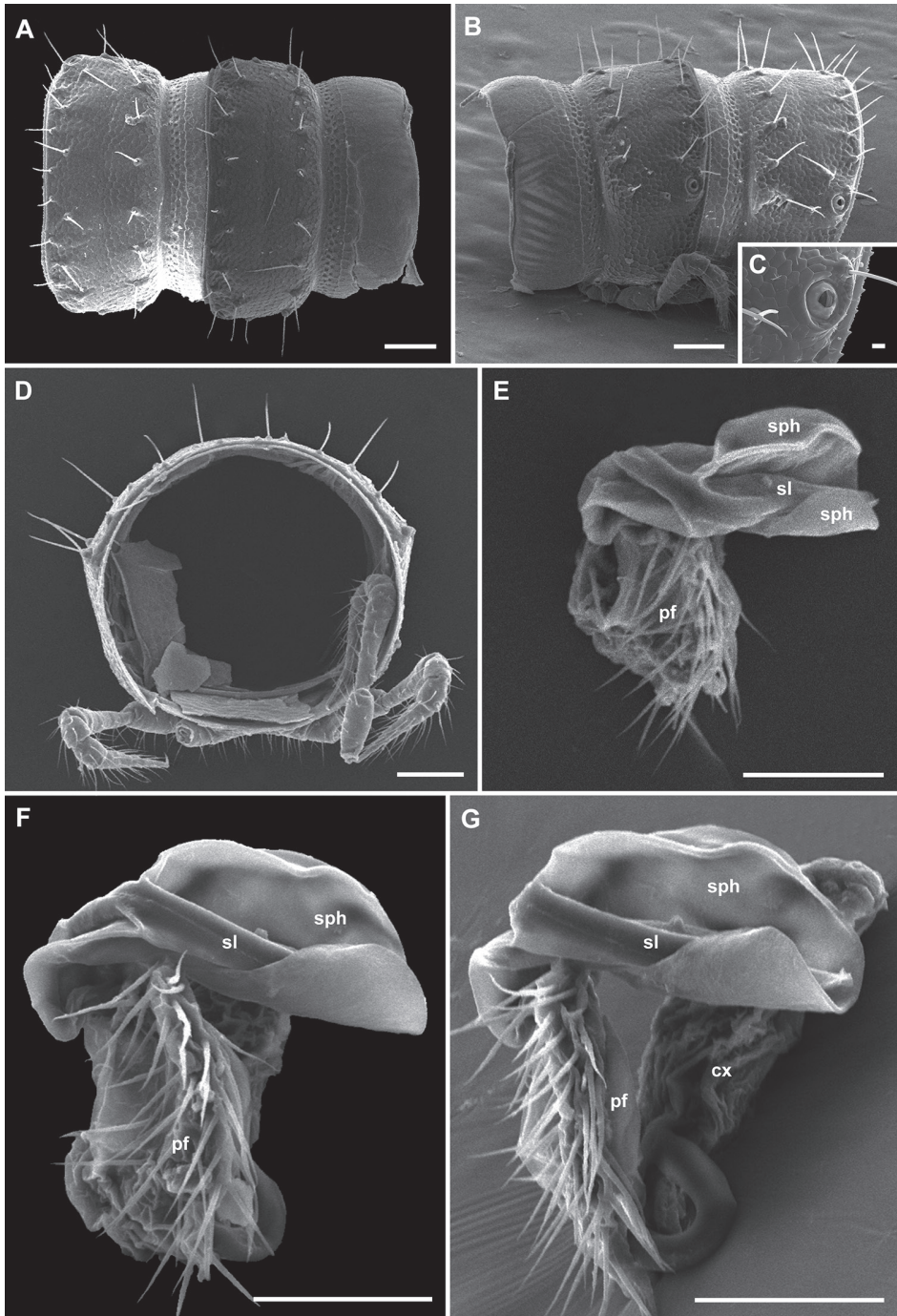
Figure 8. *Metonomastus radjai* sp. n., **A, B, C, D** paratype ♀ (IZB) **A** body rings 9 and 10, dorsal view **B** body rings 9 and 10, lateral view **C** body ring 10, ozopore lateral view **D** body ring 11, caudal view **E, F, G** paratype ♂ (IZB), right gonopod **E** oral (distal) view **F** ventral view **G** ventromesal view. Abbreviations: **cx** coxite, **pf** prefemorite, **sl** solenomere, **sph** solenophore. Scale bars: 0.1 mm (**A, B, D**), 0.05 mm (**E, F, G**), 0.01 mm (**C**).

Figure 9. *Metonomastus radjai* sp. n. paratype ♂ (IZB), right gonopod **A** dorsal view **B** mesal view **C** ventral view **D** lateral view. Abbreviations: **cx** coxite, **pf** prefemorite, **sl** solenomere, **sph** solenophore. Scale bar: 0.1 mm.

Discussion

Based on gonopod characters, species of *Metonomastus* may provisionally be divided into two groups. The first group is characterized by a two-branched acropodite, while the second group includes species 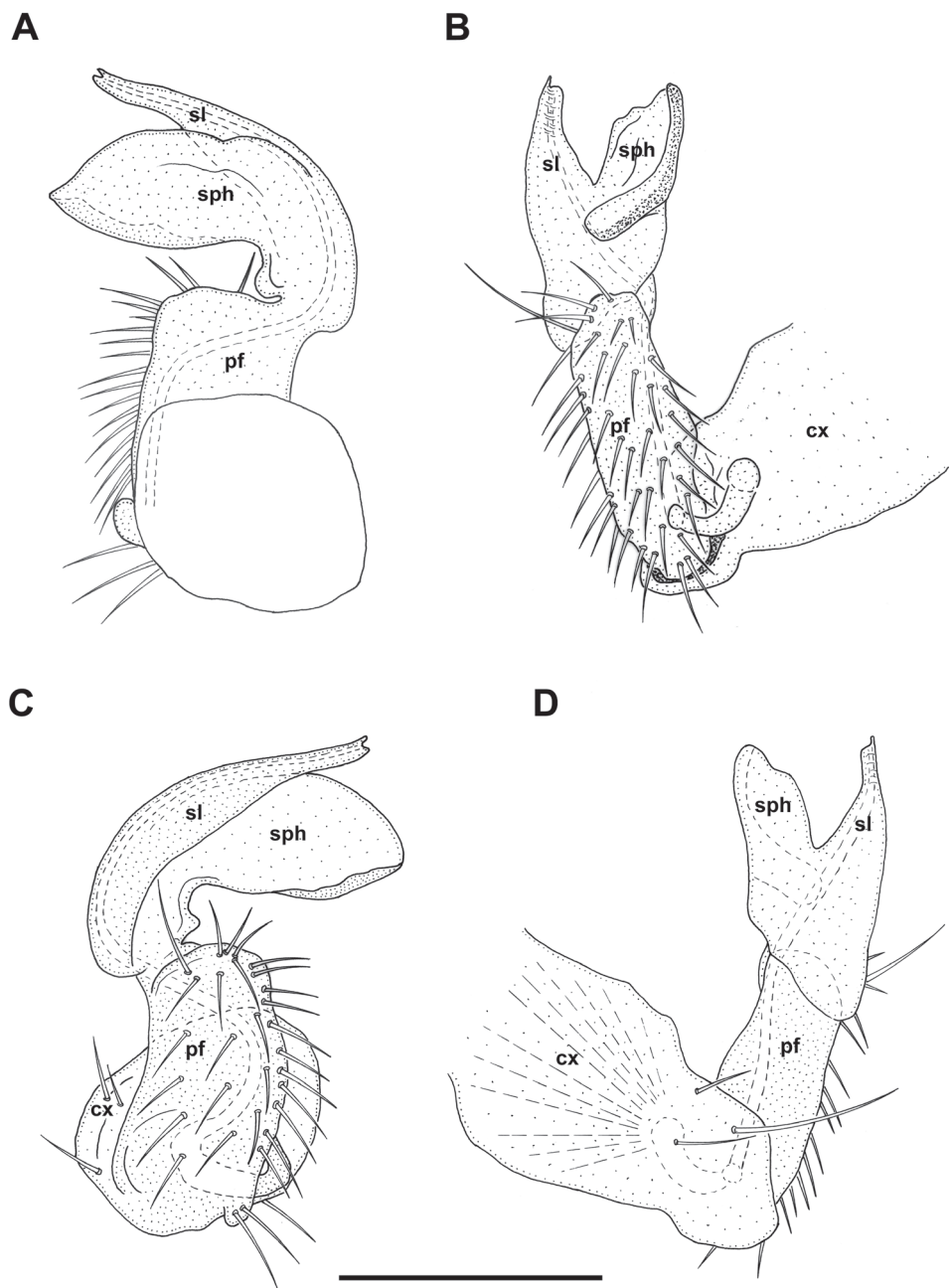with three branches. Such a division is also supported biogeographically. Taxa with two acropodital branches appear in the central Mediterranean: in northeastern and central Italy and along the Adriatic coast of the western Balkans. This group contains ten species, including *Metonomastus radjai* sp. n. Among these congeners, *M. capreae* (Verhoeff, 1942), *M. hirtellus* (Silvestri, 1903), *M. mariae* (Strasser, 1965), *M. patrizii* Manfredi, 1950, and *M. romanus* (Verhoeff, 1951) are all known from central Italy [*M. hirtellus* was recently found also in Croatia (Antić et al. 2018)], also showing a similar pattern of gonopodal structure. The prefemorite seems to be somewhat elongated, at least equal in length to the acropodite, the solenomere is a well-developed and more or less erect outer branch, with an additional small process in *M. mariae* and *M. patrizii* (this could also be true for the other three species?), while the inner branch, the solenophore (= tibiotarsus) is curved mesad. On the other hand, the very common and abundant *M. albus*, known from Slovenia, Croatia and Bosnia and Herzegovina, has gonopods with a much shorter prefemorite, while the solenophore is broad, lamellar, erect, obviously more strongly developed than the solenomere, with a deep rift between the two latter structures. Although our new island species, *M. radjai* sp. n., occurs geographically much closer to the coast-inhabiting *M. albus*, it seems to show more similarities to central Italian forms, viz., a somewhat elongated prefemorite which is almost equal in length to the acropodite, the solenophore curved mesad, and a shallow rift present between the solenophore and solenomere. However, *M. radjai* sp. n. clearly differs by both acropodital branches being strongly curved mesad. In addition, the solenophore is very broad, lamellar, and with a ventrally curved proximal edge. Similarities in the gonopodal structure between *M. radjai* sp. n. and the mostly central Italian *Metonomastus* species could be evidence of a trans-Adriatic distribution of this (sub)group. Such a distribution pattern is already known not only in some millipedes, but also in such arthropods as isopods or endogean beetles (see Antić et al. 2018). Even if it has a habitus usual for the genus, the Albanian *M. petrelensis* Mauriès, Golovatch & Stoev, 1997 has gonopods with significantly different postfemoral branches from those of the above species. Both solenomere and solenophore are simple and slender, whereas the solenomere is mesal in position and spinulose distally. This species differs also from the above ones by the absence of adenostyles on the pregonopodal femora (Mauriès et al. 1997). If we consider the habitus, one species in this group is clearly distinguished from the others: *M. saetosus* (Strasser, 1960). It is characterized by very abundant and irregular metatergal pilosity, contrary to the presence of two or three transverse rows of setae in the other known *Metonomastus* species (the exception is *M. bosniensis*, reported to lack setae, but this observation requires verification). Originally, *M. saetosus* was placed in the genus *Microdesminus* Strasser, 1960, but it was synonymized under *Metonomastus* by Golovatch and Stoev (2004).

The second group within *Metonomastus* includes three species, viz. *M. pomak*, *M. strasseri*, and *M. petrovi* sp. n. All three species are characterized by the presence of three acropodital branches. Unlike the previous, central Mediterranean group, these taxa inhabit the eastern Mediterranean within Greece and northwestern Anatolia (*M. strasseri*) or the Rhodopian part of Bulgaria (*M. pomak* and *M. petrovi* sp. n.). In both previously described species, the solenophore appears as the main, long and curved branch above the solenomere which can be long and slender in *M. strasseri* or lamelliform and broad in *M. pomak*. The new species clearly differs from both of them by the presence of a strongly developed, robust and somewhat beak-shaped solenomere which appears as the main branch, while a solenophore is fully reduced.

As already stated by Golovatch and Stoev (2004), the somewhat disjunct distribution of the representatives of *Metonomastus* may be evidence of the group being ancient and relict. On the other hand, the very small bodies and a cryptic life in the soil or caves can also account for such a sporadic known distribution. Future research in the Mediterranean and southeastern Europe, including the application of various collecting techniques, will surely result in a considerable increase in the knowledge of millipede diversity, including further progress in our knowledge of the species richness and distribution of the genus *Metonomastus*.

Key to *Metonomastus* species

1	Metatergal setae absent	***M. bosniensis***
–	Metatergal setae present	**2**
2	Gonopods with three acropodital branches	**3**
–	Gonopods with two acropodital branches	**5**
3	Solenophore absent	***M. petrovi* sp. n.**
–	Solenophore present	**4**
4	Solenomere lamelliform and broad	***M. pomak***
–	Solenomere elongated and slender	***M. strasseri***
5	Metaterga densely setose	***M. saetosus***
–	Metaterga with 2–3 rows of setae	**6**
6	Gonopod prefemorite suboval and considerably shorter than acropodite ....***M. albus***
–	Gonopod prefemorite subquadrate and about as long as acropodite	**7**
7	Acropodital branches slender and sinuate	***M. petrelensis***
–	Acropodital branches stouter	**8**
8	Solenomere strongly curved mesad	***M. radjai* sp. n.**
–	Solenomere not curved mesad, but erect ....***M. capreae, M. hirtellus, M. mariae, M. patrizii, M. romanus***

Acknowledgements

References

Antić DŽ, Dražina T, Rađa T, Lučić LR, Makarov SE (2018) Review of the genus *Typhloiulus* Latzel, 1884 in the Dinaric region, with a description of four new species and the first description of the male of *Typhloiulus insularis* Strasser, 1938 (Diplopoda: Julida: Julidae). Zootaxa 4455(2): 258–294. https://doi.org/10.11646/zootaxa.4455.2.2

Attems C (1937) Myriapoda 3. Polydesmoidea I. Fam. Strongylosomidae. Das Tierreich 68: 300 pp.

Chamberlin RV (1943) On nine North American polydesmoid millipeds. Proceedings of the Biological Society of Washington 56: 35–40.

Golovatch SI, Stoev P (2004) A new species of the millipede genus *Metonomastus* Attems, 1937 from a cave in the Eastern Rhodopes (Bulgaria), with some remarks on its congeners (Diplopoda: Paradoxosomatidae). In: Beron P, Popov A (Eds) Biodiversity of eastern Rhodopes (Bulgaria and Greece). [Biodiversity of Bulgaria 2.] [Pensoft Series Faunistica No 41.] National Museum of Natural History, Sofia, 199–205.

Hoffman RL, Lohmander H (1968) The Diplopoda of Turkey. Part III. Order Polydesmida. – Mitteilungen aus dem Hamburgischen Zoologischen Museum und Institut 63: 61–121.

Manfredi P (1950) Miriapodi italiani, VI. contributo - Specie e varieta nuove. Atti della Società italiana di scienze naturali, e del Museo civico di storia naturale 89: 33–42.

Mauriès J-P, Golovatch SI, Stoev P (1997) The millipedes of Albania: recent data, new taxa; systematical, nomenclatural and faunistical review (Myriapoda, Diplopoda). Zoosystema 19: 255–292. http://sciencepress.mnhn.fr/sites/default/files/articles/pdf/z1997n2_3a7_0.pdf

Silvestri F (1903) Classis Diplopoda. Vol. 1a. Anatome: Pars I, Segmenta, Tegumentum, Musculi. In: Berlese A. Acari, Myriapoda et Scorpiones huscque in Italia reperta 346: 1–272. Portici.

Strasser K (1960) Diplopoden aus Alpen-, Apenninen- und Balkanländern. Fragmenta Entomologica (Roma) 3(6): 95–140.

Strasser K (1965) Diplopodi raccolti in alcune grotte dell'Abruzzo. Bollettino della Società adriatica di scienze naturali in Trieste 53: 173–182.

Verhoeff K (1901) Beiträge zur Kenntniss paläarktischer Myriopoden. XIX. Aufsatz: Diplopoden aus Herzegowina, Ungarn und Baiern. Archiv für Naturgeschichte 67A(1): 221–240.

Verhoeff KW (1942) Diplopoden der Insel Kapri. Zoologischer Anzeiger 139: 213–233.

Verhoeff KW (1951) Diplopoda, Chilopoda und Isopoda terrestria vom Mt. Soratte in Latium. Zoologische Jahrbücher, Abteilung für Systematik, Ökologie und Geographie der Tiere 80: 205–253.

RESEARCH ARTICLE

One generic synonym and one new species of Phlaeothripidae from India (Thysanoptera)

Kaomud Tyagi[1], Devkant Singha[1,2], Goutam Kumar Saha[2], Vikas Kumar[1]

1 *Centre for DNA Taxonomy (CDT), Molecular Systematics Division, Zoological Survey of India, Kolkata, West Bengal, India* **2** *Department of Zoology, University of Calcutta, West Bengal, India*

Corresponding author: Kaomud Tyagi (kumud.tyagi5@gmail.com)

Citation: Tyagi K, Singha D, Saha GK, Kumar V (2018) One generic synonym and one new species of Phlaeothripidae from India (Thysanoptera). ZooKeys 786: 59–68. https://doi.org/10.3897/zookeys.786.28332

Abstract

Haplothrips shivendraii Tyagi & Kumar, **sp. n.** is described from Rajasthan state of India. The monobasic Austro-oriental genus *Dyothrips* Kudô is formally synonymised with *Haplothrips*.

Keywords

Dyothrips, *Haplothrips*, India, new species, synonym.

Introduction

The genera *Haplothrips*, *Dyothrips*, and *Plicothrips* belong to tribe Haplothripini in the subfamily Phlaeothripinae, family Phlaeothripidae (Mound and Minaei 2007, Minaei and Mound 2008). *Haplothrips* was erected by Amyot and Serville (1843) for the single species, *Phloeothrips albipennis* Burmeister, 1836. It is the second largest genus in the family Phlaeothripidae and comprises the two subgenera *Haplothrips* and *Trybomiella*. These are distinguished by the presence or absence of fore wing duplicated cilia, present in *Haplothrips* and absent in *Trybomiella*. The genus currently includes 242 extant

species, of which 219 are in *Haplothrips* and 23 in *Trybomiella* (ThripsWiki 2018). From India, 22 *Haplothrips* species are recorded, 16 in the subgenus *Haplothrips* and six in *Trybomiella* (Tyagi and Kumar 2016).

Dyothrips was first described as a subgenus by Kudô (1974) to include the single species *Haplothrips* (*Trybomiella*) *cingulatus* Pelikan, 1963 from China, and he simultaneously recorded this species from Taiwan (Kudô 1974). However, two further species described from Australia, *Zygothrips pallescens* Hood, 1919 and *Watsoniella helena* Girault, 1928 were later synonymized with *cingulatus* (Pitkin 1973). Bhatti (1995) elevated the status of *Dyothrips* from subgenus to genus to include the single species *Dyothrips pallescens* (Hood, 1919). This was based on two morphological characters: incomplete notopleural sutures, and complete mesopresternum. The genus *Plicothrips* Bhatti, 1979 included two species, *Hindsiana apicalis* Bagnall, 1915 from India and *Hindsiana cameroni* Priesner, 1934 from Sudan.

The genus *Dyothrips* is closely related to *Plicothrips* by the presence of one sense cone on antennal segment III and incomplete notopleural sutures. However, it can be separated by the presence of two pairs of wing retaining setae in *Dyothrips* and one pair in *Plicothrips*. Furthermore, according to the key to Australian genera of the *Haplothrips* lineage group (Mound and Minaei 2007) *Dyothrips* is distinguished from *Haplothrips* based solely on incomplete notopleural sutures. Those authors pointed out that *Dyothrips* and *Haplothrips* do not differ in the mesopresternum because this structure is completely sclerotised in the type species of *Haplothrips*. Recently, we collected a Haplothripini species from Rajasthan state of India and found the notopleural sutures were incomplete in eight specimens, but complete in four specimens, and in a further specimen this suture was incomplete on the left side but complete on the right side. These ten specimens were all collected from the same locality on the same plant, and this variation suggests that the complete or incomplete condition of these sutures is not robust enough to separate the genus *Dyothrips* from *Haplothrips*. As a result, the genus *Dyothrips* is formally synonymized under the subgenus *Trybomiella* of the genus *Haplothrips*.

The objective of the present study is to describe a new species of *Haplothrips* from Rajasthan state of India and to synonymise the genus *Dyothrips* under the subgenus *Trybomiella* of genus *Haplothrips*.

Materials and methods

Holotype and paratypes are deposited in the National Zoological Collections (**NZC**) at Zoological Survey of India, Kolkata. The specimens were collected by beating vegetation over a white tray, and picked by using a camel-hair brush wet in 70% alcohol and stored in -20 °C. The specimens were then mounted onto the glass slides in Canada balsam for identification. Morphological terminology for adult structures mainly follows Mound and Minaei (2007). Photographs and illustrations were taken with a Leica Trinocular Microscope (Leica DM-1000) using Leica software application suite (LAS EZ 2.1.0). The identification was done using available keys (Pitkin 1976; Ananthakrishnan and Sen 1980; Mound and Minaei 2007; Minaei and Mound 2008).

Taxonomy

Haplothrips Amyot & Serville, 1843

Haplothrips Amyot & Serville, 1843: 640.
Dyothrips Kudô, 1974: 114. Syn. n.

Remarks. The Austro-oriental genus *Dyothrips* is known by the single species *D. pallescens* Hood, 1919 from China, Taiwan, Thailand, Japan, Australia, Fiji, and India. Because of variation in the notopleural sutures in the new species described below, *Dyothrips* can no longer be distinguished from *Haplothrips*, and they are here formally synonymised. The new combination, *Haplothrips pallescens* (Hood, 1919), is established here.

Haplothrips shivendraii Tyagi & Kumar, sp. n.
http://zoobank.org/31D6F646-D7E9-4D29-960B-05A86D23B121
Figures 1–9

Diagnosis. Both sexes macropterous. Body dark brown, fore wing transparent. Antennae 8-segmented, III with two and IV with four sense cones. Head longer than broad, maxillary stylets widely separated, maxillary bridge complete; with one pair of postocular setae, capitate. Pronotal epimeral setae (ep) well developed, capitate, notopleural sutures incomplete or incomplete. Mesopresternum divided into two lateral triangles. Fore wing without duplicated cilia. Fore tarsal tooth small in female and developed in male. Pelta triangular.

 Description. Female macroptera. Body dark brown, all femora, mid and hind tibiae, mid and hind tarsi brown; fore tibiae light brown, fore tarsi yellow with unguitractor dark, fore wing transparent, shaded with brown basally (Figure 1). Antennae brown except light brown segment III. Head longer than broad, dorsal surface with few transverse striae (Figure 3). Maxillary stylets retracted to postocular setae and one third of width apart, maxillary bridge present; one pair of postocular setae well developed, capitate; eyes enlarged dorsally than ventrally; ocelli present. Antennae 8-segmented; segment II with campaniform sensilla situated apically; segment III with two sense cones, IV with four sense cones, V with three-one-one sense cones situated outer and inner margin of apex, and one small sense cone on apex, VI with two, VII with one sense cone; segment VIII not constricted at base (Figure 4). Mouth cone rounded. Pronotum rectangular, 1.7 times as broad as long, and 0.6 times as long as head; dorsal surface with few striae laterally and posteriorly and many small setae; anteroangular setae (aa) small and blunt apically, anteromarginal (am) and midlateral (ml) setae small, pointed or reduced, posteroangular setae (pa) capitate, little longer than aa and shorter than ep, epimeral setae (ep) well developed, capitate, and longer than posteroangular (pa); notopleural sutures incomplete or complete. Mesonotum dorsal surface with faint transversely reticulate sculpture, median and submedian setae little far from posterior

Figures 1. *Haplothrips shivendraii* sp. n.: Female

margin; lateral setae expanded at apex. Metanotum weakly sculptured with reticulation, with well-developed median pointed setae. Mesopresternum divided into two lateral triangles (Figure 5). Fore wing with median constriction, without duplicated cilia; sub-basal wing setae arranged in one row, well developed and capitate, and S3 the longest (Figure 6). Fore tarsal tooth small (Figure 3). Pelta triangular in shape, surface with reticulation (Figure 7). Tergites III–VII with 2 pairs of wing retaining setae (Figure 8); tergite IX setae S1 bluntly pointed, S2 and S3 finely acute (Figure 9). Sternites II–VIII with accessory setae. Tube shorter than head, anal setae shorter than tube.

Measurements. (holotype female in microns). Body length 2020; head length 225, width across eyes 170, across cheeks 176, across cheeks just before basal collar 159;
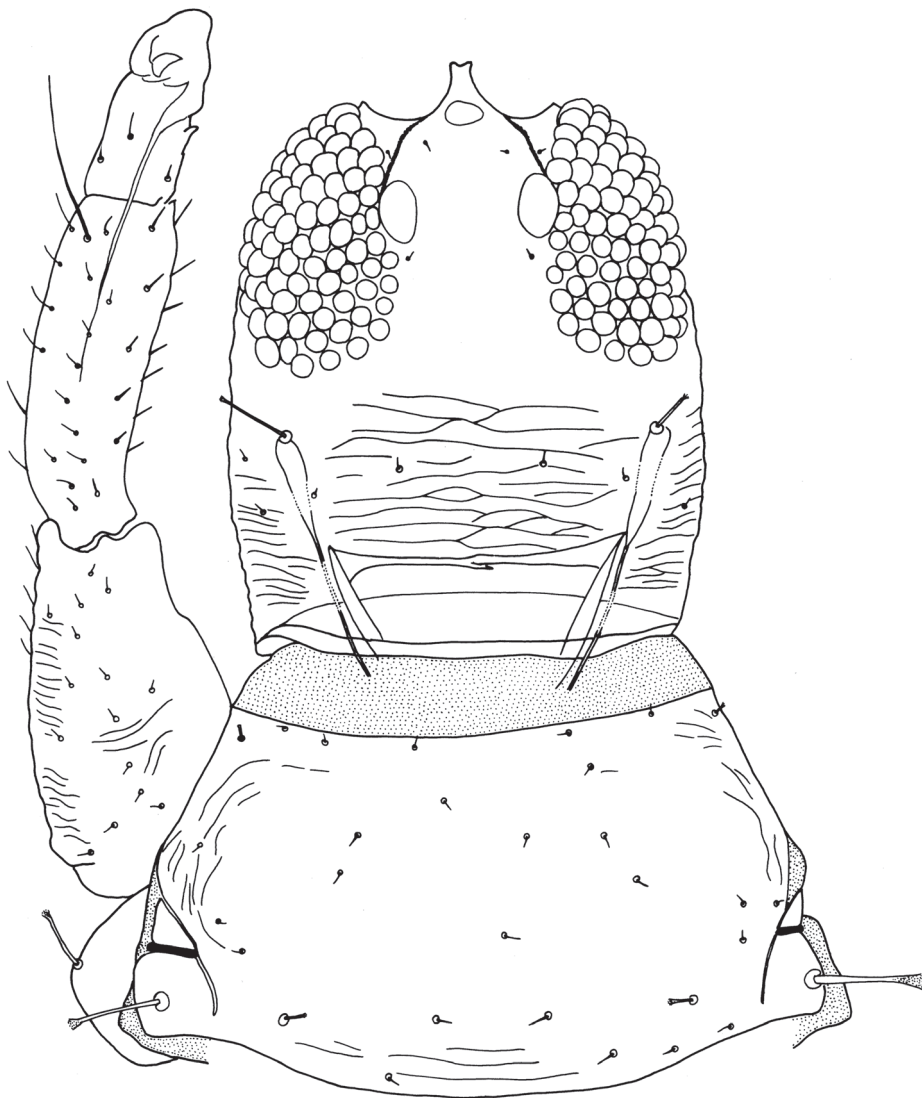
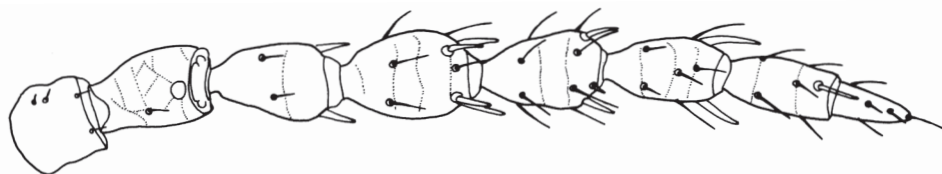**Figures 2.** *Haplothrips shivendraii* sp. n.: Male

eye length 98–100, width 50–55; postocular setae lengths 25–28; pronotum median length 133, width 238, lengths of major setae: pa 10, epim 36–42; pelta length 96, width at base 120; antenna length 318, L(W) of antennal segments I 27–29(29), II 39–42 (29), III 43(28), IV 46–49(32), V 41–43(28), VI 40(23), VII 37(20), VIII 27–29(11); fore wing basal setae length S1 39–40, S2 52–54, S3 62–63; tergite IX length 70; setae S1 102–104, setae S2 87–88; tube length 153, width at base 34, at apex 62; anal setae length 99–117.

Male. Macropterous. Colour and structure similar to female (Figure 2). Fore tarsus with distinct and well developed tooth. Male sternite VII without pore areas.

Material studied. Holotype female, **INDIA:** Rajasthan, Jodhpur, Desert Regional Centre, ZSI, collected from grass, 1.i.2015, (Reg. No.9542/H17), Coll. Shivendra Kumar Singh, in National Zoological Collections (NZC). Paratypes: 8 females 4 males, taken with holotype (Reg. No. 9543/H17 to 9554/H17).

Figures 3. *Haplothrips shivendraii* sp. n.: Head and Prothorax with fore leg

Figures 4. *Haplothrips shivendraii* sp. n.: Antenna, female

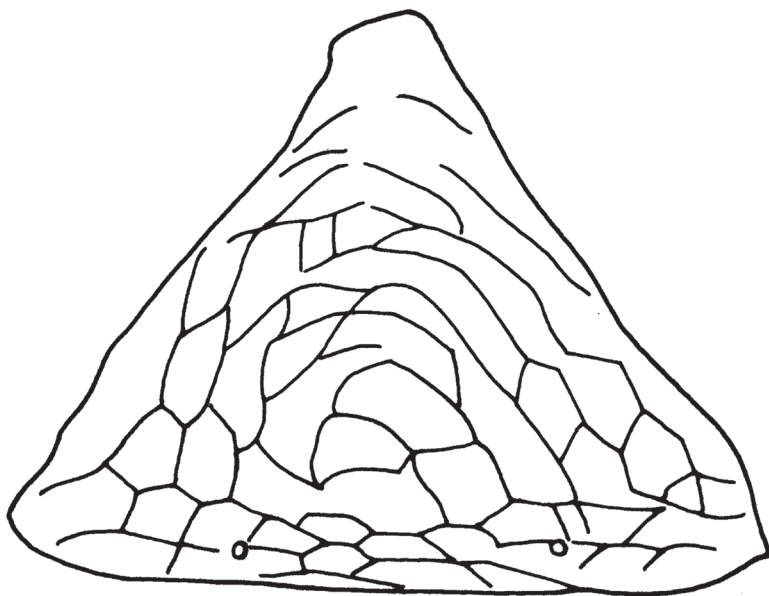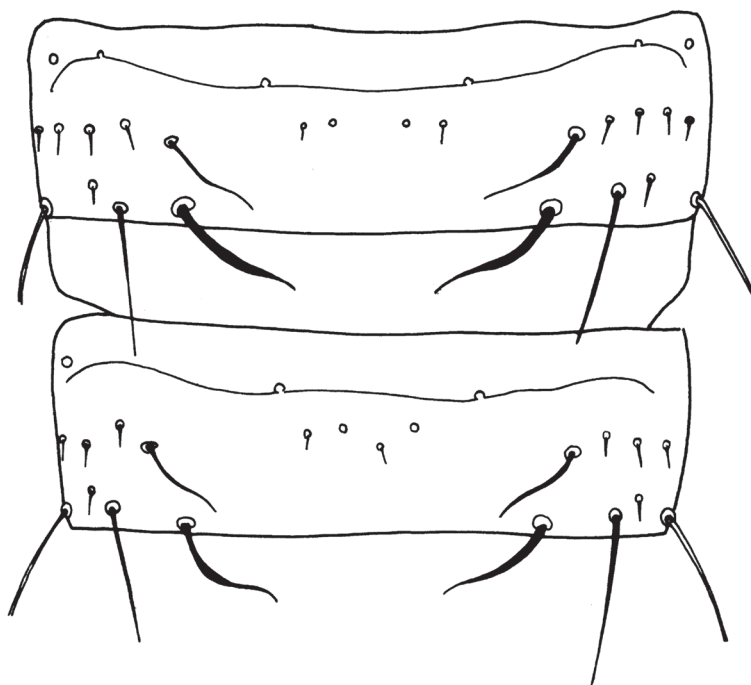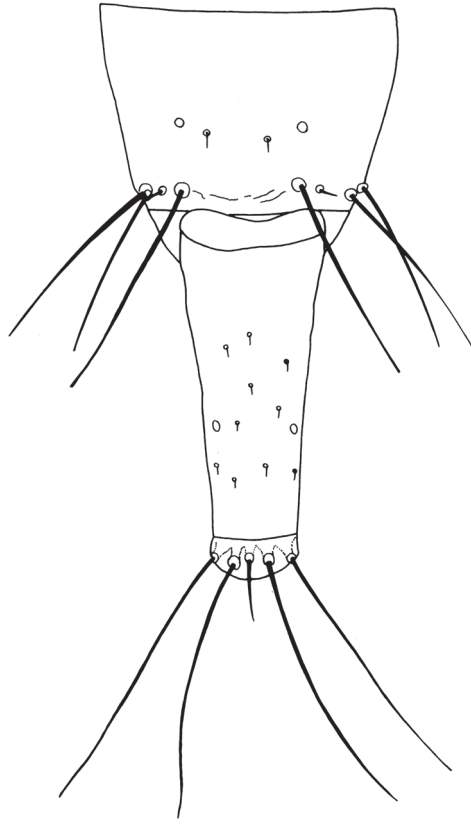**Figures 5.** *Haplothrips shivendraii* sp. n.: Prothroax, ventral view, female
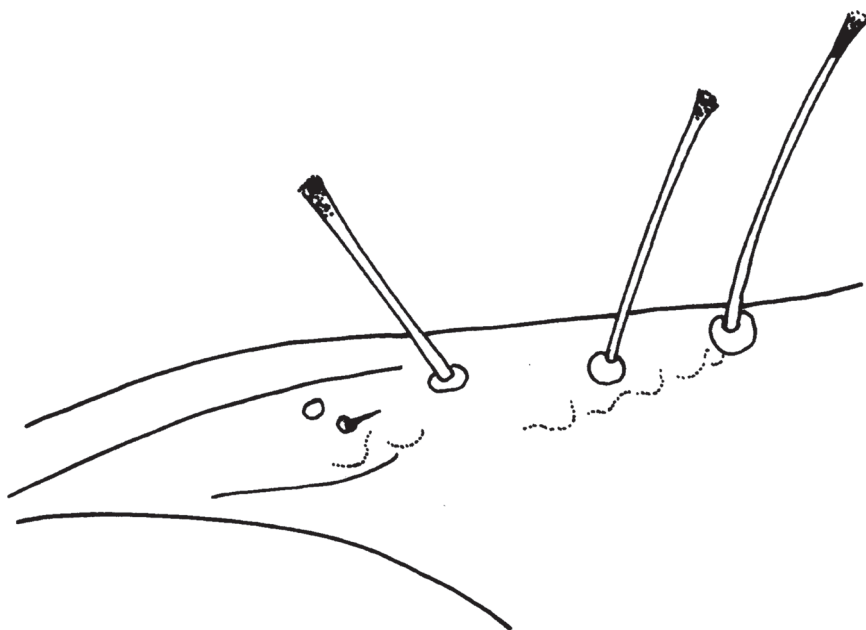
Figures 6. *Haplothrips shivendraii* sp. n.: part of fore wing, female

Figures 7. *Haplothrips shivendraii* sp. n.: Pelta, female

Figures 8. *Haplothrips shivendraii* sp. n.: Tergites IV–V, female

Figures 9. *Haplothrips shivendraii* sp. n.: Tergites IX–X, female

Etymology. This species is credited to Shivendra Kumar Singh for his keen interest and untiring effort for thrips collection dating back to his childhood.

Distribution. India (Rajasthan).

Remarks. This new species is similar to *Haplothrips pallescens* in having incomplete notopleural sutures in ten specimens. It can be distinguished by the body colour, which is brown in the new species but bicoloured in *pallescens*; the pronotal anteroangular and anteromarginal setae are not developed in *shivendraii*, but well developed and capitate in *pallescens*. There are two sense cones on antennal segment III and four on IV in *shivendraii* but one sense cone on III and three on IV in *pallescens*.

According to Indian key to the order Thysanoptera (Ananthakrishnan and Sen 1980), the new species is similar to *Haplothrips nigricornis* (Bagnall) by the length of the pronotal midlateral setae and anteroangular setae. It can be distinguished by the yellow fore tarsus (yellowish brown in *nigricornis*), light brown fore tibia (fore tibia brown with slightly paler apex), presence of four sense cones on segment IV (4+1 in *nigricornis*); pronotum with posteroangular setae developed (reduced in *nigricornis*); and maxillary stylets are more widely separated in *shivendraii* than *nigricornis*.

Acknowledgements

References

Ananthakrishnan TN, Sen S (1980) Taxonomy of Indian Thysanoptera. Zoological Survey of India, Handbook Series No. 1: 1–234.

Bhatti JS (1979) Studies in some haplothripine forms. Nouvelle Revue Entomologique 9: 305–311.

Bhatti JS (1995) Studies on some Phlaeothripidae (Insecta: Tubulifera). Zoology (Journal of Pure and Applied Zoology) 5: 97–110.

Pitkin BR (1973) A revision of the Australian Haplothripini, with descriptions of three new species (Thysanoptera: Phlaeothripidae). Journal of the Australian Entomological Society 12: 315–339. https://doi.org/10.1111/j.1440-6055.1973.tb01680.x

Pitkin BR (1976) A revision of the Indian species of *Haplothrips* and related genera (Thysanoptera: Phlaeothripidae). Bulletin of the British Museum (Natural History), Entomology 34: 221–280.

Kudô I (1974) Some graminivorous and gall-forming Thysanoptera of Taiwan. Kontyu 42: 110–116.

Minaei K, Mound LA (2008) The Thysanoptera Haplothripini (Insecta: Phlaeothripidae) of Iran. Journal of Natural History 42: 2617–2658. https://doi.org/10.1080/00222930802354159

Mound LA, Minaei K (2007) Australian thrips of the *Haplothrips* lineage (Insecta: Thysanoptera). Journal of Natural History 41(45–48): 2919–2978. https://doi.org/10.1080/00222930701783219

ThripsWiki (2018) Thrips Wiki – providing information on the World's thrips. http://thrips.info/wiki [accessed 1 June 2018]

Tyagi K, Kumar V (2016) Thrips (Insecta: Thysanoptera) of India – An Updated Checklist. Halteres 7: 64–98.

RESEARCH ARTICLE

A new species and a key to the species of *Corticarina* from Guatemala (Coleoptera, Latridiidae)

Jose Carlos Otero[1], José Manuel Pereira[1]

1 *University of Santiago de Compostela, Department of Zoology, Genetics and Physical Anthropology, Santiago de Compostela 15782, Spain*

Corresponding author: *José Manuel Pereira* (josse33@hotmail.es)

Citation: Otero JC, Pereira JM (2018) A new species and a key to the species of *Corticarina* from Guatemala (Coleoptera, Latridiidae). ZooKeys 786: 69–73. https://doi.org/10.3897/zookeys.786.26553

Abstract

A new species of *Corticarina* Reitter, 1881 (Coleoptera: Latridiidae), *Corticarina oscargloriorum* **sp. n.** from Guatemala is described and illustrated. The differential diagnosis is established in relation to a group of other species of the genus.

Keywords

Introduction

Latridiidae is a moderately large family with approximately 500 species which is represented in all major biogeographic regions. The genus *Corticarina* is distributed in the Holarctic, Neotropical, Afrotropic and Oriental regions (Rücker 2009). In Central America, the fauna of Corticariinae is presumably extraordinarily rich, however, little known despite the attention that some authors (Johnson 1978, 1981, 1997; Reike

2015; Rücker 1981a, 1981b, 1987; Sharp 1902) have paid to some genera of this family (*Melanophthalma* Motschulsky, *Corticarina* Reitter, *Cortinicara* Johnson, etc.). Twenty species of *Corticarina* are known from Central America. Four of them, considered in this article, are distributed exclusively in Guatemala (Rücker 2009). As a result of that work, we have had the opportunity to study additional material collected in Central America (Zoological Museum, University of Lund, Sweden). Presumably most species considered in this article are endemic to Guatemala. The present paper presents part of the material collected at Sierra Madre Oriental in Guatemala.

Materials and methods

The terminology and the measurements of the new species follow Otero (1997) and Otero and López (2016). Structures were measured under a Leica M205C- stereomicroscope equipped with an Application Suite analysis system.

Abbreviations:

L   length;
WL   width/length ratio;
E   eccentricity of the eyes (width/half of the length).

The width is measured across the widest part of a line joining the anterior and posterior limit of the eye. Length is the maximum length of the eye. **L** is used for length in dorsal view, **W** for width, and **Ø** for diameter.

Institutional abbreviations:

USC   Universidad de Santiago de Compostela, Spain;
ZML   Zoological Museum, University of Lund, Sweden.

Taxonomy

Gen. *Corticarina* Reitter, 1881

Type species. *Corticarina truncatella* Mannerheim, 1844

Diagnosis. Head generally much narrower than the pronotum. Pronotum rather broad, usually strongly curved at the sides, with or without a circular post median impression; hind angles clearly toothed. Basal segment of the tarsi (especially the hind) strongly produced ventrally so that its apex almost reaches the apex of the second segment; second tarsomere reduced, arising dorsally from the basal segment nearly at the middle. Male: front tibia with a tooth situated at or a little in front of the middle; aedeagus strongly sclerotized, asymmetrical, the ostium ventral and covered with a plate which is usually strongly projecting apically.

Corticarina oscargloriorum **sp. n.**

http://zoobank.org/8A6EE954-93DB-49BB-9E47-B635F64AD1DE

Figures 1–4

Material examined. "Holotype m*. **GUATEMALA.** Jalapa, Pino Dulce, Mataquescuintla, 14.5256528°N, 90.1453500°W, 28.X.2016, 2.400 m". Holotype placed in Coll. J. C. Otero (USC).

Diagnosis. Morphologically, *Corticarina oscargloriorum* is very similar to other *Corticarina* in many external features, but can be distinguished by the configuration of the male genital apparatus and the features in the key below.

Description. Length: 1.1 mm. Body oval, convex and little bright (Figure 1). Yellowish grey-brown; antennae (except for the two first articles) and tibiae dark grey-brown; two first articles of antennae and legs yellowish grey-brown. Metathoracic wings fully developed.

Head (Figure 1) slightly transverse (WL = 1.8–1.9). Labrum arcuate at anterior margin. Eyes large (L = 0.073 mm) and little protruding (E = 0.5–0.6); eye facets as large as head punctures. Puncturation very fine (Ø = 0.006–0.007 mm) and sparse, barely distinct. Temples indistinct. Antennae (Figure 2) long (L = 0.398 mm). First antennomere spherical, almost as wide as long; second slightly shorter and half as thin as first; from fourth to seventh almost identical and half as short as second; eighth as wide as long; ninth sub-conical, longer than wide and 1.2 times as long as tenth; tenth 1.1 times longer than wide; eleventh twice as long.

Pronotum (Figure 1) moderately convex and little transverse (WL = 1.2–1.3); greatest width at anterior third. Lateral margins regularly rounded and denticulate. Postmedial circular depression present; lateral impressions somewhat distinct. Pubescence whitish, short (L = 0.019–0.020 mm) and recumbent. Punctation fine (Ø = 0.011–0.012 mm) and sparse.
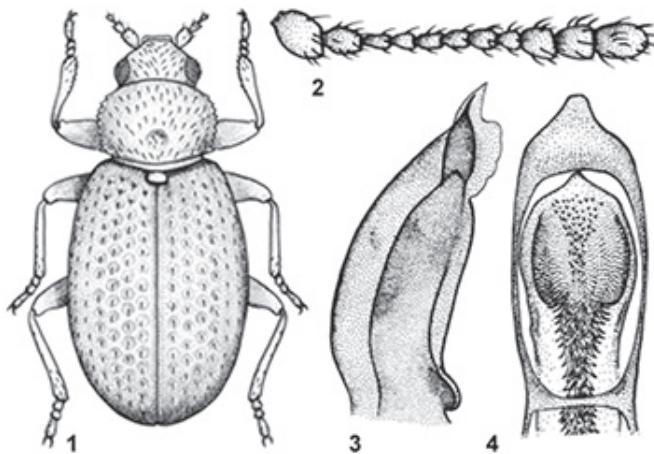
Figures. 1–4. *Corticarina oscargloriorum* sp. n., male, holotype: (**1**) habitus; (**2**) antenna; (**3–4**) aedeagus (lateral and ventral views).

Elytra 1.5 times as long as wide. Callosity humeralwell-marked and posteriorly prolonged until becoming slightly carenated in the humeral region. Pubescence short (L = 0.016–0.018 mm) and recumbent. Punctation fine (Ø = 0.014 mm) and sparse. Six abdominal sternites visible. Male pro-tibiae with a tooth on internal apical third.

Aedeagus (Figs. 3, 4) sub-lanceolate with a small apical protuberance. Internal sac with numerous small spines.

Etymology. This species is dedicated to Óscar Medinilla and Gloria de Dios, Guatemala.

Distribution. Guatemala.

Biology. It has been captured by stirring different types of plant formations.

Key to the *Corticarina* species from Guatemala

1   Tenth antennomere distinctly transverse; ninth squared. Spine of male pro-tibiae on the last quarter of the internal margin. Aedeagus (Fig.5). L: 1.4–1.5 mm. Guatemala..***guatemalica* Johnson**
–   Tenth antennomere as long as wide or longer than wide **2**
2   Ninth antennomere conical, wider than long; tenth as long as wide. Light brown; legs yellowish grey-brown; antennae pale on the base however darkening towards the apex. Spine of male pro-tibiae in the middle of the internal margin. Aedeagus (Fig. 7). L: 1.4–1.6 mm. Guatemala..... ***conjuncta* Johnson**
–   Ninth antennomere markedly longer than wide..**3**
3   Pale colour; head and pronotum slightly darker; antennae and legs entirely (except for the antennal club) yellowish grey-brown. Ninth antennomere conical and longer than wide; tenth longer than wide and slightly shorter than ninth. Spines of male pro-tibiae arranged on the middle of the internal margin. Aedeagus (Fig. 6). L: 1.4–1.6 mm. Guatemala.................................
       ....***impensa* Johnson**
–   Yellowish grey-brown; antennae (except for the two first articles) and tibiae dark greybrown; two first articles of the antennae and legs yellowish grey-brown. Ninth antennomere (Fig. 2) sub-conical, longer than wide; tenth 1.1 times longer than wide and slightly shorter than ninth. Spines of pro-tibiae on apical third. Aedeagus (Figs. 3& 4). L: 1.1 mm. Guatemala....................
       ....***oscargloriorum* sp. n.**

Discussion

Four species for *Corticarina* have been recorded from the Guatemala to date, and the four species are known to the authors. Morphologically, *Corticarina oscargloriorum* is very similar to other *Corticarina* which are remarkably uniform in appearance. Their male genitalia fortunately provide excellent diagnostic characters and are thus essential for identification.
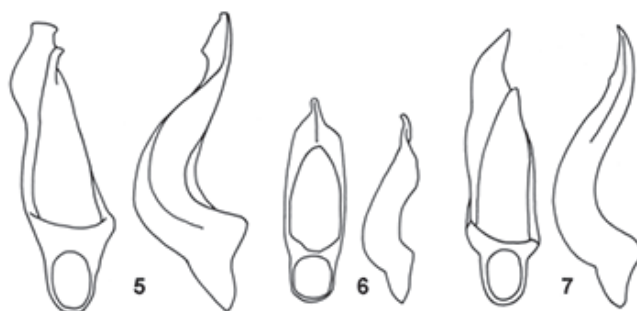
Figures. 5–7. Adeadeagi of species of *Corticarina*, ventral and lateral views: (**5**) *Corticarina guatemalica*; (**6**) *Corticarina impensa*; (**7**) *Corticarina conjuncta*.

Acknowledgements

References

Johnson C (1978) New species of *Corticarina* Reitter (Col., Latridiidae). Entomologist's Monthly Magazine 114: 55–62.

Johnson C (1981) New species of *Corticarina* Reitter (Col., Lathridiidae), part 2. Entomologist's Monthly Magazine 117: 117–123.

Johnson C (1997) Ten new species of *Corticarina* Reitter (Col.: Latridiidae) from Central and South America. Entomologist's Record 109: 115–124.

Otero JC (1997) Three new species and distributional records of *Micrambe* C. G. Thomson, 1863 and *Cryptophagus* Herbst, 1792 (Coleoptera: Cryptophagidae) from Israel and Turkey. Revue Suisse de Zoologie 104(1): 207–216. https://doi.org/10.5962/bhl.part.79997

Otero JC, López MJ (2016) *Coleoptera* Latridiidae. In: Ramos MA, et al (Eds) Fauna Ibérica, vol. 42. Museo Nacional de Ciencias Naturales, CSIC, Madrid, 288 pp.

Reike H-P (2015) Eine neue Art der Gattung *Corticaria* aus der sylvicola-Gruppe und eine neue *Corticarina* (Coleoptera, Latridiidae). Latridiidae and Merophysiinae 18: 1–4.

Rücker HW (1981a) Neue Arten der Gattung *Melanophthalma* Motschulsky aus Panama (Coleoptera, Lathridiidae). Entomologische Blätter 77: 161–164.

Rücker HW (1981b) Revision der Motschulsky-Typen aus Nord-und Südamerika, Coleoptera: Lathridiidae, Melanophthalma Motschulsky. Entomologische Blätter 77: 161–164.

Rücker HW (1987) Neue Arten der Gattung *Melanophthalma* Motschulsky aus der neotropischen Region (Coleoptera: Latridiidae). Entomologische Blätter 83 (1): 1–12.

Rücker HW (2009) Checklist Latridiidae and Merophysiinae of the world. Latridiidae: Mitteilungsblatt für Systematik und Taxonomie nder Latridiidae, 9: 1–15.

Sharp D (1902) Lathridiidae in Biologia Centrali Americana. Insecta Coleoptera 2(1): 626–638.

RESEARCH ARTICLE

A new genus and species of clingfish from the Rangitāhua Kermadec Islands of New Zealand (Teleostei, Gobiesocidae)

Kevin W. Conway[1,2], Andrew L. Stewart[3], Adam P. Summers[4,5]

1 *Department of Wildlife and Fisheries Sciences and Biodiversity Research and Teaching Collections, Texas A&M University, College Station, TX 77843, USA* **2** *Research Associate, Ichthyology, Australian Museum Research Institute, 1 William Street, Sydney, NSW 2010, Australia* **3** *Museum of New Zealand Te Papa Tongarewa, 169 Tory Street, Wellington, New Zealand* **4** *Friday Harbor Laboratories, University of Washington, Friday Harbor, WA 98250, USA* **5** *Burke Museum of Natural History and Culture, University of Washington, Seattle, WA 98105, USA*

Corresponding author: *Kevin W. Conway* (kevin.conway@tamu.edu)

Abstract

Flexor incus, new genus and species, is described from 15 specimens (14.0–27.2 mm SL) collected from shallow (0–9 meters) intertidal and sub-tidal waters of the Rangitāhua Kermadec Islands, New Zealand. The new taxon is distinguished from all other members of the Gobiesocidae by a combination of characters, including a heterodont dentition comprising both conical and distinct incisiviform teeth that are laterally compressed with a strongly recurved cusp, an oval-shaped opening between premaxillae, a double adhesive disc with a well-developed articulation between basipterygia and ventral postcleithra, and many reductions in the cephalic lateral line canal system. The new taxon is tentatively placed within the subfamily Diplocrepinae but shares a number of characteristics of the oral jaws and the adhesive disc skeleton with certain members of the Aspasminae and Diademichthyinae.

Keywords

Introduction

> "*The discovery of this and several other new genera in recent years makes it necessary to reconsider the characterization and relationships of various subfamilies within the Gobiesocidae*" Briggs (1993: 197)

The family Gobiesocidae contains over 170 species and 50 genera of predominately small-bodied marine fishes found in coastal areas of the Atlantic and Indo-Pacific oceans (Briggs 1955; Conway et al. 2015), from the intertidal zone down to ~500 meters (Hastings and Conway 2017). Seven species also are known to inhabit freshwater streams in the Neotropics (Briggs and Miller 1960; Conway et al. 2017a). Commonly referred to as clingfishes, members of this family generally exhibit a well-developed ventral adhesive disc (formed by elements of the paired fins and paired-fin girdles; Guitel 1888), with which they can attach to smooth or even heavily structured substrates with great tenacity (Wainwright et al. 2013; Ditsche et al. 2014).

Clingfishes are considered archetypal crypto-benthic fishes (Brandl et al. 2018) and it is not surprising that new species continue to be discovered and described on an almost annual basis. Since 2010, this includes 19 new species (Fricke et al. 2010, 2015, 2016; Allen and Erdmann 2012; Moore et al. 2012; Sparks and Gruber 2012; Conway et al. 2014, 2017b, c, 2018; Fricke 2014; Craig et al. 2015; Shinohara and Katayama 2015; Bilecenoğlu et al. 2017; Fricke and Wirtz 2017; Hastings and Conway 2017; Fujiwara and Motomura 2018; Fujiwara et al. 2018), three of which were also considered to represent new genera at the time of description (Fricke 2014; Fricke et al. 2016; Conway et al. 2017b).

Specimens of a reportedly new species of clingfish have been known from the remote Rangitāhua Kermadec Islands (here after Kermadec Islands) of New Zealand since at least 1980s (Francis et al. 1987; Francis 1993) and have been referred to in recent literature as *Aspasmogaster* sp. (Stewart 2015; Trnski et al. 2015) and by the common name "Kermadec clingfish" (Stewart 2015). These specimens differ markedly in a number of characters from the currently recognized species of *Aspasmogaster*, a genus reported to date only from temperate Australia (Hutchins 1984, 2008), and from members of other Australasian and Indo-Pacific genera of the Gobiesocidae. The purpose of the present paper is to provide a formal description for the "Kermadec clingfish", which represents a new genus and species of the Gobiesocidae.

Materials and methods

Specimens used in this study were obtained from the following museum collections:

ANSP   Academy of Natural Sciences of Drexel University, Philadelphia
AMS   Australian Museum, Sydney

AIM   Auckland War Memorial Museum, Auckland
NMNZ   Museum of New Zealand Te Papa Tongarewa, Wellington
ROM   Royal Ontario Museum, Toronto
NMST-P   National Museum of Nature and Science, Tsukuba
SAIAB   South African Institute of Aquatic Biodiversity, Grahamstown
TCWC   Biodiversity Research and Teaching Collections, Texas A&M University, College Station
USNM   National Museum of Natural History, Washington D.C.
WAM   Western Australian Museum, Perth.

Head and body measurements reported follow Conway et al. (2014) and are expressed as percent of standard length (SL) or head length (HL). Adhesive disc papillae terminology follows Briggs (1955) and Hutchins (2008). Cephalic lateral line pore terminology follows Shiogaki and Dotsu (1983), except that we also use numbers to refer to individual pores following Conway et al. (2017b), with pores numbered along a particular canal from anterior to posterior or dorsal to ventral (lachrymal canal only). General osteological terminology follows that of Springer and Fraser (1976), except that we use the term anguloarticular instead of articular, anterior ceratohyal instead of ceratohyal, autopalatine instead of palatine, epicentral instead of epipleural (following Gemballa and Britz 1998), pharyngobranchial instead of infrapharyngobranchial, posterior ceratohyal instead of epihyal, and retroarticular instead of angular.

Select specimens were cleared and double stained (C&S) for bone and cartilage investigation using the protocol of Taylor and Van Dyke (1985). Select specimens were reversibly stained using cyanine blue following Saruwatari et al. (1997) to aid examination of adhesive disc papillae and cephalic lateral line canal pores. Specimens or parts thereof were observed and photographed using a ZEISS SteREO Discovery V20 stereomicroscope equipped with a ZEISS Axiocam MRc5 digital camera. Digital images were typically stacked using ZEISS Axiovision software. Computed tomography (CT) scans of select specimens were also obtained at the Karel F. Liem BioImaging Center (Friday Harbor Laboratories, University of Washington) using a Bruker (Billerica, MA) SkyScan 1173 scanner with a 1 mm aluminium filter at 60 kV and 110 µA on a 2240 × 2240 pixel CCD at a resolution of 8.8 µm. Specimens were scanned simultaneously in a 50ml plastic Falcon tube (Corning, NY), in which they were wrapped with cheesecloth moistened with ethanol (70%) to prevent movement during scanning. The resulting CT data were visualised, segmented, and rendered in Horos (www.horosproject.org) and Amira (FEI). The premaxilla and dentary from the right side were removed from select specimens and prepared for scanning electron microscopy (SEM) following the protocol outlined in Conway et al. (2015). Coated specimens were examined using a Tescan Vega3 SB scanning electron microscope. All digital images were processed using Adobe Photoshop and Adobe Illustrator.

Systematics

Flexor gen. n.
http://zoobank.org/23E32F56-CAF3-4B3D-938A-0BF6A590C070

Diagnosis. A genus of the Gobiesocidae differing from all other genera by a combination of characters, including: head and anteriormost part of body similar in width; a relatively elongate body with a small, double adhesive disc located beneath anteriormost part of body; an oval-shaped gap between premaxillae formed by a semicircular indentation along medial edge of premaxilla; premaxilla with a single row of teeth, comprising 2–3 peg-like, conical teeth anteriorly at, and adjacent to, symphysis and 10–12 strongly laterally compressed, incisiviform teeth with strongly recurved cusp, along outer margin of bone; lower jaw with a single row of 14–16 small, conical teeth with sharply pointed and slightly recurved tip; posterior tip of basipterygium expanded and articulating with anteromedial edge of ventral postcleithrum via a shallow concave facet; mandibular portion of preoperculo-mandibular lateral line canal absent; lachrymal canal with two pores; upper and lower lip simple, uniform in thickness along jaw margin.

Etymology. New Latin, anatomical term for muscles, from the Latin *flexus*, past participle of *flectere*, to bend. In reference to the great flexibility of clingfishes, many of which have the ability to bend the body so that the tail end comes to lie close to the head. Masculine.

Type species. *Flexor incus*, new species

Flexor incus sp. n.
http://zoobank.org/CFA9314B-78DB-4B46-9F7D-64BCD829E86D
Figs 1–10

Aspasmogaster sp.: Stewart 2015: 1539, 1544; Trnski et al. 2015: 473, 476, Table 1.

Holotype. **NMNZ P.060717**, 20.8 mm SL; New Zealand, Kermadec Islands, Raoul Island, Fishing Rock Landing (29°15'03.0"S, 177°54'12.0"W), 0–1 meters depth, 18 May 2011, M. Francis.

Paratypes. All Kermadec Islands. **AIM MA655142**, 1 (C&S), 20.0 mm SL; Raoul Island, North Meyer Islet, northwest side of island (29°14'40.4"S, 177°52'41.3"W), 0–1.3 meters depth, 13 May 2011. – **AIM MA655401**, 2, 18.0–24.0 mm SL; Raoul Island, Fishing Rock Landing (29°15'02.7"S, 177°54'11.7"W), 0–1 meters depth, 18 May 2011. – **AIM MA655316**, 1 (CT scan; https://doi.org/10.17602/M2/M56344), 23.0 mm SL; **AMS I.45807-001**, 1, 19.7 mm SL; **NMNZ P.049965**, 1, 24.3 mm SL; **NMNZ P.049966**, 1, 27.2 mm SL; Raoul Island, Herald Islets, west side of North Chanter Island (29°15'06.0"S, 177°51'21.0"W), 1–12 meters depth, 16 May 2011, A. Ballance.

Figure 1. *Flexor incus*, NMNZ P.060717, holotype, 20.8 mm SL; New Zealand, Kermadec Islands, Raoul Island.

– **AMS I.45823-010**, 1, 19.1 mm SL; same as holotype. – **NMNZ P.017760**, 1, 14.0 mm SL; Raoul Island, rockpool on Fishing Rock Landing (29°15'S, 177°54'W) 17 Aug 1985. – **NMNZ P.041114**, 1, 22.4 mm SL; Raoul Island, Meyer Islet (29°14'48.0"S, 177°52'51.0"W), 0–1.5 meters depth, 7 November 2004. – **NMNZ P.024500**, 1, not measured; Fishing Rock, Raoul Island (29°10'S, 177°54'W), November 1980 – **NMNZ P.025315**, 1, 19.4 mm SL; Raoul Island (29°14'55.0"S, 177°58'22.6"W), 1975. – **NMNZ P.028570**, 1, 27.2 mm SL; Raoul Island, Meyer Islet, Boat Harbour (29°14'54.0"S, 177°52'12.0"W), 0–3 meters depth, 03 June 1992. – **NMNZ P.029570**, 1, 27.1 mm SL; Meyer Islet, Boat Harbour (29°14'54.0"S, 177°52'12.0"W), 03 June 1992. – **NMNZ P.050069**, 1, 21.1 mm SL; Raoul Island, Fishing Rock Landing (29°15'04.6"S, 177°54'12.9"W), 1 meter depth, 14 September 2011. – **NMNZ P.057561**, 1, 16.9 mm SL; Raoul Island (29°14'55.2"S, 177°58'22.8"W), 1975.

Diagnosis. See generic diagnosis.

Description. General body shape as in Figures 1, 2. Morphometric characters listed in Table 1. Head relatively small (less than one third of body length), slightly

Table 1. Select morphometric characters obtained from the holotype and six paratypes of *Flexor incus*. Ranges include value obtained for holotype.

	Holotype	Range	Mean	St. Dev.
Standard Length (SL)	20.8	16.9–27.2	–	–
In % of SL				
Head length (HL)	31.7	29.4–34.5	31.9	1.9
Body depth	14.9	10.0–14.9	13.6	1.9
Predorsal length	75.5	73.3–82.2	76.3	2.9
Preanal length	72.6	72.6–77.7	74.2	1.7
Preanus length	63.0	60.7–63.0	61.7	0.9
Anus to disc	15.9	14.1–18.6	16.8	1.5
Anus to anal fin	8.9	8.0–9.7	8.6	0.8
Caudal peduncle length	10.1	8.0–10.1	8.9	0.9
Caudal peduncle depth	11.1	8.2–11.1	9.4	0.9
Disc length	18.8	17.8–26.0	20.2	3
Disc width	16.3	16.3–20.1	17.7	1.3
In % of HL				
Head depth at orbit	34.8	25.9–34.8	29.1	3.4
Head width at orbit	47.0	42.6–51.9	47.6	3.1
Head width at widest point	60.6	52.9–67.3	58.3	5.4
Interorbital width	21.7	19.5–23.1	21.4	1.5
Snout length	30.3	28.1–36.5	32.2	2.7
Eye diameter	21.2	17.2–22.2	20.1	1.7

dorso-ventrally compressed. Body moderately elongate, circular in cross-section anteriorly, becoming increasingly laterally compressed posteriorly. Widest point of body immediately behind head; as wide as widest point of head. Body width tapering gradually posteriorly. Body depth relatively uniform anterior to dorsal and anal fins; shallowest along caudal peduncle. Eye large, positioned on dorsolateral surface of head; orbit barely visible in ventral view. Centre of eye closer to tip of snout than to posterior margin of operculum. Snout of moderate length, broad, anterior margin rounded (Figs 1–3). Anterior nostril a small tubular opening (Figure 3). Posterior nostril surrounded by a low, fleshy rim; situated along anterodorsal margin of orbit (Figure 3). Gill membranes free from isthmus.

Mouth terminal, small; posterior tip of upper jaw reaching imaginary vertical line through anterior nostril when mouth closed. Upper and lower lip narrow; upper lip uniform in thickness along length of jaw; lower lip thicker along lateral margins of lower jaw, narrower at jaw symphysis (Figure 3). Upper jaw slightly wider and longer than lower jaw, creating a narrow gap between teeth of upper and lower jaws when jaws closed (Figure 5). Premaxilla with a single row of teeth, comprising 2–3 peg-like, conical teeth anteriorly at and adjacent to symphysis, and 10–12 strongly laterally compressed incisiviform teeth, each with a single strongly recurved cusp, along outer margin of bone (Figure 7A–C). Dentary with a single row of 14–16

Figure 2. *Flexor incus*, Te konui Point, Raoul Island, Kermadec Islands, 28 meters depth, photographed by R. Robinson (www.depth.co.nz) during the 2011 Kermadec Islands Biodiscovery Expedition, a project led by the Auckland Museum. Specimen not retained.

small, conical teeth with sharply pointed and slightly recurved tip (Figure 7D). Pharyngeal jaws comprising patch of 4–6 small conical teeth with slightly recurved tips on pharyngobranchial toothplate 3 and row of 3–5 small conical teeth with slightly recurved tips along ceratobranchial 5 (Figure 8D). 5–6 small triangular gill rakers located along anterior and posterior edge of ceratobranchials 2–3 and anterior edge of ceratobranchial 4; one or two tiny gill rakers located along anterior edge of ceratobranchial 1 (Figure 8D). Paired rows of gill filaments (holobranch) on gill arches I-III (three gill filaments of Briggs 1955). Basihyal an elongate rod, widest posteriorly at point of articulation with dorsal hypohyals; anterior edge tipped with cartilage (Figure 8C). Six brachiostegal rays (Figure 8A); anteriormost ray sepa-
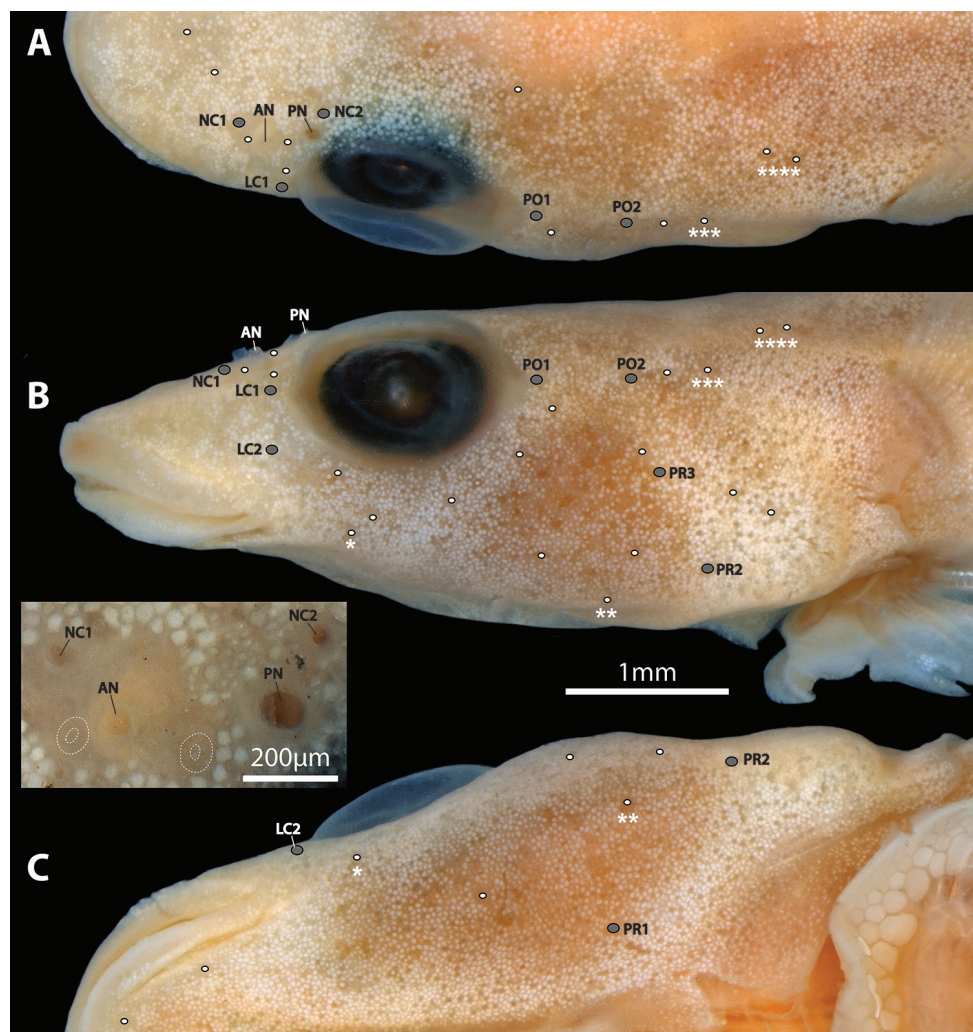
Figure 3. Head of *Flexor incus* (NMNZ P.025315, paratype, 19.4 mm SL) in dorsal (**A**), lateral (**B**), and ventral (**C**) view highlighting position of cephalic lateral line canal pores (grey circles) and superficial neuromasts (white circles) on the left side of the head. Close-up view of nostrils shown in inset image between **B** and **C** Superficial neuromasts highlighted by white dotted line in inset image. Single scale bar shared between **A–C**. Skin on ventral surface of head damaged on right side of specimen. Superficial neuromasts on surface of body not highlighted. Asterisks (*, **, ***, ****) label individual superficial neuromasts that are visible in different views. Abbreviations: AN, anterior nostril; LC1-2, lachrymal canal pores 1–2; NC1–2, nasal canal pores 1–2; PN, posterior nostril; PO1–2, postorbital canal pores 1–2; PR1–3, preopercular canal pores 1–3.

rate from hyoid bar; second ray articulating medially with hyoid bar along anterior ceratohyal; posterior rays articulating with hyoid bar laterally, including two along posteriormost part of anterior ceratohyal, one straddling junction between anterior and posterior ceratohyals, and posteriormost along anteriormost part of posterior
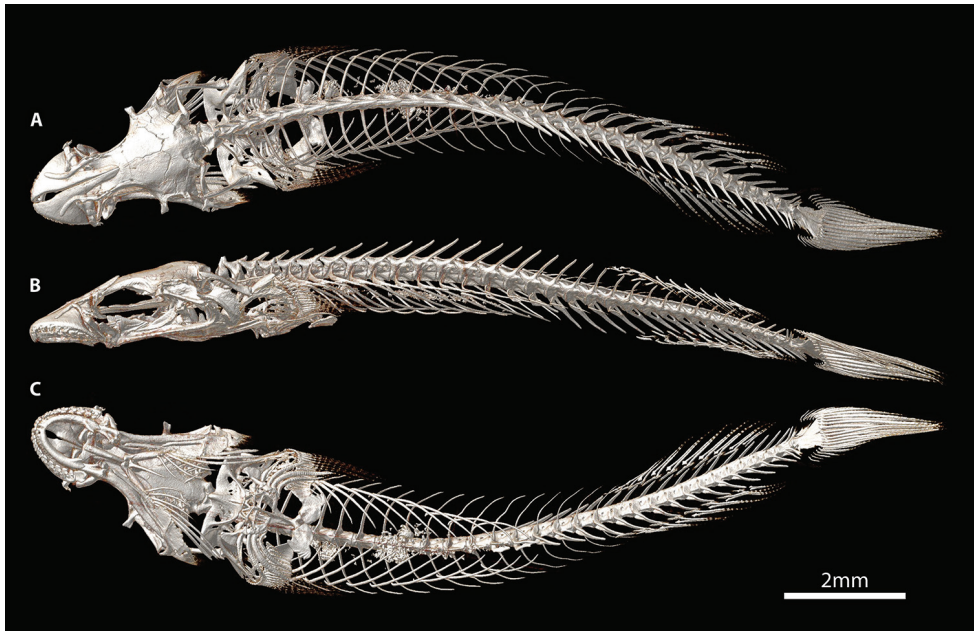
Figure 4. CT scanned skeleton of *Flexor incus*, AIM MA655316, paratype, 23.0 mm SL. **A** Dorsal view.
B Lateral view (left side) **C** Ventral view.

ceratohyal (Figure 8B). Anteriormost branchiostegal ray shorter than posterior rays.
Three posteriormost branchiostegal rays similar in width and length, approximately
twice as long and thick as anteriormost ray. Intervening rays intermediate in width
and length (Figure 8B).

Cephalic lateral-line system with 2 pores in nasal canal; 2 pores in postorbital ca-
nal; 2 pores in lachrymal canal; 3 pores in preopercular canal (Figure 3). Mandibular
canal absent. Canal pores minute; typically flush with surface of skin and difficult to
locate. Supraorbital canals (including nasal canal plus anteriormost region of postorbi-
tal canal of Shiogaki and Dotsu 1983) connected across midline via epiphyseal com-
missure (Figure 6A). Superficial neuromasts on surface of head not arranged in obvious
rows (Figure 3); each surrounded by a shallow groove.

Dorsal-fin rays 9 or 10. Anal-fin rays 8 or 9 (first in serial or supernumerary as-
sociation with anteriormost proximal-middle radial). Principal caudal-fin rays 5+5,
dorsal procurrent rays 6 or 7, ventral procurrent rays 6. Pectoral-fin rays 24 or 25;
uppermost ray a tiny splint-like element comprised of a single hemitrichium. Pelvic-
fin rays I, 4. All fins rays, excluding anteriormost 4–5 procurrent caudal-fin rays, un-
branched and segmented; anteriormost 4–5 procurrent caudal-fin rays unsegmented,
azygous elements. Caudal fin marginally truncate, tips of principal caudal-fin rays ex-
tended beyond fin margin. Caudal-fin skeleton comprised of upper and lower hypural
plates; epural triangular, with broad cartilaginous dorsal margin; parhypural absent,
parahypural cartilage roughly triangular (Figure 10). Neural and hemal spine of PU2
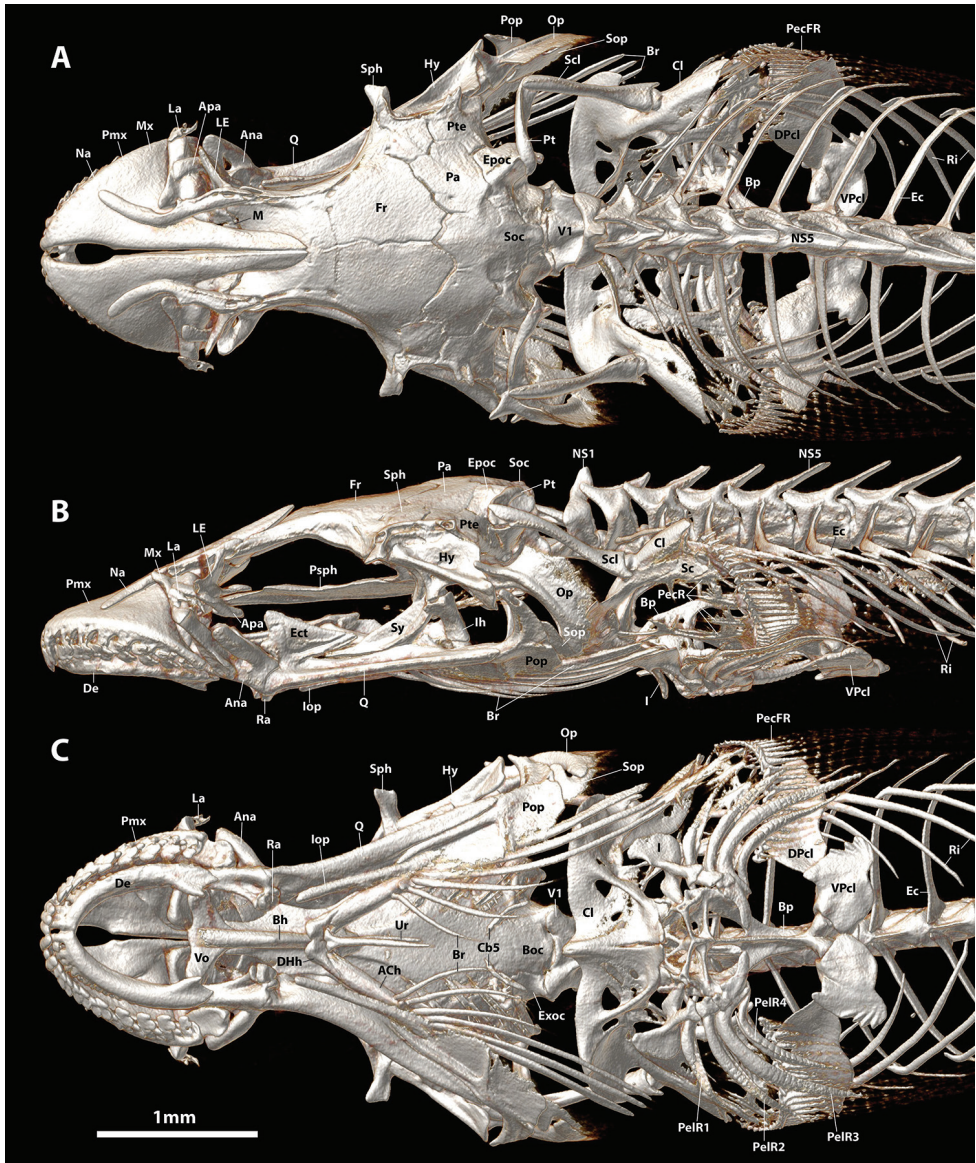
Figure 5. CT scanned anterior skeleton of *Flexor incus*, AIM MA655316, paratype, 23.0 mm SL. **A** Dorsal view **B** Lateral view (left side) **C** Ventral view. Abbreviations: ACh, anterior ceratohyal; Ana, anguloarticular; Apa, autopalatine; Boc, basioccipital; Bp, basipterygium; Br, branchiostegal rays; Cb5, ceratobranchial 5; Cl, cleithrum; DHh, dorsal hypohyal; DPcl, dorsal postcleithrum; Ec, epicentral; Ect, ectopterygoid; Epoc, epiotic; Exoc, exoccipital; Fr, frontal; Hy, hyomandibular; I, pelvic-fin spine; Iop, interopercle; La, lachrymal; LE, lateral ethmoid; M, mesethmoid; Na, nasal; NS1, 5, neural spine of vertebral centrum 1, 5; Op, opercle; Pa, parietal; PecR, pectoral radial; PecFR, pectoral-fin ray; PelFR1-4, pelvic-fin ray 1–4; Pop, preopercle; Pro, prootic; Psph, parasphenoid; Pt, posttemporal; Pte, pterotic; Q, quadrate; Ra, retroarticular; Ri, rib; Sc, scapula; Scl, supracleithrum; Soc, supraoccipital; Sop, subopercle; Sph, sphenotic; Ur, urohyal; V1, vertebral centrum 1; Vo, vomer; VPcl, ventral postcleithrum.

Figure 6. Neurocranium of *Flexor incus*, AIM MA655142, paratype, 20.0 mm SL. **A** Dorsal view **B** Lateral view (left side) **C** Ventral view. Abbreviations: Boc, basioccipital; Ec, epicentral; EpC, epiphyseal commissure of supraorbital canal; Epoc, epiotic; Exoc, exoccipital; Fr, frontal; La, lachrymal; LE, lateral ethmoid; M, mesethmoid; Na, nasal; NS1, neural spine of vertebral centrum 1; Pa, parietal; Pro, prootic; Psph, parasphenoid; Pte, pterotic; SC, supraorbital canal; Soc, supraoccipital; Sph, sphenotic; V1, vertebral centrum 1; Vo, vomer.
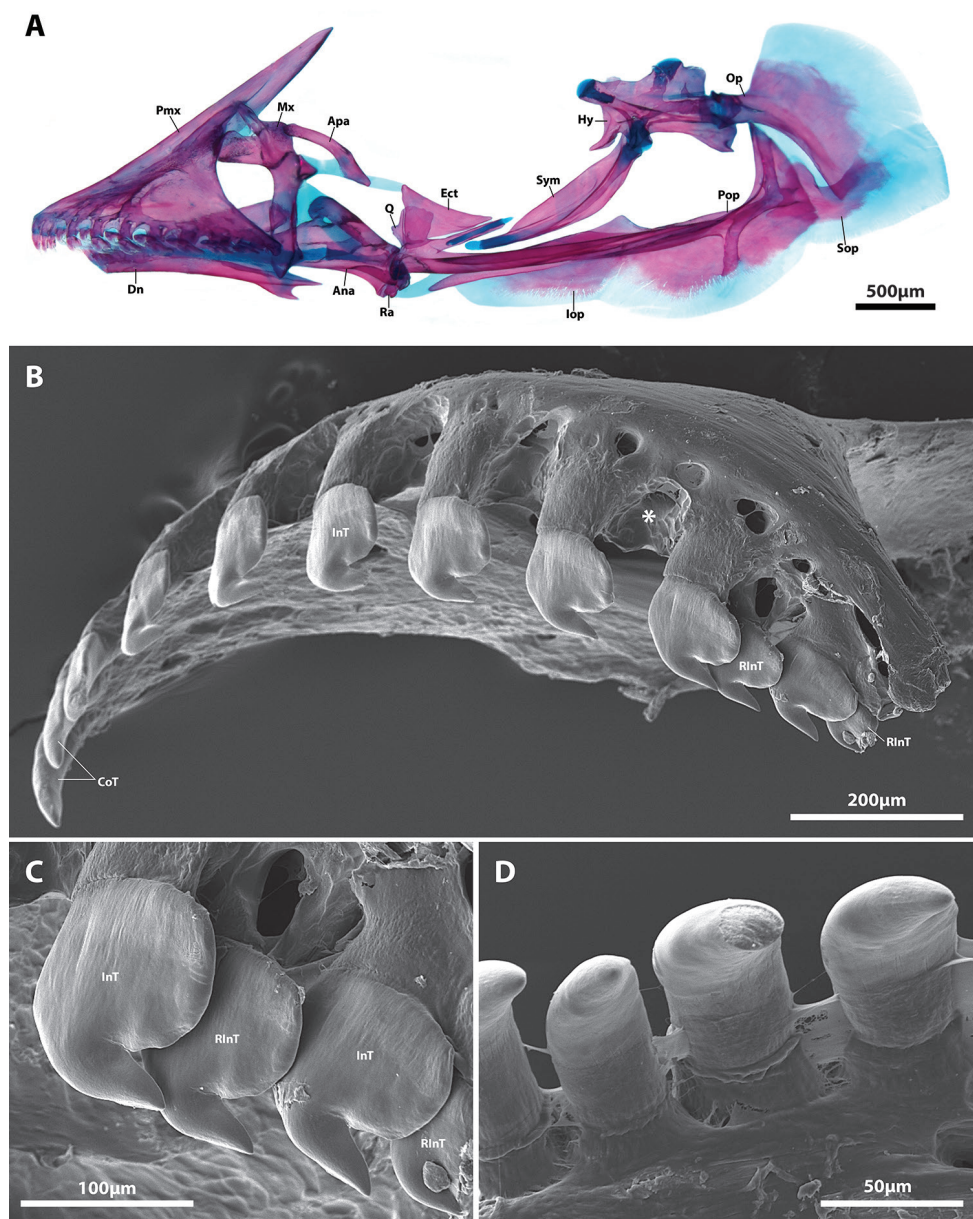
Figure 7. *Flexor incus,* AIM MA655142, paratype, 20.0 mm SL. **A** Hyopalatine arch and opercular series, right side in lateral view (image reversed) **B** Scanning electron micrograph of premaxilla, right side in oblique lateral view (image reversed). Asterisk (*) highlights location of replacement tooth crypt **C** Close up of posteriormost incisiform teeth of premaxilla shown in **A D** Scanning electron micrograph of conical teeth located close to middle of dentary, right side in medial view (image reversed). Abbreviations: Ana, anguloarticular; Apa, autopalatine; CoT, conical tooth; Dn, dentary; Ect, ectopterygoid; Hy, hyomandibular; InT, incisiform tooth; Iop, interopercle; Mx, maxilla; Op, opercle; Pop, preopercle; Q, quadrate; Ra, retroarticular; RInT, replacement incisiform tooth; Sop, subopercle; Sym, symplectic.
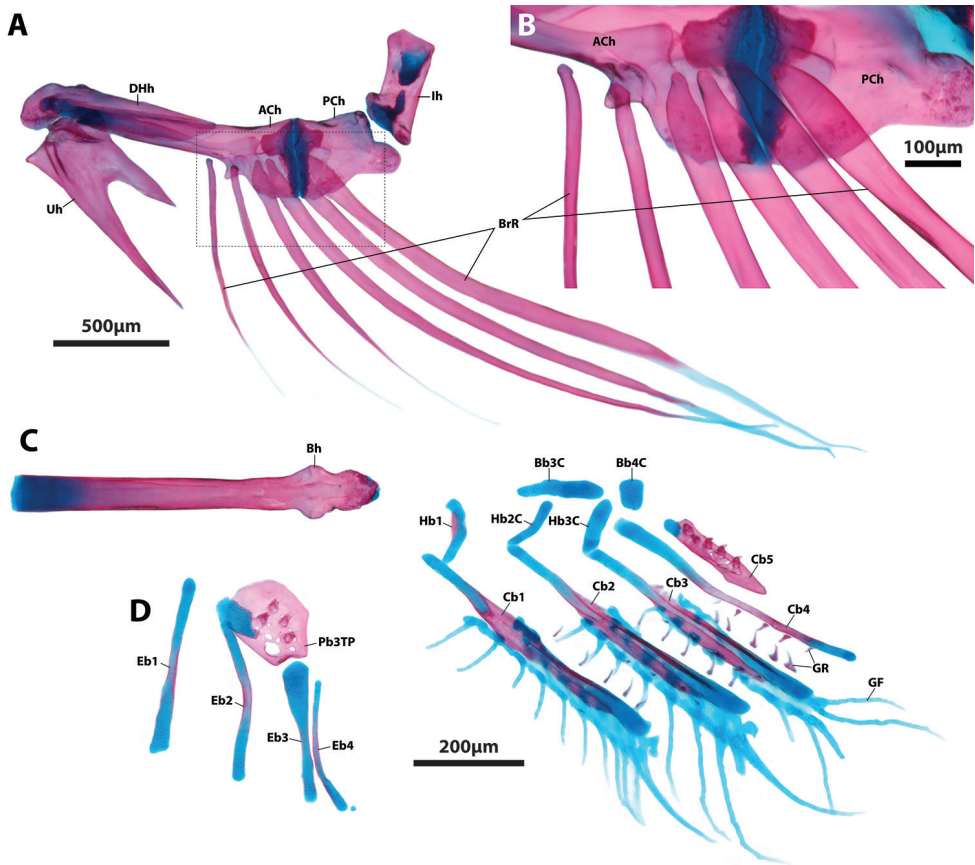
Figure 8. Hyoid bar (**A–B**) and gill arches (**C–D**) of *Flexor incus,* AIM MA655142, paratype, 20.0 mm SL. **A** Hyoid bar, right side in lateral view (image reversed) **B** Close up of box in **A** showing articulating between heads of branchiostegal rays and hyoid bar **C** Lower gill arches in dorsal view, paired elements of right side omitted **D** Upper gill arches of left side in ventral view. A single scale bar shared between **C** and **D**. Abbreviations: ACh, anterior ceratohyal; Bb3-4C, basibranchial 3 or 4 cartilages; Bh, basihyal; BrR, branchiostegal rays; Cb1-5, ceratobranchial 1-5; DHh, dorsal hypohyal; EB1-4, epibranchials 1-4; GF, gill filament; GR, gill raker; Hb1, hypobranchial 1; Hb2-3C, hypobranchial 2 or 3 cartilage; Pb3TP, pharyngobranchial 3 toothplate; Uh, urohyal.

bifurcated in single CT scanned specimen (Figure 4); singular in C&S specimen (Figure 10). Dorsal-fin origin situated slightly anterior to imaginary vertical line through anal-fin origin (Figs 1, 4). First dorsal-fin pterygiophore inserted between neural spines of vertebrae 17/18. First anal-fin pterygiophore inserted between hemal spines of vertebrae 18/19 or 19/20. Total number of vertebrae 33, consisting of 13 or 14 abdominal vertebrae and 19 or 20 caudal vertebrae (Figure 4). Ribs 12, associated with vertebrae 3–14. Epicentrals 20, associated with vertebrae 2–21.

Adhesive disc small (18–26% of SL), double (Figure 9A); anterior margin weakly crenulated medially, becoming smooth at point corresponding to location of expanded
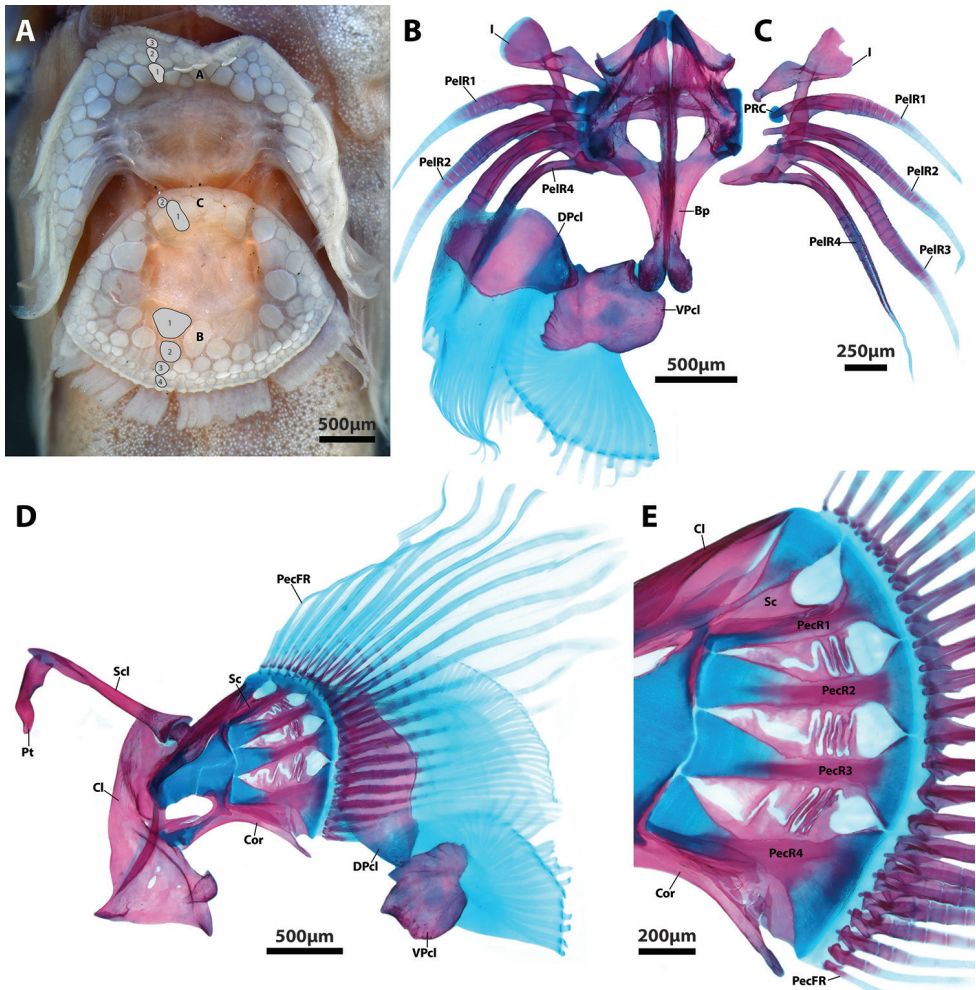
Figure 9. Surface features of the adhesive disc (**A** NMNZ P.025315, paratype, 19.4 mm SL) and internal supporting skeleton of the paired-fin girdles (**B–E** AIM MA655142, paratype, 20.0 mm SL) of *Flexor incus*. **A** Adhesive disc in ventral view (anterior to top of page); a single row of papillae highlighted in grey in each region (A–C) of the adhesive disc **B** Adhesive disc supporting skeleton, including elements of the pelvic and pectoral-fin girdle in dorsal view (anterior to top of page); postcleithra and pelvic-fin rays of the right side removed **C** Pelvic-fin rays of right side in dorsal view (anterior to top of page) **D** Pectoral-fin girdle of right side in medial view (anterior to left) **E** Close-up of elements of the pectoral-fin endoskeleton articulating with pectoral-fin rays of the right side in medial view (anterior to left). Abbreviations: A, disc region A; B, disc region B; Bp, basipterygium; C, disc region C; DPcL, dorsal postcleithrum; I, pelvic-fin spine; PecR1–4, pectoral radial 1–4; PecFR, pectoral-fin ray; PelR1–4, pelvic-fin rays 1–4 VPcL, ventral postcleithrum.

tip of spinous ray; posterior margin bordered by a broad, thin and weakly crenulated skin flap. Skin of posterior flap delicate, easily damaged; supported internally by fimbrae of ventral postcleithrum. Disc region A with 3–4 transverse rows of papillae. Disc region B with 4–5 transverse rows of papillae. Disc region C with 2–3 rows of papillae.
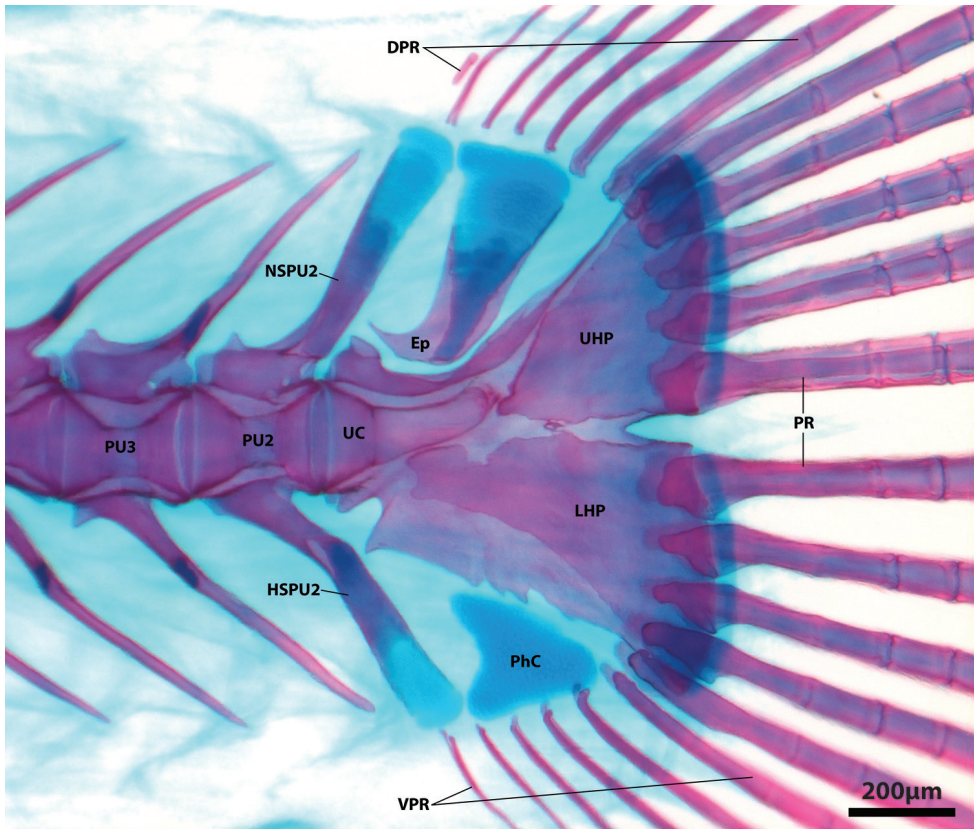
Figure 10. Caudal-fin skeleton (left side, lateral view) of *Flexor incus*, AIM MA655142, paratype, 20.0 mm SL. Abbreviations: DPR, dorsal procurrent caudal-fin rays; Ep, epural; HSPUS, hemal spine of preural centrum 2; LHP, lower hypural plate; NSPU2, neural spine of preural centrum 2; PhC, parhypural cartilage; PR, principal caudal-fin ray; PU2-3, preural centrum 2, 3; UC, ural centrum; UHP, upper hypural plate; VPR, ventral procurrent caudal-fin ray.

Papillae of disc region A decreasing in diameter gradually towards outer margin of disc. Papillae of disc region B and C decreasing in diameter towards outer margin of inner disc. Decrease in size of papillae of disc region C abrupt, with papillae of inner row 2–3 times larger than papillae of outer rows. Dorsal postcleithrum a well ossified shield-shaped bone with ~25 long, poorly ossified and distally bifurcated fimbrae (Figure 9B). Ventral postcleithrum well ossified, irregular in shape; approximately equal in size to dorsal postcleithrum (Figure 9B). ~20 long, poorly ossified and distally bifurcated fimbrae restricted to posterolateral margin of ventral postcleithrum; point of fimbrae bifurcation located distally on medial fimbrae, shifting gradually to a more proximal location on lateral fimbrae. A strong articulation between anteromedial edge of ventral postcleithrum and posterior tip of basipterygium (Figs 5B, 9B). Skin associated with last pelvic-fin ray attaching to base of pectoral fin opposite 5th–6th lowermost pectoral-fin rays. Skin over base of ventral pectoral-fin rays smooth. Pectoral radials with well-

developed bony struts along ventral (pectoral radial 1), dorsal (pectoral radial 4), or both ventral and dorsal margins (pectoral radials 2 and 3) that interdigitate with struts borne on element(s) directly above and/or below (Figure 9D, E).

Colouration. In alcohol, head and body background colour typically uniformly pale cream to yellow (Figure 3). Holotype (Figure 1) has retained pinkish purple colour of live individuals and is an exception. Fins hyaline.

In life (Figure 2), body uniformly pinkish purple to grey, with diffuse, pale markings ranging from bars to irregular blotches. Head pinkish purple to grey, with diffuse, pale areas around nostrils and tip of snout. Iris red. Fins transparent.

Distribution and habitat. Known to date only from intertidal and subtidal waters of the Kermadec Islands (Figure 11), including Raoul Island (type locality) and L'Esperance Rock. The majority of available specimens were collected from rock pools and from shallower subtidal areas (down to 9 meters) over rock and coral rubble substrates using ichthyocides (Stewart 2015). However, a single specimen of the new species has been observed (and photographed) at 28 meters in depth (Figure 2).

Etymology. *Incus* is the Latin word for anvil, in reference to the anvil-like outline of Raoul Island, the largest island in the Kermadec archipelago and type locality of the new species. A noun in apposition.

Gut content. Hard and irregular shaped items ranging in size from 50–300 μm are scattered throughout the stomach of the CT scanned individual (Figure 12A). Smaller elements have smooth surfaces and could not be identified. Several of the larger elements appear to exhibit a porous (potentially stereomic) surface and are tentatively identified as echinoderm remains. Hard elements inside the stomach of the single C&S individual survived the clearing and staining process and could be dissected and photographed (Figure 12B, C). These elements are tentatively identified as either stereomic ossicles from the terminal disc of an echinoid (Figure 12B) or ossicles from the body of a holothuroid (Figure 12C) suggesting that the new species consumes echinoderms or parts of echinoderms.

Discussion

The Kermadec Islands are a group of tiny remote islands almost 1,000 km from New Zealand, about half way between Tonga and Auckland, and lie between 29°15'S and 31°21'S. The Kermadec-Tonga arc is the longest submarine arc on the planet, running 2,500 km along the boundary of the Pacific and Australian Plates. It is a region of high geothermal activity with 83% of investigated volcanic centres venting (de Ronde et al. 2007). Directly to the east of the ridge lies the Kermadec Trench, the fourth deepest in the world which reaches to ca 10,000 meters deep at the deepest point. The Kermadec Islands constitute a series of four small emergent islands (Raoul, Macauley, Curtis, and Nugent) and two large rocks (L'Esperance and Havre). The largest of these islands is Raoul Island (2,040 ha, rising to 520 m asl) and the smallest L'Esperance Rock (4.8 ha, 70 m als) (Trnski and de Lange 2015). Havre Rock only just breaks the surface at
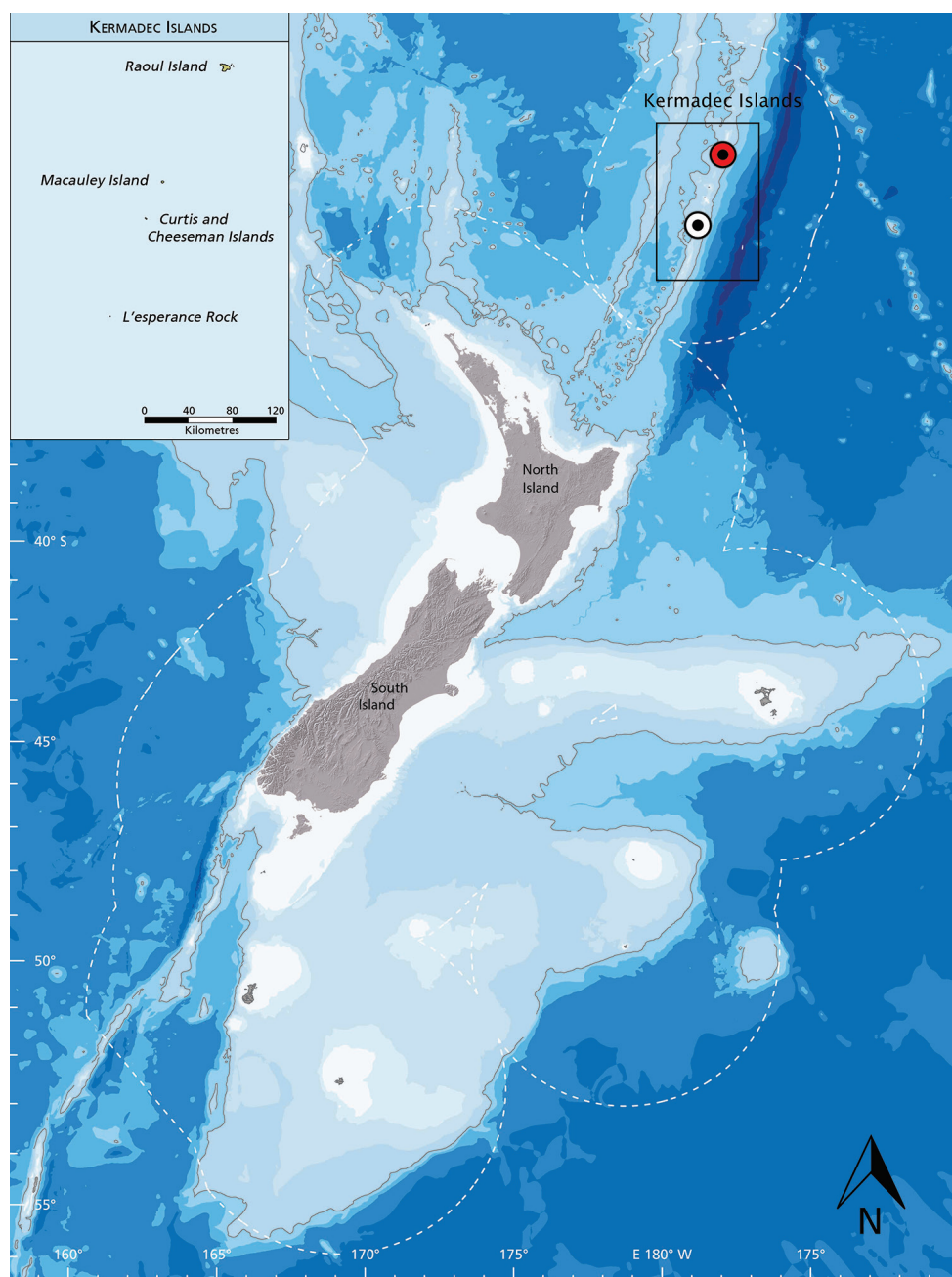
Figure 11. Distribution of *Flexor incus*. Type locality in red.

low tide. The total land area of these islands and rocks is ca. 33 km² (Mortimer and Campbell 2014). The cones have had a highly dynamic recent history with explosive emergence and collapse (Lloyd et al. 1996). In spite of geothermal activity and remote-
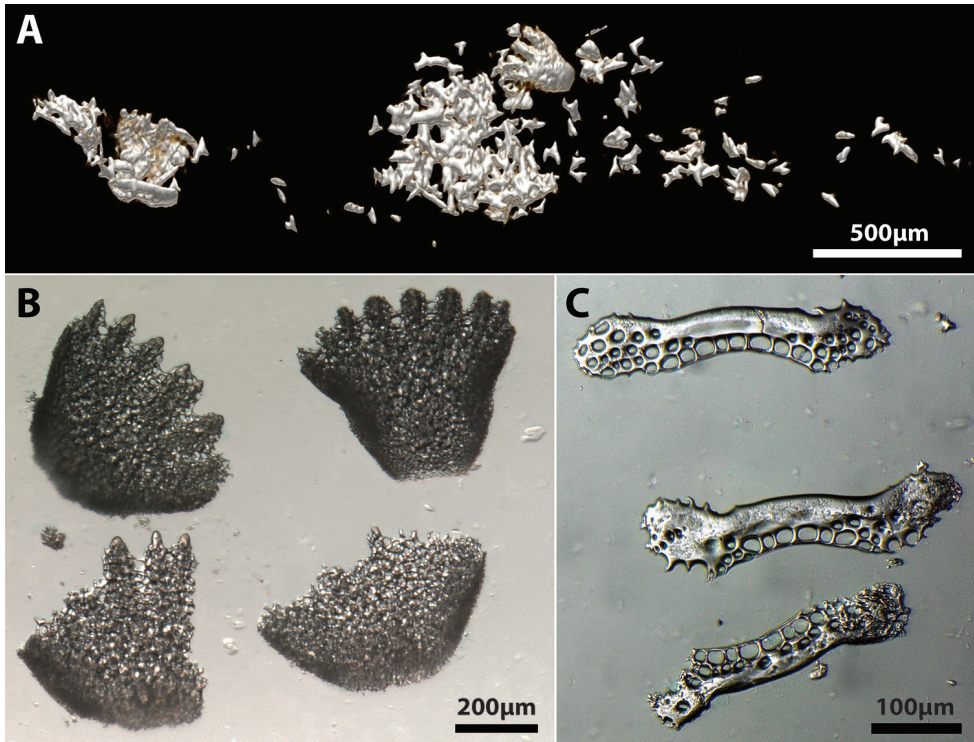
Figure 12. Gut content of *Flexor incus*. **A** Hard gut content of AIM MA655316, paratype, 23.0 mm SL, as revealed by CT scanning. Isolated elements from the gut of AIM MA655142, paratype, 20.0 mm SL **B** Stereomic ossicles tentatively identified as elements from the terminal disc of an echinoid **C** Rod-like elements tentatively identified as ossicles from the body of a holothuroid.

ness, the Kermadec Ridge and adjacent trench is inhabited by over 2,000 taxa (Duffy and Ahyong 2015) including 397 species of fishes (Te Papa unpublished records), of which nine are known to be endemic to the shelf (0–200 m depth). These include *Anarchias supremus*, *Microbrotula punicea*, *Lepidotrigla robinsi*, *Hypoplectrodes* sp. n., *Enneapterygius kermadecensis*, *Eviota kermadecensis*, *Arnoglossus* sp. n., *Lophonectes* sp. n., and the new clingfish species described herein (Roberts et al. 2015; Duff and Ahyong 2015; Te Papa unpublished records).

Specimens of *Flexor incus* have been referred to previously as *Aspasmogaster* sp. (Stewart 2015; Trnski et al. 2015). This taxonomic assignment, considered "tentative" by Stewart (2015), was based on preliminary attempts to identify the new species by B. Hutchins in 1980s (A. Stewart pers. obs.). *Aspasmogaster* is currently represented by four species (viz. *A. costata*, *A. liorhynchus*, *A. occidentalis* and *A. tasmaniensis*) and restricted to coastal areas of temperate Australia (Hutchins 1984; Hutchins 2008). The new species differs most obviously from *Aspasmogaster* by features of the oral jaw dentition, including both the arrangement (teeth in both jaws arranged in a single row vs. teeth in both jaws arranged in a broad patch anteriorly, tapering to a single row
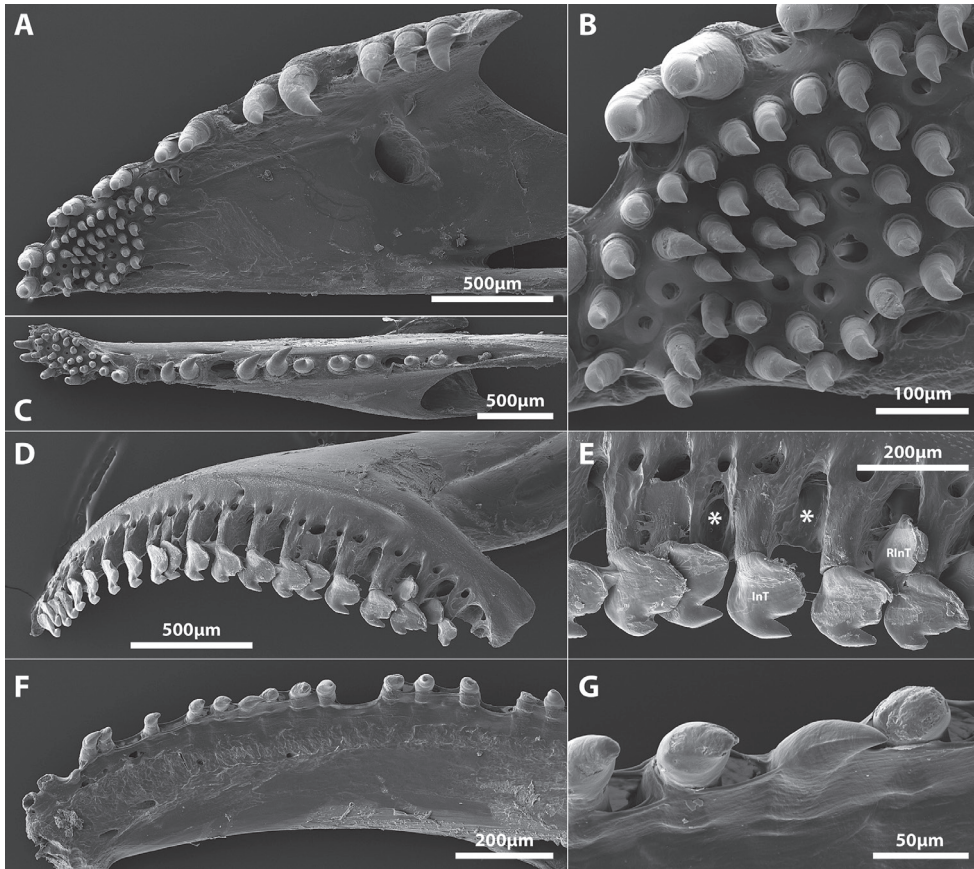
Figure 13. Scanning electron micrographs of the tooth-bearing oral jaw bones of *Aspasmogaster costata* (AMS I.19103-015, 32.0 mm SL) and *Lepadichthys coccinotaenia* (SAIAB 49396, 31.0 mm SL). **A** Premaxilla of *A. costata*, right side in ventral view (image reversed) **B** Close up of lingual toothpatch on premaxilla of *A. costata* shown in **A** **C** Dentary of *A. costata*, right side in ventral view (image reversed) **D** Premaxilla of *Lepadichthys coccinotaenia*, right side in lateral view (image reversed) **E** Close up of incisiviform teeth located on posterior part of premaxilla of *L. coccinotaenia* shown in **D** Asterisks (*) highlight locations of crypts associated with dislodged replacement teeth **F** Dentary of *Lepadichthys coccinotaenia*, right side in medial view **G** Close up of conical teeth located along midregion of dentary of *L. coccinotaenia* shown in **F** Abbreviations: InT, incisiviform tooth; RInT, replacement incisiviform tooth.

posteriorly; Figure 13A, C) and the type of teeth present on the premaxilla (*Flexor* is a heterodont with both conical and incisiviform teeth on the premaxilla [Figure 7A, B] vs. premaxilla with conical teeth only [Figure 13A, B]). It can be further distinguished from *Aspasmogaster* by having an oval opening between the premaxillae formed by a characteristic indentation along the medial edge of each premaxilla (vs. medial edge of premaxilla straight, premaxillae abutting along entire medial edge or separated only by a narrow gap [Figure 14A]), simple lips, both of which are relatively thin and uniform in thickness along the length of the jaws (vs. lower lip expanded adjacent to the sym-
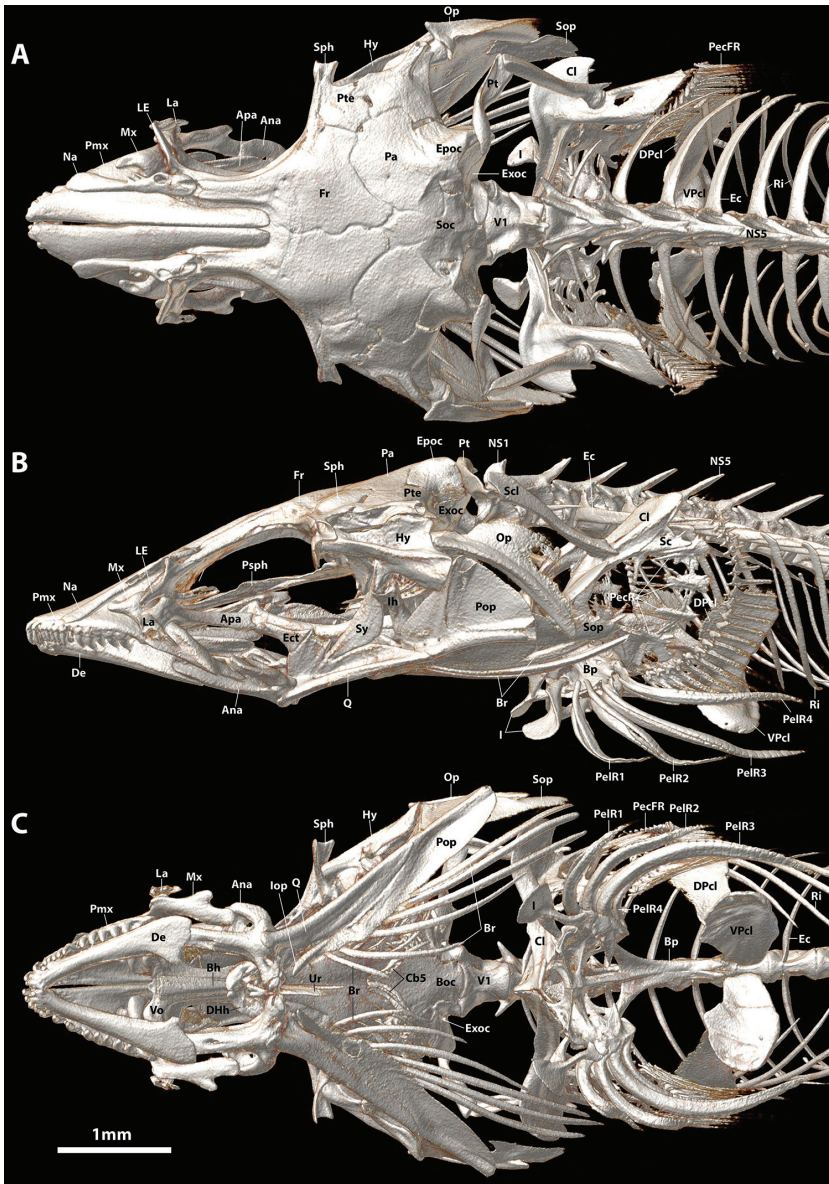
Figure 14. CT scanned anterior skeleton of *Aspasmogaster costata*, TCWC 17166.01, 30.0 mm SL. **A** Dorsal view **B** Lateral view (left side) **C** Ventral view. Abbreviations: ACh, anterior ceratohyal; Ana, anguloarticular; Apa, autopalatine; Boc, basioccipital; Bp, basipterygium; Br, branchiostegal rays; Cb5, ceratobranchial 5; Cl, cleithrum; DHh, dorsal hypohyal; DPcl, dorsal postcleithrum; Ec, epicentral; Ect, ectopterygoid; Epoc, epiotic; Exoc, exoccipital; Fr, frontal; Hy, hyomandibular; I, pelvic-fin spine; Iop, interopercle; La, lachrymal; LE, lateral ethmoid; Na, nasal; NS1, 5, neural spine of vertebral centrum 1, 5; Op, opercle; Pa, parietal; PecR, pectoral radial; PecFR, pectoral-fin ray; PelFR1-4, pelvic-fin ray 1–4; Pop, preopercle; Pro, prootic; Psph, parasphenoid; Pt, posttemporal; Pte, pterotic; Q, quadrate; Ra, retroarticular; Ri, rib; Sc, scapula; Scl, supracleithrum; Soc, supraoccipital; Sop, subopercle; Sph, sphenotic; Ur, urohyal; V1, vertebral centrum 1; Vo, vomer; VPcl, ventral postcleithrum.

physis into a prominent fleshy fold in all four species of *Aspasmogaster*; upper lip also expanded and overlapping anterolateral margin of snout in *A. occidentalis*; Hutchins 1984), by features of the adhesive disc, including a lower number of transverse rows of papillae in all disc regions (3–4 rows in region A, 4–5 in region B and 2–3 in region C vs. 5–8 rows in region A, 6–9 in region B and 3–5 in region C; Briggs 1955; Hutchins 1984), a well-developed articulation between the posterior tip of the basipterygium and the anteromedial edge of the ventral postcleithrum (vs. basipterygium and ventral postcleithrum without contact; Figure 14C, see also Hutchins 1984: figure 5), and by features of the cephalic lateral line canals, including the absence (vs. presence) of the mandibular portion of the preoperculo-mandibular canal, and 2 (vs. 3) openings in the lachrymal canal.

Based on the characters listed in the key to the subfamilies of the Gobiesocidae (Briggs 1955: 10), *Flexor* would be considered a member of the Diplocrepinae, which in addition to *Aspasmogaster* is also hypothesised to include *Cochleoceps*, *Diplocrepis*, *Gastrocyathus*, *Gastrocymba*, *Gastroscyphus*, *Parvicrepis*, *Pherallodus* and *Propherallodus* (Briggs 1955; Shiogaki and Dotsu 1983; Hardy 1984; Fujiwara and Motomura 2018). The composition of this subfamily has been questioned previously by Briggs (1993) and we suspect that it is not monophyletic (see below). Regardless, *Flexor* can be distinguished from all of the aforementioned genera except *Pherallodus* and *Propherallodus* by features of the adhesive disc, including the absence (vs. presence) of papillae in region D and by having a well-developed articulation between the posterior tip of the basipterygium and the anteromedial edge of the ventral postcleithrum (vs. basipterygium and ventral postcleithrum without contact or with simple contact). It can be further distinguished from all but *Pherallodus* by the presence of strongly laterally compressed incisiviform teeth with a strongly recurved cusp, along the outer margin of the premaxilla (vs. simple peg-like conical teeth or strongly recurved conical teeth along the outer margin of the premaxilla), and from *Pherallodus* by the presence (vs. absence) of the preopercular portion of the preoperculo-mandibular canal, the lower jaw with conical teeth only (vs. lower jaw with both conical and incisiviform teeth), and by a complete field of papillae across the centre of region A and C of the adhesive disc (vs. papillae absent from centre of both region A and C) (Shiogaki and Dotsu 1983).

The characteristic type of incisiviform tooth present on the premaxilla of *Flexor* (Figure 7B, C) and *Pherallodus* is also present in some members of the Aspasminae (*Aspasmichthys* and *Pherallodichthys*) and the Diademichthyinae (*Diademichthys* and *Lepadichthys*) (Briggs 1955; Shiogaki and Dotsu 1983; Hayashi et al. 1986). This distinct type of incisiviform tooth appears to have been first described and illustrated by Briggs (1955: figure 71) for *Aspasma*, *Aspasmichthys, Diademichthys* and *Lepadichthys*. Briggs (1955) described these teeth as "highly compressed with reversed points [sic]" (pg. 137) or "broad with pointed reverse tips [sic]" (pg. 141). We have been unable to observe this characteristic type of incisiviform tooth in our C&S material of *Aspasma minima* (NMST-P 114701) but our observations on the dentition of *Aspasmichthys*, *Diademichthys* and *Lepadichthys* are congruent with those of Briggs (1955). In *Pherallodichthys meshimaensis, Aspasmichthys ciconiae* (Figure 16B), and some members of
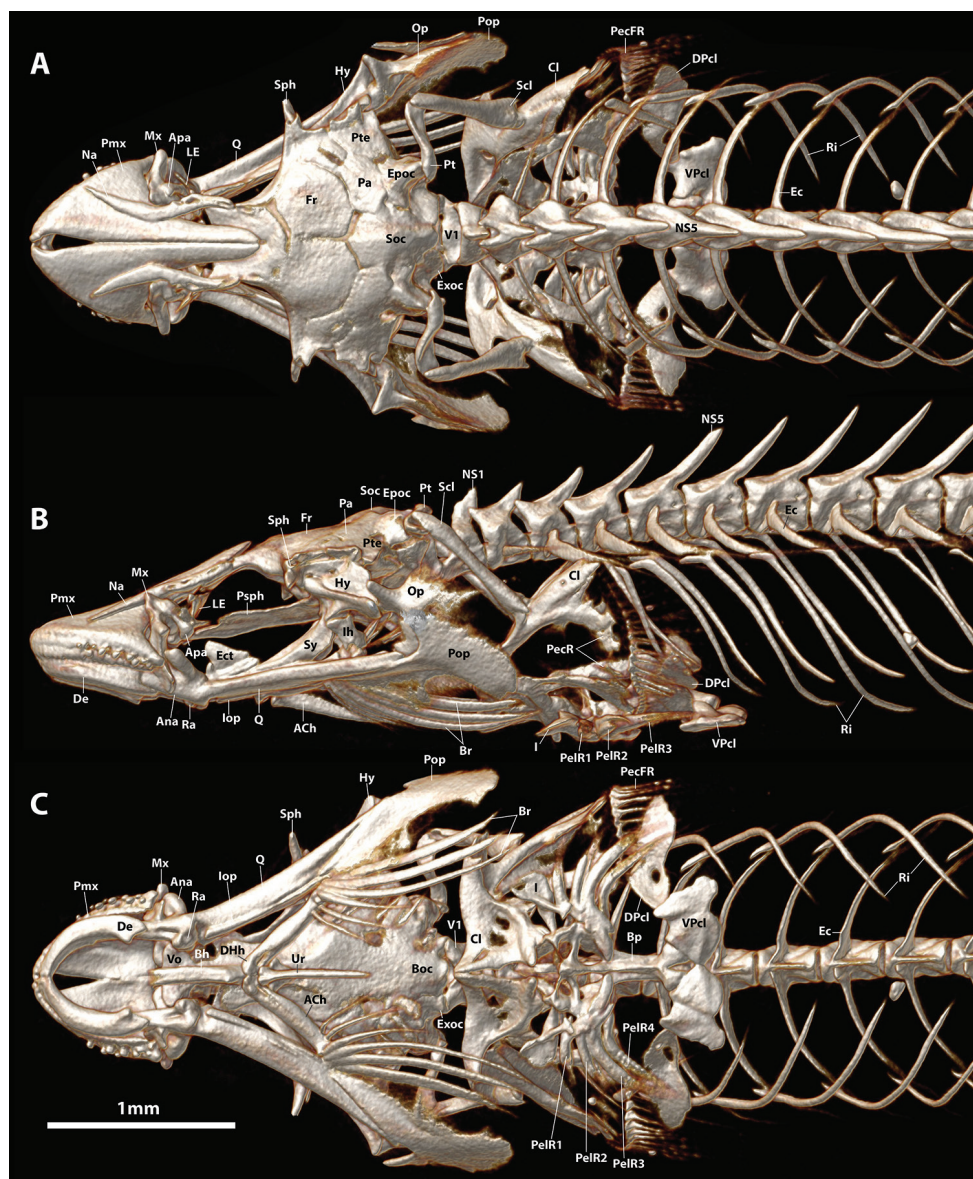
Figure 15. CT scanned anterior skeleton of *Pherallodus indicus*, NSMT-P 114703, 25.0 mm SL. **A** Dorsal view **B** Lateral view (left side) **C** Ventral view. Abbreviations: ACh, anterior ceratohyal; Ana, anguloarticular; Apa, autopalatine; Boc, basioccipital; Bp, basipterygium; Br, branchiostegal rays; Cl, cleithrum; DHh, dorsal hypohyal; DPcl, dorsal postcleithrum; Ec, epicentral; Ect, ectopterygoid; Epoc, epiotic; Exoc, exoccipital; Fr, frontal; Hy, hyomandibular; I, pelvic-fin spine; Iop, interopercle; LE, lateral ethmoid; Na, nasal; NS1, 5, neural spine of vertebral centrum 1, 5; Op, opercle; Pa, parietal; PecR, pectoral radial; PecFR, pectoral-fin ray; PelFR1-4, pelvic-fin ray 1–4; Pop, preopercle; Pro, prootic; Psph, parasphenoid; Pt, posttemporal; Pte, pterotic; Q, quadrate; Ra, retroarticular; Ri, rib; Scl, supracleithrum; Soc, supraoccipital; Sph, sphenotic; Ur, urohyal; V1, vertebral centrum 1; Vo, vomer; VPcl, ventral postcleithrum.

Lepadichthys (e.g., *L. bolini*; Figure 17B) the incisiviform teeth are arranged in a single row along the outer margin of the premaxilla and, as in *Flexor,* are combined with a small number of peg-like conical teeth anteriorly (Shiogaki and Dotsu 1983; Hayashi et al. 1986). In other members of *Lepadichthys* (e.g., *L. frenatus* and *L. coccinotaenia*; Figure 13D, E) the entire upper jaw comprises only a single row of ca. 18–20 incisiviform teeth, though there is a clear gradation in the width of the incisiviform teeth and the distinctiveness of the tooth cusp along the length of the upper jaw, with those located more anteriorly being narrower with a less defined cusp than those located posteriorly (Figure 13D). In *Diademichthys*, incisiviform teeth are arranged in a single row along both the dentary and premaxilla (Briggs 1955; Hayashi et al. 1986, Figure 7H, 8H). In addition to this characteristic incisiviform tooth, *Aspasmichthys*, *Diademichthys*, *Lepadichthys*, *Pherallodichthys* and *Pherallodus* also share a complex articulation between the posterior tip of the basipterygium and the anteromedial edge of the ventral postcleithrum with *Flexor*. Additionally, and excluding *Pherallodichthys*, these taxa also share a characteristic oval opening between the premaxillae formed by a semicircular indentation along the medial edge of each premaxilla. This opening is relatively small and restricted to the anterior part of the premaxilla only in *Flexor* (Figure 5A, C), *Pherallodus* (Figure 15A, C), *Aspasmichthys* (Figure 16A, C) and *Diademichthys* (see Briggs 1955: fig. 81; Hayashi et al. 1986: fig. 7H) but is greatly enlarged in the species of *Lepadichthys* that we have examined (excluding *L. lineatus* in which the premaxillae are unmodified) and encompassing almost the anterior 1/3 of the upper jaw (Figure 17A). In some species of *Lepadichthys* (e.g., *L. frenatus*) the semicircular indentation extends anteriorly to the symphysis of the upper jaw, where the premaxillae are without contact (Briggs, 1955). In this extreme condition, the majority of the anterior part of the upper jaw is roofed only by skin.

We consider the aforementioned characters of the oral jaws ([1] characteristic incisiviform teeth and [2] characteristic oval opening between the premaxillae formed by a semicircular indentation along the medial edge of each premaxilla) and the complex articulation between the posterior tip of the basipterygium and the anteromedial edge of the ventral postcleithrum as derived characteristics and putative evidence that the aforementioned members of the Diplocrepinae (*Flexor*, *Pherallodus*), Aspasminae (*Aspasmichthys* and *Pherallodichthys*), and Diademichthyinae (*Diademichthys* and *Lepadichthys*) are potentially more closely related to each other than they are to other members of these subfamilies that do not exhibit these characters. If correct, the relationships of *Flexor* would lie with Indo-Pacific taxa and not with the members of the endemic New Zealand gobiesocid fauna (Stewart 2015), as is the case for many other Kermadec endemic shore fishes, including *Enneapterygius kermadecensis,* which is considered a member of either the *E. hemimelas*-group (Fricke 1994) or *E. pyramis*-group (Fricke 1997), both with members distributed broadly through the eastern Pacific (from Taiwan/Ryukyu Islands to Lord Howe Island), and *Eviota kermadecensis*, which is most similar and potentially closely related to species of *Eviota* from Japan (Hoese and Stewart 2012).
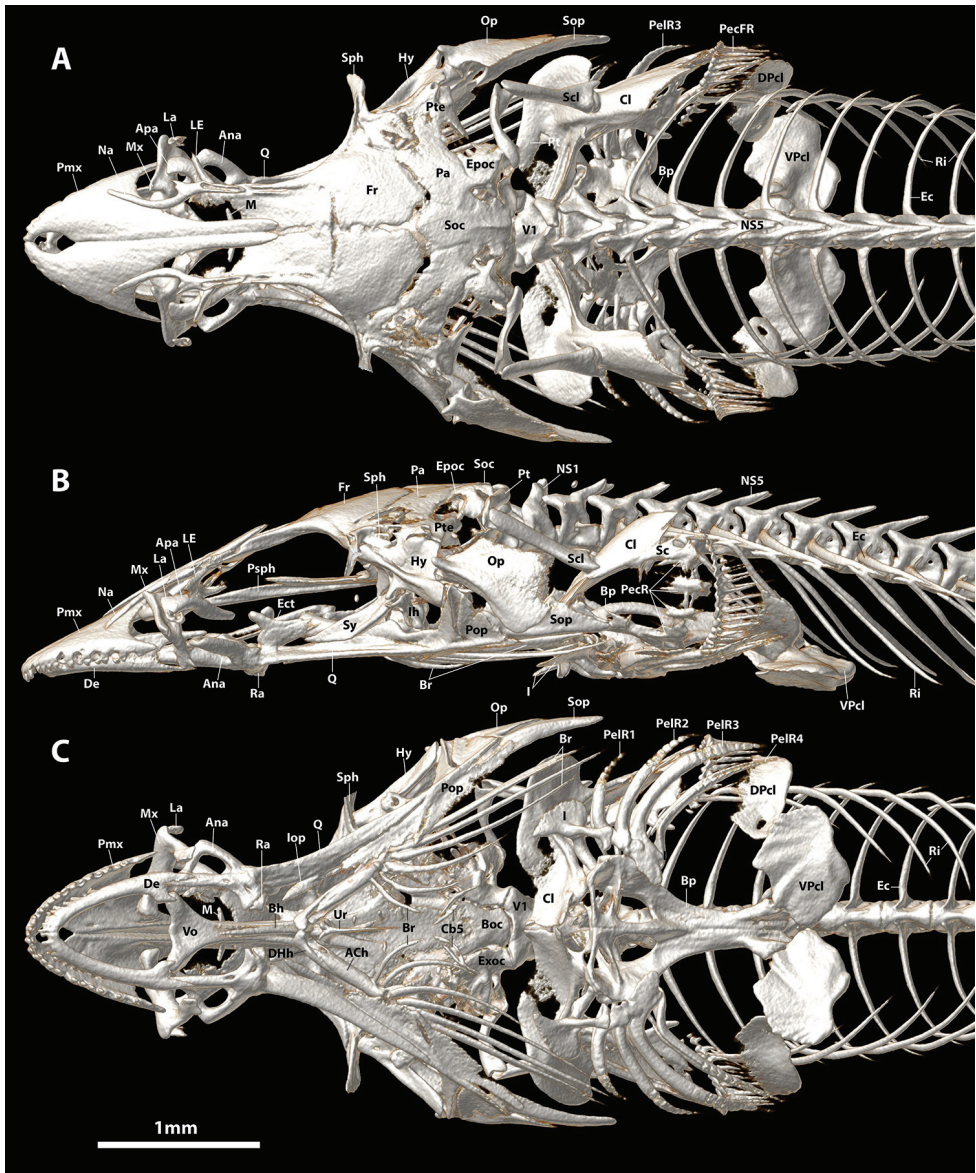
Figure 16. CT scanned anterior skeleton of *Aspasmichthys ciconiae*, TCWC 16461.02, 26.0 mm SL. **A** Dorsal view **B** Lateral view (left side) **C** Ventral view. Abbreviations: ACh, anterior ceratohyal; Ana, anguloarticular; Apa, autopalatine; Boc, basioccipital; Bp, basipterygium; Br, branchiostegal rays; Cb5, ceratobranchial 5; Cl, cleithrum; DHh, dorsal hypohyal; DPcl, dorsal postcleithrum; Ec, epicentral; Ect, ectopterygoid; Epoc, epiotic; Exoc, exoccipital; Fr, frontal; Hy, hyomandibular; I, pelvic-fin spine; Iop, interopercle; La, lachrymal; LE, lateral ethmoid; M, mesethmoid; Na, nasal; NS1, 5, neural spine of vertebral centrum 1, 5; Op, opercle; Pa, parietal; PecR, pectoral radial; PecFR, pectoral-fin ray; PelFR1-4, pelvic-fin ray 1–4; Pop, preopercle; Pro, prootic; Psph, parasphenoid; Pt, posttemporal; Pte, pterotic; Q, quadrate; Ra, retroarticular; Ri, rib; Sc, scapula; Scl, supracleithrum; Soc, supraoccipital; Sop, subopercle; Sph, sphenotic; Ur, urohyal; V1, vertebral centrum 1; Vo, vomer; VPcl, ventral postcleithrum.

Figure 17. CT scanned anterior skeleton of *Lepadichthys bolini*, ROM 55185, 21.5 mm SL. **A** Dorsal view **B** Lateral view (left side) **C** Ventral view. Abbreviations: ACh, anterior ceratohyal; Ana, anguloarticular; Apa, autopalatine; Bp, basipterygium; Br, branchiostegal rays; Cb5, ceratobranchial 5; Cl, cleithrum; Cor, coracoid; DHh, dorsal hypohyal; DPcl, dorsal postcleithrum; Ec, epicentral; Ect, ectopterygoid; Epoc, epiotic; Exoc, exoccipital; Fr, frontal; Hy, hyomandibular; I, pelvic-fin spine; Iop, interopercle; La, lachrymal; LE, lateral ethmoid; M, mesethmoid; Na, nasal; NS1, 5, neural spine of vertebral centrum 1, 5; Op, opercle; Pa, parietal; PecR, pectoral radial; PecFR, pectoral-fin ray; PelFR1-4, pelvic-fin ray 1–4; Pop, preopercle; Pro, prootic; Psph, parasphenoid; Pt, posttemporal; Pte, pterotic; Q, quadrate; Ra, retroarticular; Ri, rib; Sc, scapula; Scl, supracleithrum; Soc, supraoccipital; Sop, subopercle; Sph, sphenotic; Ur, urohyal; V1, vertebral centrum 1; Vo, vomer; VPcl, ventral postcleithrum.

We started our paper with a quote from John C. "Jack" Briggs (1920–2018): "The discovery of this and several other new genera in recent years makes it necessary to reconsider the characterization and relationships of various subfamilies within the Gobiesocidae" Briggs (1993: 197). We agree wholeheartedly.

Comparative material (C&S and/or CT scanned material only)

Aspasminae – *Aspasma*: *A. minima* – USNM 270219, 1 (C&S), 40.2 mm SL; NS-MT-P 114701, 2 (C&S), 35.0–51.0 mm SL. ***Aspasmichthys*:** *A. ciconiae* – TCWC 16461.02, 1 (CT, https://doi.org/10.17602/M2/M30821), 26.0 mm SL. ***Pherallodichthys*:** *P. meshimaensis* – NSMT-P 46753, 1 (C&S), 18.0 mm SL.

Diademichthyinae – *Diademichthys*: *D. lineatus* – ROM 65282, 1 (C&S), 34.7 mm SL; ROM 74261, 1 (CT, https://doi.org/10.17602/M2/M30748), 35.0 mm SL; USNM 213595, 3 (C&S), 21.2–42.4mm SL. ***Lepadichthys:*** *L. bolini* – ROM 55185, 2 (1 C&S; 1 CT, https://doi.org/10.17602/M2/M30731), 20.0–21.5 mm SL. *L. coccinotaenia* – SAIAB 49396, 3 (C&S), 28.4–39.1 mm SL; USNM 272920, 1 (C&S), 31.4 mm SL. *L. frenatus* – AMS I.27134-018, 1 (C&S), 28.0 mm SL. *L. lineatus* – ROM 72940, 2 (C&S), 29.1–36.5; SAIAB 9319, 2 (2 C&S), 23.5–25.0 mm SL.

Diplocrepinae – *Aspasmogaster*: *A. costata* – AMS I.19103–015, 1 (C&S), 37.0 mm SL; TCWC 17166.01, 1 (CT, https://doi.org/10.17602/M2/M30754), 30.0 mm SL. *A. tasmaniensis* – ANSP 113616, 1 (C&S), 35.2 mm SL. ***Cochleoceps*:** *C. orientalis* – AMS I.41084–007, 1 (C&S), 27.3 mm SL. *C. spatula* – WAM P.28288–002, 3 (C&S), 40.0–43.0 mm SL. *C. viridis* – WAM P.30262–001, 2 (C&S), 24.0–25.0 mm SL. ***Gastrocyathus*:** *G. gracilis* – ANSP 113604, 1 (C&S), 32.5 mm SL; NMNZ P.035573, 2 (C&S), 21.0–23.0 mm SL. ***Gastrocymba*:** *G. quadriradiata* – AMS I.21498-001, 1 (C&S), 27.5 mm SL; NMNZ P035573, 2 (C&S), – mm SL. ***Gastroscyphus*:** *G. hectoris* – TCWC 17177.04, 2 (C&S), 30.0–31.0 mm SL. ***Parvicrepis*:** *P. parvipinnis* – TCWC 17169.01, 4 (C&S), 16.0–19.0 mm SL. ***Pherallodus*:** *P. indicus* – NSMT-P 114703, 1(CT; https://doi.org/10.17602/M2/M56337), 25.0 mm SL.

References

Allen GR, Erdman MV (2012) Reef fishes of the East Indies. Volumes I–III. Tropical Reef Research, Perth, 1292 pp.

Bilecenoğlu M, Yokeş MB, Kovačić M (2017) A new species of *Diplecogaster* (Actinopterygii: Gobiesocidae) from the Mediterranean Sea. Zoology in the Middle East 63: 210–218. https://doi.org/10.1080/09397140.2017.1349119

Brandl SJ, Goatley CH, Bellwood DR, Tornabene L (2018) The hidden half: ecology and evolution of cryptobenthic fishes on coral reefs. Biological Reviews. https://doi.org/10.1111/brv.12423

Briggs JC (1955) A monograph of the clingfishes (Order Xenopterygii). Stanford Ichthyological Bulletin 6: 1–224.

Briggs JC (1993) New genus and species of clingfish (Gobiesocidae) from southern Australia. Copeia 1993: 196–199. https://doi.org/10.2307/1446310

Briggs JC, Miller RR (1960) Two new freshwater clingfishes of the genus *Gobiesox* from southern Mexico. Occasional Papers of the Museum of Zoology University of Michigan 616: 1–15.

Conway KW, Baldwin CC, White MD (2014) Cryptic diversity and venom glands in the western Atlantic clingfishes of the genus *Acyrtus* (Teleostei: Gobiesocidae). PLoS ONE 9: e97664. https://doi.org/10.1371/journal.pone.0097664

Conway KW, Bertrand NG, Browning Z, Lancon T, Club Jr FJ (2015) Heterodonty in the New World: an SEM investigation of oral jaw dentition in the clingfishes of the subfamily Gobiesocinae (Teleostei: Gobiesocidae). Copeia 2015: 973–998. https://doi.org/10.1643/OT-15-234

Conway KW, Kim DM, Rüber L, Espinosa-Perez H, Hastings PA (2017a) Molecular phylogenetics of the New World clingfish genus *Gobiesox* (Teleostei: Gobiesocidae) and the origin of a freshwater clade. Molecular Phylogenetics and Evolution 112: 138–147. https://doi.org/10.1016/j.ympev.2017.04.024

Conway KW, Moore GI, Summers AP (2017b) A new genus and species of clingfish (Teleostei: Gobiesocidae) from Western Australia. Copeia 105: 128–140. https://doi.org/10.1643/CI-16-560

Conway KW, Stewart AL, King CD (2017c) A new species of the clingfish genus *Trachelochismus* (Teleostei: Gobiesocidae) from bays and estuaries of New Zealand. Zootaxa 4319: 531–549. https://doi.org/10.11646/zootaxa.4319.3.6

Conway KW, Stewart AL, Summers AP (2018) A new species of sea urchin associating clingfish of the genus *Dellichthys* from New Zealand (Teleostei, Gobiesocidae). ZooKeys 740: 77–95. https://doi.org/10.3897/zookeys.740.22712

Craig MT, Bogorodsky SV, Randall JE, Mal AO (2015) *Lepadichthys bilineatus*, a new species of clingfish from Oman (Teleostei: Gobiesocidae), with a redescription of *Lepadichthys erythraeus* Briggs and Link from the Red Sea. Zootaxa 3990: 113–122. https://doi.org/10.11646/zootaxa.3990.1.6

de Ronde CEJ, Baker ET, Massoth GJ, Lupton JE, Wright IC, Sparks RJ, Bannister SC, Reyners EM, Walker SL, Greene RR, Ishibashi J, Faure K, Resing JA, Lebon GT (2007) Submarine hydrothermal activity along the mid-Kermadec Arc, New Zealand: Large-scale effects of venting. Geochemistry, Geophysics, Geosystems 8(7): https://doi.org/10.1029/2006GC001495

Ditsche P, Wainwright DK, Summers AP (2014) Attachment to challenging substrates-fouling, roughness and limits of adhesion in the northern clingfish (*Gobiesox maeandricus*). Journal of Experimental Biology 217: 2548–2554. https://doi.org/10.1242/jeb.100149

Duffy CAJ, Ahyong ST (2015) Annotated checklist of the marine flora and fauna of the Kermadec Islands Marine Reserve and northern Kermadec Ridge, New Zealand. Bulletin of the Auckland Museum 20: 19–124.

Francis MP (1993) Checklist of the coastal fishes of Lord Howe, Norfolk, and Kermadec Islands, southwest Pacific Ocean. Pacific Science 47: 136–170.

Francis MP, Grace RV, Paulin CD (1987) Coastal fishes of the Kermadec Islands. New Zealand Journal of Marine and Freshwater Research 21: 1–13. https://doi.org/10.1080/00288330.1987.9516194

Fricke R (1994) Tripterygiid fishes of Australia, New Zealand and the southwest Pacific Ocean, with descriptions of 2 new genera and 16 new species (Teleostei). Theses Zoologicae, Volume 24. Königstein Koeltz Scientific Books, Königstein, 585 pp.

Fricke R (1997) Tripterygiid fishes of the western and central Pacific, with descriptions of 15 new species, including an annotated checklist of world Tripterygiidae (Teleostei). Theses Zoologicae, Volume 29. Königstein Koeltz Scientific Books, Königstein, 607 pp.

Fricke R (2014) *Unguitrema nigrum*, a new genus and species of clingfish (Teleostei: Gobiesocidae) from Madang, Papua New Guinea. Journal of the Ocean Science Foundation 13: 35–42. http://www.oceansciencefoundation.org/josf/josf13d.pdf

Fricke R, Wirtz P (2017) *Lecanogaster gorgoniphila*, a new species of clingfish (Teleostei: Gobiesocidae) from São Tomé and Principe, eastern Atlantic Ocean. Arquipelago – Life and Marine Sciences 35: 1–10.

Fricke RP, Wirtz P, Brito A (2010) A new species of the clingfish genus *Apletodon* (Teleostei: Gobiesocidae) from the Cape Verde Islands, Eastern Central Atlantic. Ichthyological Research 57: 91–97. https://doi.org/10.1007/s10228-009-0139-5

Fricke R, Wirtz P, Brito A (2015) *Diplecogaster tonstricula*, a new species of cleaning clingfish (Teleostei: Gobiesocidae) from the Canary Islands and Senegal, eastern Atlantic Ocean, with a review of the *Diplecogaster-ctenocrypta* species-group. Journal of Natural History 50: 731–748. https://doi.org/10.1080/00222933.2015.1079659

Fricke R, Chen J-N, Chen W-J (2016) New case of lateral asymmetry in fishes: A new subfamily, genus and species of deep water clingfishes from Papua New Guinea, western Pacific Ocean. Comptes Rendus Biologies 340: 47–62. https://doi.org/10.1016/j.crvi.2016.11.002

Fujiwara K, Okamoto M, Motomura H (2018) Review of the clingfish genus *Kopua* (Gobiesocidae: Trachelochisminae) in Japan, with description of a new species. Ichthyological Research: 1–21. https://doi.org/10.1007/s10228-018-0633-8

Fujiwara K, Motomura H (2018) A new species, *Propherallodus longipterus*, from the Philippines and redescription of *P. briggsi* Shiogaki and Dotsu 1983 (Gobiesocidae: Diplocrepinae). Ichthyological Research: 1–14. https://doi.org/10.1007/s10228-018-0645-4

Gemballa S, Britz R (1998) Homology of intermuscular bones in acanthomorph fishes. American Museum Novitates 3241: 1–25.

Guitel F (1888) Recherches sur les *Lepadogaster*. Archives de Zoologie Expérimentale et Générale 2: 423–480.

Hardy GS (1984) A new genus and species of deepwater clingfish (family Gobiesocidae) from New Zealand. Bulletin of Marine Science 34: 244–247.

Hastings PA, Conway KW (2017) *Gobiesox lanceolatus*, a new species of clingfish (Teleostei: Gobiesocidae) from the Los Frailes submarine canyon, Gulf of California, Mexico. Zootaxa 4221: 393–400. https://doi.org/10.11646/zootaxa.4221.3.8

Hayashi M, Hagiwara K, Hayashi H (1986) Osteology of the cling fishes in Japan (Family: Gobiesocidae). Science Report of the Yokosuka City Museum 34: 39–66.

Hoese DF, Stewart AL (2012) A new species of the gobiid genus *Eviota* (Teleostei: Gobioidei) from the Kermadec Islands, New Zealand. Zootaxa 3418: 61–67.

Hutchins JB (1984) Description of a new gobiesocid fish from south-western Australia, with a key to the species of *Aspasmogaster*. Records of the Western Australian Museum 11: 129–140. https://biodiversitylibrary.org/page/53024868

Hutchins JB (2008) Family Gobiiesocidae Clingfishes, shore-eels. In: Gomon MF, Bray DJ, Kuiter RH (Eds) Fishes of Australia's Southern Coast. New Holland Publishers, Sydney, 722–742.

Lloyd EF, Nathan S, Smith IEM, Stewart RB (1996). Volcanic history of Macauley Island, Kermadec Ridge, New Zealand. New Zealand Journal and Geophysics 39: 295–308. https://doi.org/10.1080/00288306.1996.9514713

Moore GI, Hutchins JB, Okamoto M (2012) A new species of the deepwater clingfish genus *Kopua* (Gobiesociformes: Gobiesocidae) from the East China Sea – an example of antitropicality? Zootaxa 3380: 34–38.

Mortimer N, Campbell H (2014) Zealandia. Our Continent Revealed. Penguin Books, Auckland, 271 pp.

Roberts CD, Stewart AL, Struthers CD (2015) The fishes of New Zealand. In 4 volumes. Te Papa Press, Wellington, NZ, 2008 pp.

Saruwatari T, López JA, Pietsch TW (1997) Cyanine blue: a versatile and harmless stain for specimen observation. Copeia 1997: 840–841. https://doi.org/10.2307/1447302

Shinohara G, Katayama E (2015) A new species of the clingfish genus *Kopua* (Gobiesociformes: Gobiesocidae) from Japan. Ichthyological Research 62: 431–438. https://doi.org/10.1007/s10228-015-0456-9

Shiogaki M, Dotsu Y (1983) Two new genera and two new species of clingfishes from Japan, with comments on head sensory canals of the Gobiesocidae. Japanese Journal of Ichthyology 30: 111–121.

Sparks JS, Gruber DF (2012) A new mesophotic clingfish (Teleostei: Gobiesocidae) from the Bahamas. Copeia 2012: 251–256. https://doi.org/10.1643/CI-11-124

Springer VG, Fraser TH (1976) Synonymy of the fish families Cheilobranchidae (Alabetidae) and Gobiesocidae, with descriptions of two new species of *Alabes*. Smithsonian Contributions to Zoology 234: 1–23. https://doi.org/10.5479/si.00810282.234

Stewart AL (2015) 218 Family Gobiesocidae. In: Roberts CD, Stewart AL, Struthers CD (Eds) The Fishes of New Zealand. Te Papa Press, Wellington, 1539–1555.

Taylor WR, Van Dyke GG (1985) Revised procedure for staining and clearing small fishes and other vertebrates for bone and cartilage study. Cybium 9: 107–119.

Trnski T, de Lange PJ (2015) Introduction to the Kermadec Biodiversity Expedition 2011. In: Trnski T, Schlumpf HA (Eds) Kermadec Biodiversity Expedition 2011. Bulletin of the Auckland Museum, 10, 1–18.

Trnski T, Duffy CAJ, Francis MP, McGrouther MA, Stewart AL, Struthers CD, Zintzen V (2015) Recent collections of fishes at the Kermadec Islands and new records for the region. Bulletin of the Auckland Museum 20: 463–480.

Wainwright DK, Kleinteich T, Kleinteich A, Gorb SN, Summers AP (2013) Stick tight: suction adhesion on irregular surfaces in the northern clingfish. Biology Letters 9: 20130234. https://doi.org/10.1098/rsbl.2013.0234

RESEARCH ARTICLE

Tosanoides aphrodite, a new species from mesophotic coral ecosystems of St. Paul's Rocks, Mid Atlantic Ridge (Perciformes, Serranidae, Anthiadinae)

Hudson T. Pinheiro[1], Claudia Rocha[1], Luiz A. Rocha[1]

1 *California Academy of Sciences, San Francisco, CA 94118 USA*

Corresponding author: *Hudson T. Pinheiro* (htpinheiro@gmail.com)

Citation: Pinheiro HT, Rocha C, Rocha LA (2018) *Tosanoides aphrodite*, a new species from mesophotic coral ecosystems of St. Paul's Rocks, Mid Atlantic Ridge (Perciformes, Serranidae, Anthiadinae). ZooKeys 786: 105–115. https://doi.org/10.3897/zookeys.786.27382

Abstract

During a recent expedition to St. Paul's Rocks, Atlantic Ocean, a distinctive and previously unknown species of Anthiadinae was collected at a depth of 120 m. A genetic analysis indicated the undescribed species is a member of the genus *Tosanoides*, which was only known to occur in the Pacific Ocean. This new taxon is distinguishable from all other *Tosanoides* species by the following combination of characters: soft dorsal fin rays 15–16; anal fin rays 9; ventral scale rows 9–10; last dorsal spine the longest (instead first through fourth). Here *Tosanoides aphrodite* **sp. n.** is described and illustrated, only known from St. Paul's Rocks.

Keywords

Introduction

The group commonly known as anthias fishes are classified within the serranid subfamily Anthiadinae Poey, 1861 (van der Laan et al. 2014), also historically known as "Anthiinae" (but see Carvalho-Filho et al. 2016; Pyle et al. 2016; Anderson et al. 2017; Eschmeyer and Fong 2018). In their review of the Atlantic and Eastern Pacific Anthiadine fishes, Anderson and Heemstra (2012) recognized 15 genera and 37 species, describing two

new genera. Recently, one species of *Odontanthias* was described from St. Paul's Rocks (Carvalho-Filho et al. 2016), an archipelago of small islets located around 940 km from Northeastern Brazil, in the Mid-Atlantic Ridge (Viana et al. 2009). St. Paul's Rocks harbors one of the highest levels of endemism for reef fishes among Atlantic oceanic islands (Floeter et al. 2008, Pinheiro et al. 2018), even sheltering a genetic isolated population of a widespread species of Anthiadinae (Anderson et al. 2017).

The mesophotic coral ecosystems (MCEs; Hinderstein et al. 2010) of St. Paul Rocks were recently characterized by remote operated vehicles: Rosa et al. (2016) reported an assemblage of fishes at depths of 30–90 m depth dominated by two species, *Prognathodes obliquus* (Lubbock & Edwards, 1980) and *Chromis enchrysura* Jordan & Gilbert, 1882, while bryozoans, black corals and sponges were the main features of the benthic community. During a recent expedition to explore St. Paul Rocks that included diving to depths of up to 130 m, we collected specimens of a previously unknown Anthiadinae species. Here we describe it as a *Tosanoides* species, the first species of this genus to be recorded in the Atlantic Ocean, currently only known from St. Paul's Rocks.

Materials and methods

We collected using hand nets while diving on mixed-gas, closed-circuit rebreathers (Hollis Prism 2). We performed all counts using a microscope, with exception of vertebrae and caudal rays (primary, procurrent and rudimentary), which were counted from X-rays, and morphological characters were measured to the nearest 0.01 mm following Anderson and Heemstra (2012) and Pyle et al. (2016). We counted dorsal and ventral scale rows above and below lateral line to origins of dorsal and anal fins, respectively, including small truncate scales at bases of respective fins. Vertebral counts include the first vertebra fused to the skull, and the last vertebra fused to the hypural plate. Lateral-line scale counts include only those with pores. Caudal ray counts are presented as following: upper procurrent and rudimentary unbranched caudal rays + upper principal branched caudal rays + lower principal branched caudal rays + lower procurrent and rudimentary unbranched caudal rays. Rudimentary caudal rays are those only visible in the X-ray. In the description, counts and measurements for the holotype are presented followed by ranges for paratypes (in parentheses). Morphometric and meristic data for the type specimens are presented in Table 1. We deposited the specimens in the fish collection of the California Academy of Sciences (**CAS**), Universidade Federal do Espírito Santo (**CI-UFES**), Universidade Estadual de Campinas (**ZUEC**), Bernice Pauahi Bishop Museum (**BPBM**), U.S. National Museum of Natural History (**USNM**) and Museu de Zoologia da Universidae de São Paulo (**MZUSP**).

We sequenced and analyzed the Mitochondrial Cytochrome c oxidase subunit I (COI) DNA for the new species. DNA extraction and PCR amplification of the COI were performed following Weigt et al. (2012) protocols. We compared the DNA sequences to all species of Anthiadinae available in GenBank (*Tosanoides obama*: KY370754; *Tosana niwae*: JF952878; *Odontanthias perumali*: KR105805; *Plectranthi-*

Table 1. Morphometric and meristic data for selected characters of type specimens of *Tosanoides aphrodite* sp. n. Values of morphometric data are presented in mm.

Morphometrics	Holotype	Paratypes					
	CIUFES 3444	CAS 244382	ZUEC 16842	BPBM 41351	CAS 244383	MZUSP 123538	USNM 440405
Sex	Male	Male	Male	Female	Female	Female (juvenile)	Female (juvenile)
Total length (TL) in mm	78.3	74.1	86.9	73.4	63.9	52.5	46.2
Standard length (SL) in mm	56.77	54.89	59.88	57.09	47.55	38.91	33.09
Head length	20.32	18.58	20.79	19.54	16.53	12.76	9.39
Body depth	17.83	18.5	19.13	18.55	15.23	13.14	10.67
Body width	9.42	9.15	10.82	8.89	8.53	6.47	5.46
Snout length	3.34	2.98	4.26	3.04	2.88	1.87	1.32
Predorsal length	18.6	17.93	18.71	17.94	14.95	12.58	10.33
Preanal length	34.45	33.69	36.68	35.07	28.4	23.4	21.16
Base of dorsal fin	33.09	31.56	33.45	33.11	27.12	20.58	18.25
Base of anal fin	13.75	13.85	14.81	13.28	13.56	8.57	6.54
Orbit diameter	6.08	5.59	6.61	6.3	5.36	4.62	3.79
Interorbital width	5.16	5.39	5.16	5.09	4.49	3.66	3.38
Caudal peduncle depth	6.34 i	6.41	5.84	6.53	5.41	4.51	4.03
Pelvic spine	9.08	8.74	8.45	10.23	8.29	6.32	5.33
Pelvic fin	16.15	14.72	18.11	21.16	14.17	10.34	10.51
First dorsal spine length	4.16	3.72	5.07	4.37	4.78	2.29	2.46
Second dorsal spine length	5.33	4.59	5.97	4.92	5.96	3.41	2.98
Third dorsal spine length	7.21	6.21	8.1	6.28	6.92	4.25	4
Fourth dorsal Spine length	9.34	7.82	9.35	8.25	7.8	5.31	4.65
Fifth dorsal spine length	9.98	broken	10.89	8.55	7.92	5.62	4.85
Last dorsal spine length	10.39	10.19	11.16	9.12	7.95	5.87	5.03
Longest dorsal ray length (third)	10.98	9.25	12.63	11.04	8.32	6.34	5.33
First anal spine length	3.4	3.05	3.73	3.07	3.36	2.35	2.51
Second anal spine length	7.74	7.12	8.18	8.06	6.81	4.75	4.85
Third anal spine length	8.33	7.77	9.12	8.97	6.84	4.87	4.97
Longest anal ray length (third)	9.98	10.77	12.72	12.4	7.58	6.61	5.45
Caudal fin length	22.9	20.8	26.94	17.38	16.45	13.31	11.83
Pectoral fin length	20.86	19.55	20.72	20.62	16.82	12.77	11.34
maxilla	9.43	8.9	10.34	9.98	7.64	5.94	4.43
Meristics							
Dorsal spines	X	X	X	X	X	X	X
Dorsal rays	15	15	15	16	16	15	16
Anal spines	III	III	III	III	iii	III	iii
Anal rays	9	9	9	9	9	9	9
Pectoral rays	I 13 i	I 13	I 13 i	I 14	I 13 i	I 13	I 13i
Caudal rays	9+7+6+8	9+7+6+9	9+7+6+8	broken	9+7+6+8	9+7+6+9	9+7+6+8
Pored lateral line scales	24	23	23	25	loosen	26	23
Dorsal scale rows	3	3	3	3	3	3	3
Ventral scale rows	10	10	9	10	9	10	10
Gill rakers			8+22				

as japonicus: KP267602; *Sacura margaritacea*: KF202522; *Anthias anthias*: JQ774769; *Serranocirrhitus latus*: FJ584094; *Pseudanthias pascalus*: FJ583931; *Pronotogrammus martinicensis*: MF322587; *Baldwinella aurorubens*: MG856775; *Acanthistius pictus*: KY572857; *Meganthias natalensis*: KU176438; *Luzonichthys seaver*: KP110514; *Nemanthias carberryi*: JQ350133; *Caprodon longimanus*: DQ107894). GenBank accession number for the new species is MH817857.

Results

Tosanoides aphrodite sp. n.
http://zoobank.org/A2E4E1E2-0F05-4FAF-AC25-0CFE96ED9212
Figures 1–4, Table 1

Type locality. Saint Paul's Rocks, Brazil.

Material. Holotype. CIUFES 3444 (Field number: CR 055). 56.8 mm SL, male, Saint Paul Rocks, Brazil. 00°56'N, 029°22'W, depth 120 m, collected by LA Rocha and HT Pinheiro using hand nets, 25 June 2017 (Figure 1). **Paratypes.** CAS 244382 (Field number: CR 071). 54.9 mm SL, male, Saint Paul Rocks, Brazil. 00°56'N, 029°22'W, depth 120 m, collected by LA Rocha and HT Pinheiro using hand nets, 25 June 2017. ZUEC 16842 (Field number: CR 077). 59.9 mm SL, male, Saint Paul Rocks, Brazil. 00°56'N, 029°22'W, depth 120 m, collected by LA Rocha and HT Pinheiro using hand nets, 25 June 2017. BPBM 41351 (Field number: CR 070). 57.1 mm SL, female, Saint Paul Rocks, Brazil. 00°56'N, 029°22'W, depth 120 m, collected by LA Rocha and HT Pinheiro using hand nets, 25 June 2017. MZUSP 123538 (Field number: CR 079). 38.9 mm SL, female (juvenile), Saint Paul Rocks, Brazil. 00°56'N, 029°22'W, depth 120 m, collected by LA Rocha and HT Pinheiro using hand nets, 25 June 2017. CAS 244383 (Field number: CR 078). 47.5 mm SL, female, Saint Paul Rocks, Brazil. 00°56'N, 029°22'W, depth 120 m, collected by LA Rocha and HT Pinheiro using hand nets, 25 June 2017 (Figure 2). USNM 440405 (Field number: CR 080). 33.1 mm SL, female (juvenile), Saint Paul Rocks, Brazil. 00°56'N, 029°22'W, depth 120 m, collected by LA Rocha and HT Pinheiro using hand nets, 25 June 2017.

Comparative material. We compared *Tosanoides aphrodite* to other Anthiadinae species using the keys for the Western Central Pacific Anthiadinae species in Heemstra and Randall (1999) and for the Atlantic and Eastern Pacific Anthiadinae species in Anderson and Heemstra (2012). Data from *Tosanoides obama* Pyle, Green & Kosaki, 2016, *Tosanoides flavofasciatus* Katayama & Masuda, 1980, and *Tosanoides filamentosus* Kamohara 1953 are from Pyle et al. (2016), Katayama and Masuda (1980), and Kamohara (1953), respectively.

Diagnosis. The new species differs from all other Anthiadinae by the following combination of characters: Dorsal-fin spines X; last dorsal spine the longest, 1.8–2.2 in head length; dorsal-fin rays 15–16; 7th dorsal ray the longest, 2.65–2.80 in head

Figure 1. *Tosanoides aphrodite* sp. n. holotype (CIUFES 3444), 56.8 mm SL, male, collected at a depth of 120 m in Saint Paul Rocks, Brazil. Photographs by J Fong.

length; anal-fin rays 9; pored lateral-line scales 32–35; ventral scale rows 9–10; body slender and compressed, greatest depth 2.96–3.18 in SL, and the width 1.77–2.09 in depth. Our phylogenetic analysis shows the new species belongs to *Tosanoides* Kamohara 1953, from which it differs of the other known species by: a divergence of at least 12.35% at the cytochrome oxidase I gene, last dorsal spine the longest (instead first through fourth), fewer dorsal-fin rays (15–16 vs. 16–17), and more anal-fin rays (9 vs. 8 in the other *Tosanoides*).

Description. Morphometric and meristic data for type specimens are provided in Table 1. Dorsal fin X, 15 (15–16), last soft ray branched to base; anal fin III,9, last soft ray branched to base; pectoral-fin rays 14 (14–15); pelvic-fin rays I,5; principal branched caudal rays 7 + 6 (7 + 6), upper procurrent and rudimentary unbranched caudal rays 9 (9), lower procurrent and rudimentary unbranched caudal rays 8 (8–9); pored lateral-line scales 34 (32–35); scale rows above lateral line to origin of dorsal fin 3; scale rows below lateral line to origin of anal fin 10 (9–10); gill rakers on upper limb 8, on lower limb 22; vertebrae 27 (10 precaudal + 17 caudal).

Body slender, compressed, its greatest depth 3.18 (2.96–3.13) in SL, the width just posterior to gill opening, 1.89 (1.77–2.09) in depth; head length 2.79 (2.88–3.52) in SL; snout short, its length 6.08 (4.88–7.12) in head; orbit diameter 3.34 (2.48–3.32) in head; interorbital convex, the least bony width 3.94 (2.78–4.03) in head; caudal peduncle depth 3.21 (2.33–3.56) in head. Mouth large and oblique; lower jaw not

Figure 2. *Tosanoides aphrodite* sp. n. paratype (CAS 244383), 47.5 mm SL, female, collected at a depth of 120 m in Saint Paul Rocks, Brazil. Photographs by J Fong.

projecting beyond the upper when mouth closed; maxilla 2.15 (1.96–2.16) in head, diagonal (45°), and reaching the center of pupil. One pair of nostrils in front of each eye with no membranous tube or rims. One pair of pores on top of head between eyes, slightly anterior to center of eyes. Posterior margin of eye bordered with eight to ten pores. Lateral line very high, parallel with dorsal profile, forming an angle below last few dorsal rays and extending along middle of caudal peduncle to base of caudal fin.

Teeth in upper jaw villiform, forming a band broader anteriorly with two canines on each side, one externally directed forward and other internally directed backward, an outer row of approximately 14 slender canines on each side of jaw curved forward; lower jaw with a patch of villiform teeth anteriorly; two canines on each side anteriorly curved backwards and a third canine on each side facing forward and curved internally, an outer row of approximately 15 slender canines like those of upper jaw, pointing forward; small teeth on vomer and palatines; tongue pointed, smooth. Preopercle with a round angle, upper limb serrate with approximately 25 spinules, lower limb smooth; opercle with two flat spines, upper one longest and at apex; subopercle and interopercle smooth.

Color in life. *Tosanoides aphrodite* is sexually dichromatic. Males (Figure 3A): body pinkish and reddish, darker dorsally fading to white ventrally; two alternating bright yellow and pink stripes from anterior end of body through nape across the operculum, continuing to area below middle of spinous dorsal fin and becoming series of irregular

Figure 3. Fresh specimens of *Tosanoides aphrodite* sp. n. collected in St. Paul's Rocks, Brazil. **A** Male **B** Female. Photographs by LA Rocha.

spots on posterior third of body; third yellow stripe of similar pattern from lower jaw to caudal fin becoming series of irregular blotches under pectoral fin; eye yellow with bright pink upper and lower edges; snout and region anterior to eye bright yellow with a thin pink stripe extending dorsally to two thirds distance to origin of dorsal fin; scales on ventral portion of head and body with bright yellow margins; dorsal fin yellow with bright purplish pink margin; anal fin yellow also with bright pink margin from first to seventh ray and along posterior margin of last ray; pelvic fin yellow with pink anterior margin; caudal fin pink posteriorly and yellow with irregular pink markings anteriorly; filaments in upper and lower edges yellow; pectoral fin translucent yellow.

Females and juveniles (Figure 3B) predominantly reddish orange slightly darker dorsally; snout and region anterior to eye bright yellow with a thin red stripe extending dorsally to two thirds distance to origin of dorsal fin; two alternating yellow and red stripes from anterior end of body through nape to the operculum; third yellow stripe from lower jaw to base of pectoral fin; eye greenish yellow with bright purple upper and lower edges; scales on body with red margins; dorsal fins predominantly yellow with orange rays and dark red blotch covering first three dorsal spines; anal fin predominantly yellow with orange rays and orange margin; pelvic fin yellow with purplish red anterior margin; caudal fin yellow with pinkish orange margins and vertical lines forming ocellated and irregular markings; pectoral fin translucent orange.

Figure 4. *Tosanoides aphrodite* sp. n. in its natural environment, photographed at a depth of 120 m in St. Paul's Rocks, Brazil. Photograph by LA Rocha.

Color in alcohol. Straw-colored; fins transparent; eyes black (Figure 1). Females retain dark blotch on first three dorsal fin spines (Figure 2).

Etymology. The name "*aphrodite*" refers to the ancient Greek goddess of love and beauty. While we were collecting the Aphrodite anthias, a large Six-gill shark (*Hexanchus griseus*) came very close to both of us (HTP and LAR), but that didn't divert our attention from the new exquisitely beautiful species, and we never even saw the shark (https://youtu.be/pSZrmoEwR0Q). The beauty of the Aphrodite anthias enchanted us during its discovery much like Aphrodite's beauty enchanted ancient Greek gods.

Distribution and habitat. *Tosanoides aphrodite* is only known from Saint Paul's Rocks, off Brazil. It was found on mesophotic coral ecosystems of the island, observed between 100 and 130 m depth while rebreather diving, and a single observation at 260 m depth, taken from a submersible dive. The species inhabits small crevices of complex rocky reefs (Figure 4). The ambient seawater temperature at the collecting depth (~120 m) varied between 13 and 15 °C during the two-week period we stayed in the area.

Comparative remarks. The COI gene sequence of *Tosanoides aphrodite* is 12.65% divergent from *Tosanoides obama*, and on average 14–20% divergent from other genera of Anthiadinae. Because we do not have sufficient representation for members of this subfamily, no phylogenetic tree is provided here. In addition to the unique characters presented in the diagnosis section, *Tosanoides aphrodite* also differs from *Tosanoides filamentosus* in having a shorter snout and larger orbit (4.9–7.1 and 2.5–3.3 vs 4.6

and 3.7 in HL, respectively). *Tosanoides flavofasciatus* differs from *Tosanoides aphrodite* in having a shorter fourth (2.55–2.75 vs. 2.02–2.40 in HL) and last (3.11–3.44 vs. 1.82 and 2.17 in HL) dorsal spine length, 7th dorsal ray the longest instead the third, smaller third anal spine (2.65–2.80 vs. 1.89–2.62 in HL), and longer pectoral fin length (2.36–2.71 vs. 2.72–3.05 in SL). *Tosanoides obama* also differs from *Tosanoides aphrodite* in having a shorter fourth (2.4–2.68 vs. 2.02–2.40 in HL), fifth (2.4–2.88 vs. 1.94–2.29 in HL) and last (2.67–3.06 vs. 1.82–2.17 in HL) dorsal spine length, 7th or 8th dorsal ray the longest instead the third, and longer pectoral fin length (2.49–2.63 vs. 2.72–3.05 in SL).

Discussion

Initially, differences in counts, body proportions, morphology of dorsal and caudal soft rays, and distribution (a single locality in the Atlantic versus wide range in the Pacific Ocean) made us believe that *T. aphrodite* constituted a new genus. However, preliminary genetic analysis based on the COI gene placed *T. aphrodite* between two pairs of *Tosanoides* species (including an undescribed new species from Pohnpei, Micronesia; Pyle et al., submitted). Therefore, we provisionally place this new species in *Tosanoides*, but future genetic analyses with multiple loci might clarify the Anthiadinae classification and change the generic placement of *T. aphrodite*.

The isolation of Saint Paul's Rocks, from both the American and African coastlines, and its extremely small size, are likely the main causes for the high endemism and low diversity in the local marine biodiversity. Previously, there were seven endemic reef fishes that were exclusively found at St. Paul's Rocks, while another six restricted range species were shared with the Brazilian oceanic islands of Fernando de Noronha and Rocas Atoll (Pinheiro et al. 2018). Thus, *Tosanoides aphrodite* is the eighth endemic to St. Paul's Rocks, adding to the uniqueness of this locality. However, like other inhabitants of the poorly sampled mesophotic reefs, the Aphrodite Anthias might have a wider distribution. For example, another Anthiadinae, *Anthias asperilinguis* Günther 1859, is widespread along deep reefs of the western Atlantic (usually below the MCEs), and is also found at St. Paul's Rocks, where it shows a slight genetic divergence (Anderson et al. 2017). The few studies of deep reefs in the southwestern Atlantic are mostly restrict to shallower mesophotic coral ecosystems between 30 and 80m depth (Pinheiro et al. 2015, Rosa et al. 2016, Simon et al. 2016), what limits the understanding of the biogeography of deep fishes in the province.

Acknowledgements

References

Anderson WD, Baldwin CC, Carvalho-filho A, Júnior TV (2017) Redescription of the Jeweled Gemfish, *Anthias asperilinguis* (Serranidae: Anthiadinae), with comments on its ontogeny, phylogeny, and ecology. Aqua, International Journal of Ichthyology 23: 73–95.

Anderson WD, Heemstra PC (2012) 102 Review of Atlantic and Eastern Pacific Anthine Fishes (Teleostei: Perciformes: Serranidae), with Descriptions of Two New Genera. American Philosophical Society, 204 pp.

Carvalho-Filho A, Macena BCL, Nunes DM (2016) A new species of Anthiadinae (Teleostei: Serranidae) from São Pedro and São Paulo Archipelago, Brazil, Equatorial Atlantic. Zootaxa 4139: 585–592. https://doi.org/10.11646/zootaxa.4139.4.10

Eschmeyer W, Fong J (2018) Species by Family/Subfamily in the Catalog of Fishes. http://researcharchive.calacademy.org/research/ichthyology/catalog/SpeciesByFamily.asp

Floeter SR, Rocha LA, Robertson DR, Joyeux JC, Smith-Vaniz WF, Wirtz P, Edwards AJ, Barreiros JP, Ferreira CEL, Gasparini JL, Brito A, Falcón JM, Bowen BW, Bernardi G (2008) Atlantic reef fish biogeography and evolution. Journal of Biogeography 35: 22–47. https://doi.org/10.1111/j.1365-2699.2007.01790.x

Hinderstein LM, Marr JCA, Martinez FA, Dowgiallo MJ, Puglise KA, Pyle RL, Zawada DG, Appeldoorn R (2010) Theme section on "Mesophotic Coral Ecosystems: Characterization, Ecology, and Management." Coral Reefs 29: 247–251. https://doi.org/10.1007/s00338-010-0614-5

Kamohara T (1953) Marine fishes newly found in Prov. Tosa, Japan, with description of a new genus and species. Research Reports Koshi University 2(11): 1–10.

Katayama M, Masuda H (1980) *Tosanoides flavofasciatus*, a new Anthiine fish from Sagami Bay, Japan, and the Tonga Ridge, Melanesia. Japanese Journal of Ichthyology 27: 51–55.

van der Laan R, Eschmeyer WN, Fricke R (2014) Family-group names of Recent fishes. Zootaxa 3882: 1–230. https://doi.org/10.11646/zootaxa.3882.1.1

Pinheiro HT, Mazzei E, Moura RL, Amado-Filho GM, Carvalho-Filho A, Braga AC, Costa PAS, Ferreira BP, Ferreira CEL, Floeter SR, Francini-Filho RB, Gasparini JL, Macieira RM, Martins AS, Olavo G, Pimentel CR, Rocha LA, Sazima I, Simon T, Teixeira JB, Xavier LB, Joyeux J-C (2015) Fish biodiversity of the Vitória-Trindade Seamount Chain, southwestern Atlantic: an updated database. PloS ONE 10: e0118180. https://doi.org/10.1371/journal.pone.0118180

Pinheiro HT, Rocha LA, Macieira RM, Carvalho-Filho A, Anderson AB, Bender MG, DiDario F, Ferreira CEL, Francini-Filho RB, Gasparini JL, Joyeux J-C, Luiz OJ, Mincarone M, Moura RL, Nunes J de ACC, Quimbayo JP, Rosa RS, Sampaio CLSS, Sazima I, Simon T, Vila-Nova DA, Floeter SR (2018) Southwestern Atlantic reef fishes: zoogeographic patterns and ecological drivers reveal a secondary biodiversity center in the Atlantic Ocean. Diversity and Distributions 24(7): 951–965. https://doi.org/10.1111/ddi.12729

Pyle RL, Greene BD, Kosaki RK (2016) *Tosanoides obama*, a new basslet (Perciformes, Percoidei, Serranidae) from deep coral reefs in the Northwestern Hawaiian Islands. ZooKeys 641: 165–181. https://doi.org/10.3897/zookeys.641.11500

Rosa MR, Alves AC, Medeiros DV, Coni EOC, Ferreira CM, Ferreira BP, de Souza Rosa R, Amado-Filho GM, Pereira-Filho GH, de Moura RL, Thompson FL, Sumida PYG, Francini-Filho RB (2016) Mesophotic reef fish assemblages of the remote St. Peter and St. Pauls Archipelago, Mid-Atlantic Ridge, Brazil. Coral Reefs 35: 113–123. https://doi.org/10.1007/s00338-015-1368-x

Simon T, Pinheiro HT, Moura RL, Carvalho-Filho A, Rocha LA, Martins AS, Mazzei EF, Francini-Filho RB, Amado-Filho GM, Joyeux J-C (2016) Mesophotic fishes of the Abrolhos Shelf, the largest reef ecosystem in the South Atlantic. Journal of Fish Biology 89: 990–1001. https://doi.org/10.1111/jfb.12967

Viana DF, Hazin FHV, Souza MAC (2009) O Arquipélago de São Pedro e São Paulo: 10 anos de Estação Científica. SECIRM, Brasília, 348 pp.

Weigt LA, Baldwin CC, Driskell A, Smith DG, Ormos A, Reyier EA (2012) Using DNA barcoding to assess Caribbean reef fish biodiversity: Expanding taxonomic and geographic coverage. PLoS ONE 7(7): e41059. https://doi.org/10.1371/journal.pone.0041059

RESEARCH ARTICLE

A review of the family Trichopolydesmidae in North Africa with a description of a new species from Tunisia

Nesrine Akkari[1], Jean-Paul Mauriès[2]

1 *Dritte Zoologische Abteilung, Naturhistorisches Museum Wien, Burgring 7, A-1010 Wien, Austria* **2** *Muséum National d'Histoire Naturelle, Dpt. Origines & Evolution, Section Arthropodes, 61 rue Buffon F- 75005 Paris, France*

Corresponding author: *Nesrine Akkari* (nes.akkari@gmail.com)

Citation: Akkari N, Mauriès J-P (2018) A review of the family Trichopolydesmidae in North Africa with a description of a new species from Tunisia. ZooKeys 786: 117–128. https://doi.org/10.3897/zookeys.786.28270

Abstract

A new species of the genus *Haplocookia* Brölemann, 1915 is described from Cap Bon Peninsula in Tunisia (North Africa) and a historical account of the poorly understood genera *Haplocookia* and *Heterocookia* Silvestri, 1898 is provided. Comments on the taxonomy of the family Trichopolydesmidae are presented, as well as an identification key to the trichopolydesmid species hitherto known from North Africa and an updated list of the Polydesmida in the region.

Keywords

Haplocookia, *Heterocookia*, identification key, North Africa, new species, taxonomy, Tunisia, updated checklist

Introduction

The order Polydesmida Leach, 1815 is represented in North Africa with five families, nine genera, and 22 species (see list below). Most of these species are endemic, marginally studied, and the taxonomy of several species and genera remain far from adequate (see Brölemann 1921, Schubart 1960, Tabacaru 1975, Mauriès 1984, Hoffman 1980,

Akkari and Enghoff 2011, Enghoff et al. 2015). Among these, the genera *Haplocookia* Brölemann, 1915 and *Heterocookia* Silvestri, 1898, represented with four endemic species, have particularly been subject to taxonomic controversies and remain poorly understood in comparison with the rest of the polydesmidans in this region.

The genus *Haplocookia* is characterised by a deeply divided gonopod telopodite bearing short and simple processes. It was first established by Brölemann (1915) to accommodate *Haplocookia mauritanica*, he then described from Kabylie, Algeria. The genus remained monotypic until Schubart (1960) described *Haplocookia franzi* from Morocco. *Haplocookia franzi* Schubart, 1960 differs from the type species in the shape and processes of the distal part of the telopodite.

The genus *Heterocookia* was described much earlier, based on a species collected and described from Aïn Draham Region in northwestern Tunisia by Silvestri (1896), *Heterocookia novator* (Silvestri, 1896). The genus counts a second species, *Heterocookia tunisiaca* Ceuca, 1967 described from Le Kef (Ceuca 1967). Both genera were first placed with six other genera in the tribe Trichopolydesmini (Brölemann 1915). Subsequently, Attems (1940) considered *Haplocookia* as a junior synonym of *Heterocookia* Silvestri, 1898, listing the species *mauritanica* under the genus *Heterocookia* in his Tierreich volume on Polydesmoidea. Two decades later, Schubart (1960) re-established *Haplocookia* as a valid genus, placed it in the family Vanhoeffeniidae Attems, 1914 and described a third species, *H. franzi* from several localities in Morocco. After two more decades, Hoffman (1980) also considered *Haplocookia* as a valid genus although he listed only one of the two described species, and assigned both *Haplocookia* and *Heterocookia* to the family Polydesmidae Leach, 1815. Mauriès (1984) was the last to discuss the taxonomy of the genus *Haplocookia* and he recommended placing it back in the family Trichopolydesmidae as previously suggested by Brölemann (1915) and Tabacaru (1975). Golovatch (2013) accepts both *Haplocookia* and *Heterocookia* in Trichopolydesmidae but in the latest taxonomic overview of the order Polydesmida, the genus *Haplocookia* is absent, whereas *Heterocookia* is listed under the family Trichopolydesmidae (Enghoff et al. 2015).

In this paper, we shed light on this obscure genus, describe a new species from Tunisia, *Haplocookia enghoffi* sp. n., and we further provide an updated checklist of the polydesmidan fauna of North Africa and an identification key to the species of *Haplocookia* and *Heterocookia* in this region.

Material and methods

The material of the new species was collected by NA, stored in 70% ethanol, and deposited in the Muséum national d'Histoire naturelle (**MNHN**), Natural History Museum of Denmark, Zoological Museum – University of Copenhagen (**ZMUC**), and Naturhistorisches Museum Wien (**NHMW**). Type material of *Haplocookia mauritanica* (**MNHN**) was examined for comparison. General characters were studied with a Wild Heerbrug 308700 stereomicroscope from Zeiss. Measurements and drawings were

obtained using a camera lucida of a compound microscope Axioskop from Zeiss. Parts of some specimens were mounted on microscope preparations in lactic acid for examination. Micrographs were made in NHMW with a Nikon DS-F2.5 camera mounted on a Nikon SMZ25 stereomicroscope, using NIS-Elements Microscope Imaging Software with an Extended Depth of Focus (EDF) patch. All images were processed with Adobe Photoshop CS6 and assembled in Adobe InDesign CS6.

Taxonomy

Order Polydesmida Leach, 1815
Family Trichopolydesmidae Verhoeff, 1910
Genus *Haplocookia* Brölemann, 1915

***Haplocookia enghoffi* sp. n.**
http://zoobank.org/C2E5B414-CA4D-4710-9515-93851F54D9DD
Figs 1–3

Material. Holotype. Male, Tunisia, Cap Bon peninsula, Nabeul district, Jebel Abderrahman, Tunisia, 28.11.2004, N. Akkari leg. (MNHN – JC 380). **Paratypes**. 2 males, same data as holotype, N. Akkari leg. (MNHN – JC 380); 2 males, same data as holotype, N. Akkari leg. (NHMW 9366; NHMW 9367); 1 male, same data as holotype, N. Akkari leg. (ZMUC 00039891).

Additional material studied. *Heterocookia novator*, 1 male, Tunisia, Gov. Béja, Jebel El Jouza Amdoun, coll. & det. N. Akkari, MNHN; *Heterocookia tunisiaca*, 1 male, Algeria, wilaya El Tarf, El Kala, coll. Kahina Houd-Chaker, det. J.-J. Geoffroy, MNHN.

Diagnosis. A small polydesmidan of the genus *Haplocookia*, differing from its congeners in the shape of the distal part of the gonopod telopodite having simple curved processes.

Etymology. The species epithet honours Prof. Henrik Enghoff, a leading expert in myriapod systematics, author of major works on millipede taxonomy, and always a dear friend.

Description. (all measurements in mm). Pale, almost white (Figure 1), 20 body rings; length: 8–8.6 mm, width of the 10th metazonite, including paranota: 0.83–1.18; prozonite: 0.62–0.69.

Head occipital furrow not clear; mandibles and gnathochilarium with many small and regularly distributed setae, labrum with three teeth. Antenna (Figure 2A) 1.21 mm long, articles: 1st: 0.12, 2nd: 0.15, 3^{ed}: 0.24, 4th: 0.16, 5th: 0.18, 6th: 0.26, 7th & 8th: 0.10, no special characters observed on 6th antennomere (only the usual external long seta).

Collum (Figure 2B) semicircular, not broader than head, flattened, with four irregular transverse rows of tubercles bearing stout and long setae, paranotal edges incised into three well-developed lobes, each one bearing 1 seta.

Figure 1. *Haplocookia enghoffi* sp. n. ♂ paratype NHMW 9366: **A** Habitus, lateral view **B** Head and first body rings, lateral view.

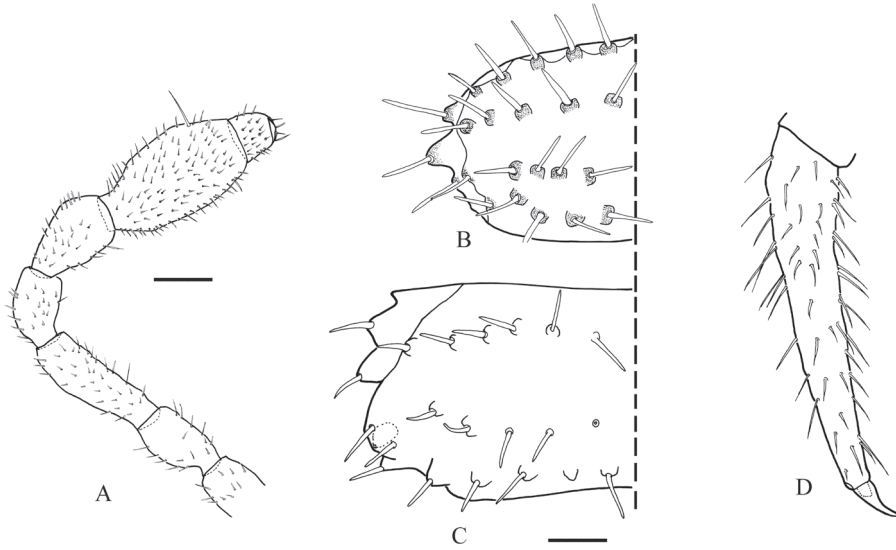**Figure 2.** *Haplocookia enghoffi* sp.n. ♂ paratype MNHN- JC 380: **A** Antenna **B** Collum **C** 10th metatergite bearing ozopore **D** leg, tarsus and apical claw. Scale bar 0.1 mm.
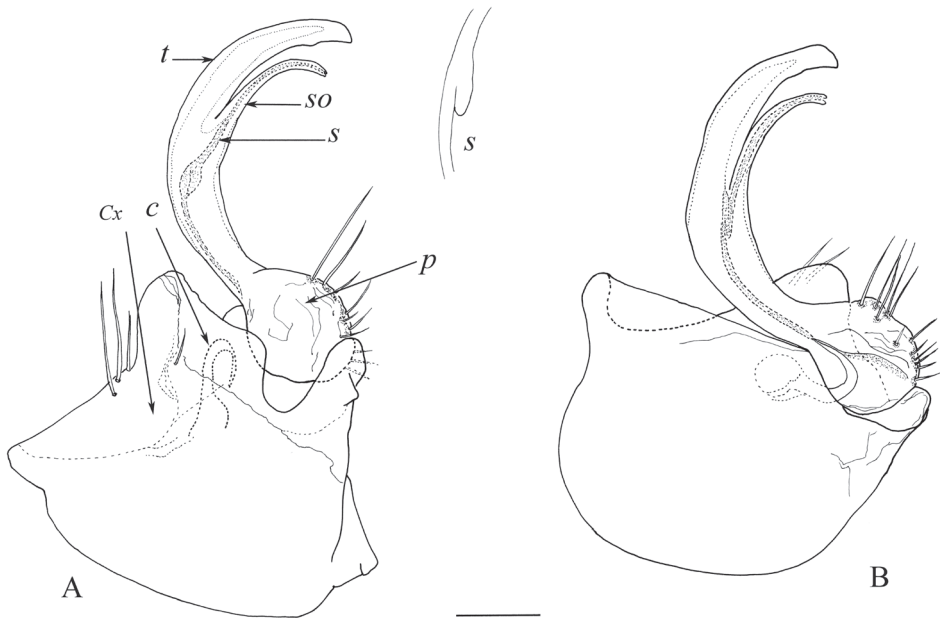

Figure 3. *Haplocookia enghoffi* sp. n. ♂ paratype: **A** Left gonopod, mesal view **B** Left gonopod, postero-lateral view. Abbreviations: C cannula, Cx Coxa, p prefemur, S seminal groove, So solenomere, t tibiotarsus. Scale bar 0.1 mm.

Metaterga (Figure 2C) with three transverse rows of 10–14 tubercles each bearing a short and stout seta (anterior and posterior rows with ten tubercles each, median row with variable number), median row closer to posterior one.

Paranota (Figure 2C) well expanded dorsolaterally, with four incised lobes bearing one long and stout seta each. Ozopore large, round and lying between the two posterior metatergal rows, present on rings 5, 7, 9, 10, 12, 13, 15 –19.

Legs (Figure 2D) without special features, articles: coxa: 0.17, prefemur: 0.20, femur: 0.08, postfemur: 0.10, tibia: 0.15, tarsus: 0.10, apical claw circa three times longer than broad (length: 0.04, basal width: 0.01).

Telson with two transverse rows of tubercles bearing long and strong setae, epiproct almost triangular, with relatively long setae.

Gonopods (Figure 3). Coxa (*Cx*) well-developed, hemispherical, internal margin not indented, external border extended in a large anterior rounded lobe with 2 long and 1 shorter setae seen in posterior view. Prefemoral part (*p*) with strong setae, medially folded and sheltering basal opening of seminal groove. Cannula (*C*) concealed in coxa, its tip entering mesal fold of the prefemur, where seminal groove (*S*) arises. Distal part of telopodite divided into solenomere (*So*) and tibiotarsus (*t*). Tibiotarsus simple, relatively broad and apically bent, with barely perceptible blunt bump on internal margin. Solenomere (*So*) slender and bent bearing the opening of the seminal groove at apex. Seminal groove (*S*) uniformly broad from femoral basis up to apex of solenomere, noticeably thickening at femoral level, just above bifurcation of telopodite.

Comments. *H. tunisiaca* is reported here for the first time from Algeria.

Discussion

Notes on the North African trichopolydesmids

Except for the special structure of the seminal groove (a small bulb-like extension, reminding of genus *Polydesmus*), the gonopod of *Haplocookia enghoffi* sp. n. is built in the same way as that of *H. mauritanica* and *H. franzi*, with a typically polydesmoid crescent-shaped telopodite arising from a large coxa (Figs 3, 5A, B). In all three species, the telopodite is divided into a tibiotarsus and a slender solenomere. However, these two processes show different configurations in the three species (Figs 3, 5A, B). In *H. mauritanica*, the two processes separate at the apical third of the telopodite and the solenomere is a very slender process orthogonal to the main telopodite axis. In *H. franzi*, the solenomere is a small and elongated branch, slightly bent and forked, laterally protected by a larger tibiotarsus. The telopodite is clearly indented in *H. franzi*, presenting a subapical triangular tooth in *H. mauritanica*, and only a small subapical blunt bump in *H. enghoffi* sp. n.

Figure 4. *Heterocookia novator* (Silvestri, 1896) and *Heterocookia tunisiaca* Ceuca, 1967, habitus. **A** *Heterocookia novator* (Tunisia, Gov. Béja, Jebel El Jouza Amdoun, coll. & det. N. Akkari, MNHN) **B** *Heterocookia tunisiaca* (Algeria, wilaya El Tarf, El Kala, coll. Kahina Houd-Chaker, det. J.-J. Geoffroy, MNHN).
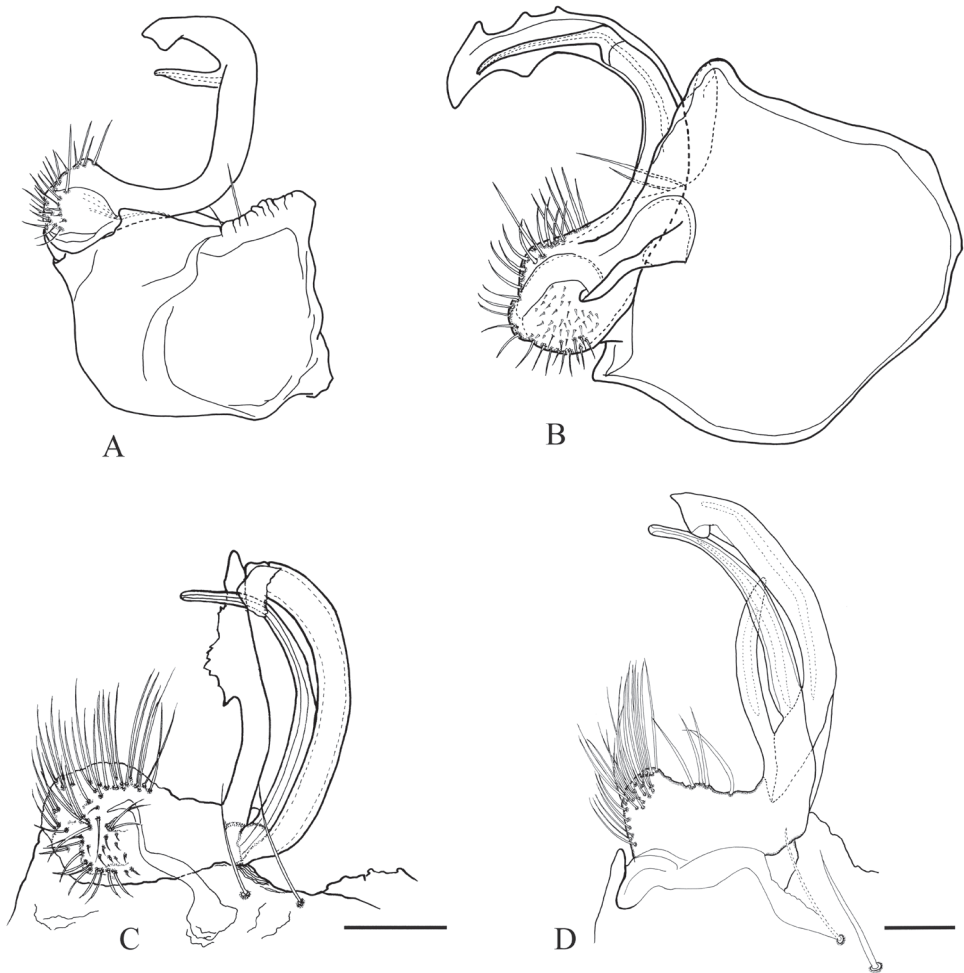
Figure 5. North African Trichopolydesmidae, right gonopod in postero-lateral view: **A** *Haplocookia mauritanica* Brölemann, 1915 (redrawn after Brölemann 1915) **B** *Haplocookia franzi* Schubart, 1960 (redrawn after Schubart 1960) **C** *Heterocookia novator* (Silvestri, 1896) **D** *Heterocookia tunisiaca* Ceuca, 1967. Scale bar 0.1 mm.

The genus *Heterocookia* includes two species from Tunisia, viz. *H. novator* (Figure 4A) and *H. tunisiaca* (Figure 4B), the latter is recorded here for the first time from El Tarf in Algeria. Both species are larger than the *Haplocookia* species despite sharing the same external characters. Their gonopods (Figure 5C, D) are characterised by a deep ramification of the telopodite, which clearly shows three slender processes composed of a simple solenomere, a more complex tibiotarsus, and a third process.

Notes on the family Trichopolydesmidae

The taxonomy of the family Trichopolydesmidae has remained controversial. Verhoeff (1910) erected the subfamily Trichopolydesminae for the two genera *Trichopolydesmus* Verhoeff, 1898 and *Bacillidesmus* Attems, 1898. Later, Attems (1926, 1940) placed the genus *Trichopolydesmus* in the family Vanhoeffeniidae Attems, 1914. Although Verhoeff (1943) reestablished the Trichopolydesmidae as a full family, Schubart (1960) described *Haplocookia franzi* in the family Vanhoeffeniidae. The families Vanhoeffeniidae and Sphaerotrichopodidae were synonymised with Dalodesmidae by Jeekel (1956). Tabacaru (1975, 1980) provided a new circumscription of Trichopolydesmidae based on the works of Verhoeff (1943), Ceuca (1958, 1974) and Kraus (1957). In his survey, Tabacaru (1980) gathered in the same group five genera: the type genus *Trichopolydesmus* [including the subgenus *Banatodesmus* Tabacaru, 1980 he then described, and which was later treated by Mauriès (1983, 1984) as a full genus and placed in the Fuhrmannodesmidae Brölemann, 1916] together with *Bacillidesmus*, *Galliocookia* Ribaut, 1955, *Verhoeffodesmus* Strasser, 1959 and *Napocodesmus* Ceuca, 1974. Following the same logic, Mauriès (1980, 1984) established a list and an identification key for the nine genera in the Trichopolydesmidae, adding *Haplocookia*, *Cottodesmus* Verhoeff, 1936, *Occitanocookia* Mauriès, 1981 [1980 in Nomenclator 3] and *Ingurtidorgius* Srasser, 1974 to the five above mentioned genera.

Almost simultaneously, Hoffman (1980) placed the genera *Galliocookia*, *Haplocookia* and *Heterocookia* in the family Polydesmidae and separated a small number of genera from the Fuhrmannodesmidae, placing them within three subfamilies of Trichopolydesmidae, viz. Trichopolydesminae (*Trichopolydesmus*), Bacillidesminae Verhoeff, 1910 (*Bacillidesmus* and *Napocodesmus*) and Ingurtidorgiinae Strasser, 1974 (*Ingurtidorgius* Strasser, 1974). Mauriès (1984) included four more genera in the Trichopolydesmidae, viz. *Haplocookia*, *Verhoeffodesmus*, *Cottodesmus* and *Occitanocookia*.

Ten years later, Simonsen (1990) underlined a clear geographical discontinuity between the Euro-Mediterranean and the Afrotropical taxa, placing them in Trichopolydesmidae and the Fuhrmannodesmidae, respectively, which was supported subsequently by Shelley (2003). Recently, Shear (2011) provided a list of Trichopolydesmoidea, where the family Trichopolydesmidae was not mentioned, very likely merged with the Fuhrmannodesmidae. Among the latest contributions, Golovatch (2013) reclassified the superfamily Trichopolydesmoidea, presented a diagnosis for the family Trichopolydesmidae, based on male sexual characters and provided a new circumscription of the family in which he included the Fuhrmannodesmidae, Macrosternodesmidae Brölemann, 1916, Mastigonodesmidae Attems, 1914 and Nearctodesmidae Chamberlin and Hoffman, 1950. This same classification was also adopted by Enghoff et al. (2015) in their classification of the Polydesmida. The Trichopolydesmidae currently includes around 75 genera and 140 species (see Golovatch 2013), among which nearly 20 genera and 40 species with Euro-Mediterranean distribution, and two genera and five species in North Africa.

Key to North African species of Trichopolydesmidae based mostly on male gonopods

1   Pale species (Fig. 1). Gonopod with two processes (Figs 3, 5A, B).................
.... ***Haplocookia* 2**
–   Pigmented species (Fig. 4). Gonopod with three processes (Figs 3, 5C, D) ...
.... ***Heterocookia* 4**
2   Tibiotarsus with strong subapical or apical indentations (Figs 3, 5A, B)...... 3
–   Tibiotarsus with a faint subapical projection (Fig. 3)....................................
....***Haplocookia enghoffi* sp. n.**
3   Tibiotarsus with apical indentation (Fig. 5A), solenomere short and bent
orthogonally to tibiotarsus ....***Haplocookia mauritanica***
–   Tibiotarsus with subapical marginal indentations; solenomere slender and
bent in same plane as tibiotarsus (Fig. 5B) ....***Haplocookia franzi***
4   Tibiotarsus with an upturned tip. Accessory process with lateral serrated
expansion (Fig. 5C) ....***Heterocookia novator***
–   Tibiotarsus with cleaver-shaped tip. Accessory process slender, without
serrations (Fig. 5D)...***Heterocookia tunisiaca***

List of species of Polydesmida in North Africa

Family Polydesmidae Leach, 1815
    Archipolydesmus chreensis Abrous-Kherbouche & Mauriès, 1996
    Archipolydesmus fodili Abrous-Kherbouche & Mauriès, 1996
    Archipolydesmus kabylianus Abrous-Kherbouche & Mauriès, 1996
    Archipolydesmus maroccanus Attems, 1898
    Polydesmus dismilus (Berlese, 1891)
    Polydesmus proximus (Latzel, 1884)
    Polydesmus superus (Latzel, 1884)
Family Pyrgodesmidae Silvestri, 1896
    Rharodesmus cherifiensis Schubart, 1960
    Rharodesmus tabarkensis Akkari & Enghoff, 2012
    ?*Tonodesmus bolivari* Silvestri, 1923
Family Trichopolydesmidae Verhoeff, 1910
    Haplocookia enghoffi sp. n.
    Haplocookia franzi Schubart, 1960
    Haplocookia mauritanica Brölemann, 1915
    Heterocookia novator (Silvestri, 1896)
    Heterocookia tunisiaca Ceuca, 1967
Family Xystodesmidae Cook, 1895
    ?*Melaphe blainvillei* (Eydoux & Gervais, 1836)
    Melaphe mauritanica (Lucas, 1844)
    Macellolophus rubromarginatus (Lucas, 1846)

Family Paradoxosomatidae Daday, 1889

    Boreviulisoma liouvillei Brölemann, 1928

    Eviulisoma abadi Mauriès, 1985

    Oranomorpha guerinii (Gervais, 1836)

    Stosatea italica (Latzel, 1886**)**

Ackowledgements

References

Akkari N, Enghoff H (2011) The genus *Rharodesmus* – a tropical element in the North African millipede fauna: a new species from Tunisia and notes on the family Pyrgodesmidae (Diplopoda: Polydesmida). Zootaxa 2985: 55–63.

Attems C (1926) Myriapoda in Kükenthal & Krumbach. Handbuch der Zoologie, Berlin, Leipzig, 4: 1–402.

Attems C (1940) Myriapoda 3. Polydesmoidea III. in Das Tierreich, Berlin & Leipzig 70: i–xxxii + 1–577.

Brölemann HW (1915) Description d'un genre nouveau et d'une espèce nouvelle de Myriapodes d'Algérie. Bulletin de la Société d'Histoire Naturelle d'Afrique du Nord, Alger 6: 88–94.

Brölemann HW (1921) Liste des Myriapodes signalés dans le Nord de l'Afrique. Bulletin de la Société des sciences naturelles du Maroc 1: 99–110.

Ceuca T (1958) Contributions à la connaissance de la Faune de la République Populaire de Roumanie III. Diplopodes cavernicoles. Studii si Cercetari de Biologie, Cluj 9, 2: 335–343.

Ceuca T (1967) Diplopodes de Tunisie (avec description d'une nouvelle espèce). Bulletin de l'Académie Polonaise des Sciences, Varsovie, Cl. 2, 15, 9: 551–554

Ceuca T (1974) Nouvelles contributions à la connaissance des Diplopodes de la faune de Roumanie. Studii Universitates Babes-Bolyai, Cluj, sér. Biologia 1: 91–97.

Enghoff H, Golovatch SI, Short M, Stoev P, Wesener T (2015) Diplopoda – taxonomic overview. In: Minelli, A. (Ed.) Treatise on Zoology – Anatomy, Taxonomy, Biology. The Myriapoda 2, 16: 363–453.

Golovatch SI (2013) A reclassification of the millipede superfamily Trichopolydesmoidea, with descriptions of two new species from the Aegean region (Diplopoda, Polydesmida). ZooKeys 340: 63–78. https://doi.org/10.3897/zookeys.93.1159

Hoffman RL (1980) Classification of Diplopoda. Muséum d'Histoire naturelle, Genève, 1979 (1980), 238 pp.

Jeekel CAW (1956) Milliped miscellany – Part III. Beaufortia, Amsterdam 5, 52: 73–99.

Kraus O (1957) Myriapoden aus Perou. V. Senckenbergiana biologica, Frankfurt a. Main, 38 (1–2): 95–114.

Mauriès JP (1981) Description d'une espèce nouvelle et d'un genre nouveau de Diplopodes polydesmides hypogés récoltés dans l'arrondissement de Béziers (Hérault). Bulletin de la Société d'Histoire Naturelle de Toulouse, 116, 3–4, 1980: 228–234.

Mauriès JP (1983) Un nouveau Diplopode Polydesmide cavernicole du département du Gard, *Mastigonodesmus fagniezi* n.sp. (Polydesmidea, Mastigonodesmidae). Bulletin de la Société d'Histoire naturelle de Toulouse, 1982, 118: 141–144.

Mauriès JP (1984) Le genre *Galliocookia* Ribaut, 1954. Deux espèces nouvelles des grottes de l'Ardèche et du Gard (Myriapoda, Diplopoda, Polydesmida). Bulletin de la Société d'Histoire Naturelle de Toulouse, 119, 1983: 103–110.

Schubart O (1960) Ein weiterer Beitrag zur Diplopoden-fauna Marokkos. Bulletin de la Société des Sciences Naturelles et Physiques du Maroc, Rabat, 40: 159–232.

Shear WA (2011) Diplopoda in Zhang ZQ (Ed.) Animal Diversity: An outline of higher-level classification and survey of taxonomic richness. Zootaxa 3148: 159–164

Shelley RM (2003) A revised, annotated, family-level classification of the Diplopoda. Arthropoda Selecta 2002 (2003), 113: 187–207.

Silvestri F (1896) Una escursione in Tunisia. Naturalista Siciliano (8–12): 143–161.

Simonsen Å (1990) Phylogeny and biogeography of the millipede order Polydesmida, with special emphasis on the suborder Polydesmidea. PhD thesis, Museum of Zoology, University of Bergen: 1–114.

Tabacaru I (1975) *Napocodesmus florentzae* n.sp; (Diplopoda, Polydesmida). Travaux de l'Institut de Spéologie «Emil Racovitza», Bucarest 14: 71–82.

Tabacaru I (1980) *Trichopolydesmus* (*Banatodesmus*) *jeanneli* n. sg., n. sp. (Diplopoda, Polydesmida). Travaux de l'Institut de Spéologie "Emil Racovitza", Bucarest 29: 155–161.

Verhoeff KW (1910) Über Diplopoden. 42. Aufsatz: Neue Polydesmiden aus Mitteleuropa und ihre Verwandten. Zoologischen Anzeiger, Leipzig, 36, 6/7: 132–145.

Verhoeff KW (1943) Chilopoden und Diplopoden. In: Beiträge zur fauna Perus I. Hamburg, 1, 2: 5–80.

RESEARCH ARTICLE

Additions to the leafhopper genus *Mimotettix* (Hemiptera, Cicadellidae, Deltocephalinae) from Yunnan Province, China

Xingtao Wei[1], Jichun Xing[1]

I *Institute of Entomology, Guizhou University; Special Key Laboratory for Development and Utilization of Insect Resources of Guizhou; Guiyang, Guizhou, 550025, P.R. China*

Corresponding author: *Jichun Xing* (xingjichun@aliyun.com)

Citation: Wei X, Xing J (2018) Additions to the leafhopper genus *Mimotettix* (Hemiptera, Cicadellidae, Deltocephalinae) from Yunnan Province, China. ZooKeys 786: 129–138. https://doi.org/10.3897/zookeys.786.26402

Abstract

Two new leafhopper species: *Mimotettix multispinosus* **sp. n.** and *M. sinuatus* **sp. n.** are described and illustrated from Yunnan, China. A checklist to the species of *Mimotettix* from Yunnan and a key to species from the region are also provided.

Keywords

Homoptera, morphology, taxonomy, distribution, Old World tropics, Scaphoideini

Introduction

The genus *Mimotettix* Matsumura, 1914 (Deltocephalinae: Scaphoideini) is one of the more distinctively marked leafhoppers in the Old World tropics (see Discussion). It was established for a single species, *M. kawamurae* Matsumura 1914, from

Taiwan. Later, Kwon and Lee (1979) described another species, *M. curticeps* from South Korea and Webb and Heller (1990) transferred five Indian species to *Mimotettix* from other genera from India. Recently, Li and Xing (2010) described another new species, *M. spinosus*, and made two new combinations: *M. slenderus* (Li & Wang, 2005) and *M. fanjingensis* (Li & Wang, 2005) from China. Meanwhile, Daiet al. (2010) reviewed this genus, based on an examination of the types of most species, and described seven new species and provided a key to the 15 known species. Xing and Li (in Xing et al. 2013) described another new species, *M. articularis* from China, and provided a key to the 10 Chinese species of the genus. Of the latter, three species are distributed in the Palearctic region, i.e., *M. tibetensis* (Tibet) and *M. curticeps* and *M. spinosus* (Gansu, Shaanxi and Henan). Conversely, in Yunnan Province (southern China), one of China's richest regions in terms of biodiversity, five species are recorded (see Checklist). In the present paper, two new species from Yunnan Province are described which form a separate group from the remaining species of *Mimotettix* based on the structure of the male genitalia (see Discussion) and a key to separate the species from Yunnan is provided. The type specimens of the new species are deposited in the Institute of Entomology, Guizhou University, Guiyang, China (GUGC).

Material and methods

Male specimens were used for the description and illustration. External morphology was observed under a stereoscopic microscope and characters were measured with an ocular micrometer. Color pictures for adult habitus were obtained by the KEYENCE VHX-1000 system. The genital segments of the examined specimens were macerated in 10% NaOH and drawn from preparations in glycerin jelly using a Leica MZ 12.5 stereomicroscope. Illustrations were scanned with a Canon CanoScan LiDE 200 and imported into Adobe Photoshop CS8 for labeling and plate composition.

The morphological terminology used in the descriptions mainly follows Dai et al. (2010) and Li et al. (2011). Absolute measurements, in millimeters (mm), are used for the body.

Taxonomy

Mimotettix Matsumura

Mimotettix Matsumura, 1914: 197; Dai et al. 2010: 2; Xing et al. 2013: 4.

Type species. *Mimotettix kawamurae* Matsumura, 1914.
  Remarks. For the relationship and diagnosis of *Mimotettix* see Dai et al. (2010: 2)
  Distribution. China, Japan and throughout the Old World tropics.

Checklist of *Mimotettix* species from Yunnan, China

M. alboguttulatus (Melichar, 1903)
    Distribution: China (Guizhou, Sichuan, Fujian, Guangxi, Yunnan), Japan, India, Sri Lanka, Thailand, Vietnam, Africa.
M. distiflangentus Dai, Zhang & Webb, 2010
    Distribution: China (Yunnan).
M. dorsocavatus Dai, Zhang & Webb, 2010
    Distribution: China (Yunnan).
M. multispinosus sp. n.
    Distribution: China (Yunnan).
M. robustistylus Dai, Zhang & Webb, 2010
    Distribution: China (Yunnan).
M. sinuatus sp. n.
    Distribution: China (Yunnan).
M. spinosus Li & Xing, 2010
    Distribution: China (Guizhou, Yunnan, Shaanxi), Malaysia.

Key to species (males) of *Mimotettix* from Yunnan Province

1   Apex of subgenital plate long and thin (Figs 7, 19); connective 'H'-shaped with distal lateral arms bracing aedeagus (Figs 10, 11, 22); aedeagal process aligned distinctly asymmetrically (Figs 8, 9, 20, 21)....................................**2**
–   Apex of subgenital plate not long and thin; connective 'Y'-shaped without distal lateral arms; aedeagal process aligned symmetrically or nearly so........**3**
2   Aedeagal process short, expanded apically with many fine spines (Figs 8, 9)..
        .... ***M. multispinosus* sp. n.**
–   Aedeagal process elongate, tapered to apex, without spines (Figs 20, 21).......
        ....***M. sinuatus* sp. n.**
3   Aedeagal shaft robust, with pair of triangular-shape flanges on dorsal surface....
        .... ***M. spinosus***
–   Aedeagal shaft thin, without pair of triangular-shape flanges on dorsal surface **4**
4   Aedeagal process with length approximately 1/2 length of shaft..................
        ....***M. distiflangentus***
–   Aedeagal process with length more than 2/3 length of shaft **5**
5   Aedeagal shaft relatively narrow throughout length in lateral view.............
        ....***M. dorsocavatus***
–   Aedeagal shaft relatively broad throughout length in lateral view **6**
6   Aedeagal shaft without flanges on dorsal surface; pygophore slightly protruding at ventroposterior angle....................................***M. robustistylus***
–   Aedeagal shaft with narrow flanges on dorsal surface; pygophore acutely rounded posteriorly..***M. alboguttulatus***

Mimotettix alboguttulatus (Melichar, 1903)

Thamnotettix alboguttulatus Melichar, 1903: 184–185; synonymised with *Mimotettix lateralis* (Walker) by Distant 1908: 395, in error.
Paralimnus albomaculatus Distant, 1908: 397; synonymised by Dai et al. 2010: 4, figs 3A–M.
Mimotettix kawamurae Matsumura, 1914: 198, fig. 7; Ishihara 1953: 268, figs 5a–i; synonymised by Dai et al. 2010: 4, figs 3A–M.
Paralimnus lefroyi Distant, 1918: 63; synonymised by Dai et al. 2010: 4, figs 3A–M.
Mimotettix albomaculatus (Distant); Webb and Heller 1990: 7.
Mimotettix lefroyi (Distant); Webb and Heller 1990: 7.
Mimotettix apicalis Li & Wang, 2005: 798, figs 7–12; synonymised by Dai et al. 2010: 4, figs 3A–M.
Mimotettix alboguttulatus (Melichar); Dai et al. 2010: 4, figs 3A–M.

Material examined. 4♂♂4♀♀, China: Guizhou Prov., Weining County, 12 August 1977, coll. Plant protection Class 77; 4♂♂7♀♀, Guizhou Prov., Suiyang County, Kuankuoshui, 1 August 1984, coll. Zizhong Li and Lianmin Wang; 2♂♂4♀♀, Guizhou Prov., Fanjing Mt., 12 August 2001, coll. Zizhong Li and Qiongzhang Song; 4♂♂5♀♀, Guizhou Prov., Yanhe County, Mayanghe, 19 May 2007, coll. Yujian Li and Qiongzhang Song; 1♂ (holotype of *Mimotettix apicalis* Li & Wang), Guangxi Autonomous Region, Yuanbaoshan, 13 December 2004, coll. Maofa Yang; 3♂♂7♀♀, Sichuan Prov., Guangyuan City, Shuimogou, 16 August 2007, coll. Jichun Xing; 1♂, Yunan Prov., Xishuangbanna, Menglun, 2 August 2012, coll. Yingjian Wang (GUGC).
    Distribution. China (Guizhou, Sichuan, Fujian, Guangxi, Yunnan), Japan, India, Sri Lanka, Thailand, Vietnam, Africa.

Mimotettix distiflangentus Dai, Zhang & Webb, 2010

Mimotettix distiflangentus Dai, Zhang & Webb, 2010: 6, figs 7A–E.

Distribution. China (Yunnan).

Mimotettix dorsocavatus Dai, Zhang & Webb, 2010

Mimotettix dorsocavatus Dai, Zhang & Webb, 2010: 6, figs 8A–F.

Distribution. China (Yunnan).

Mimotettix multispinosus sp. n.

http://zoobank.org/FD1E4759-787B-4CC5-86E3-0C046392B952

Figs 1–12

Description. Body reddish brown, vertex with two cream transverse bands anteriorly bordered with dark brown (Figs 1, 3). Eyes black, ocelli pale yellow. Forewings brownish hyaline, with scattered hyaline areas, veins dark brown (Figs 1, 2). Legs dark brown.

Head including eyes slightly wider than pronotum. Vertex roundly produced, slightly shorter medially than the distance between eyes. Ocelli located on anterior margin of vertex, separated from eyes by own diameter. Face slightly flattened, similar in length to width; frontoclypeus narrow, longer than width between eyes; anteclypeus slightly expanded apically (Fig. 4); antennae arising near mid-height of eye in facial view. Pronotum slightly longer than vertex, laterally carinate. Forewings with four apical cells and three subapical cells, outer subapical cell slightly tapered apically, inner subapical cell open basally.

Male genitalia: Pygofer very elongate and tapered posteriorly in lateral view, with long stout setae on posteroventral margins (Fig. 5). Valve triangulate (Fig. 6). Subgenital plate elongate, tapering posteriorly to lightly sclerotised elongate apex,

Figures 1–4. *Mimotettix multispinosus* sp. n., 1 ♂, dorsal view 2 ♂, lateral view 3 ♂, head and thorax, dorsal view 4 ♂, face, ventral view.
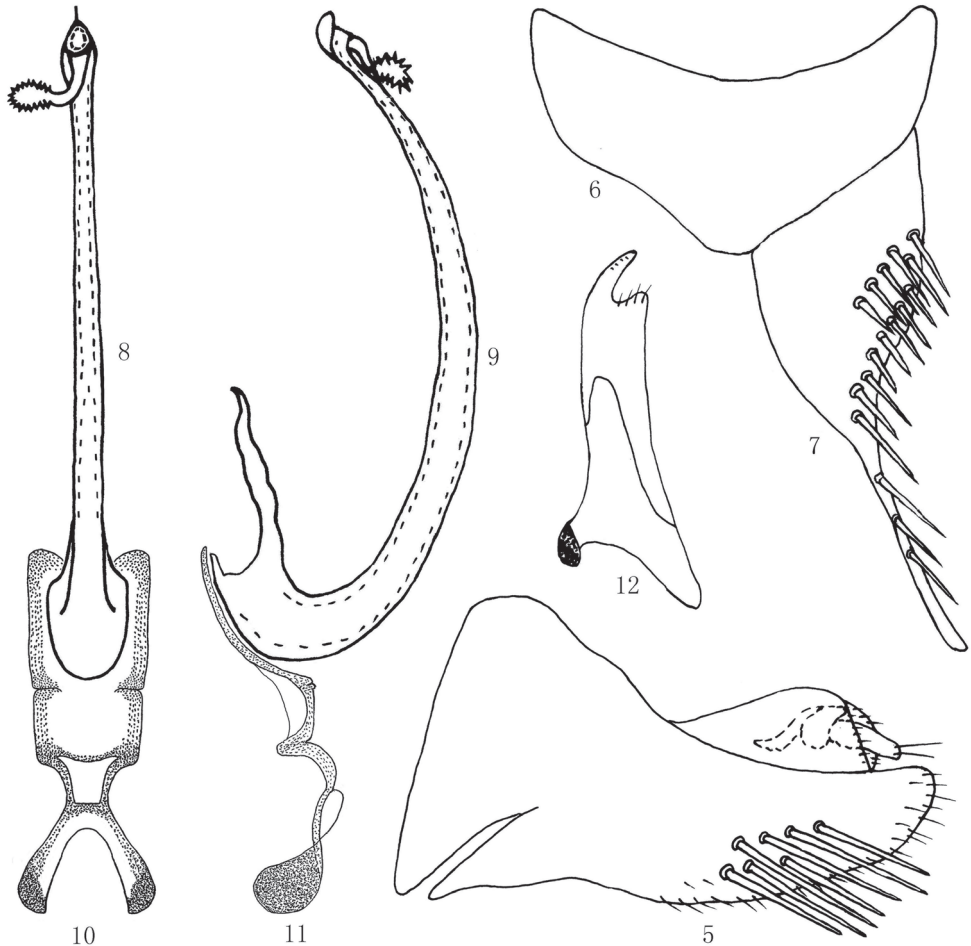
Figures 5–12. *Mimotettix multispinosus* sp. n., **5** Pygophore, left lateral view **6** Valve, ventral view **7** Subgenital plate, ventral view **8** Aedeagus, ventral view **9** Aedeagus, lateral view **10** Connective, ventral view **11** Connective, lateral view **12** Style, dorsal view.

with uniseriate submarginal row of stout setae ventrolaterally (Fig. 7). Aedeagus with shaft very elongate; apical process relatively short, its length nearly 1/7 length of shaft, curved to one side, with many fine spines; gonopore apical (Figs 8, 9). Connective 'H' shaped with arms of stem long and sinuate in lateral view, bracing base of aedeagus (Figs 10, 11). Style relatively narrow, apical process acute, turned laterally (Fig. 12).

Measurement. Length (including tegmen): ♂, 5.5–5.7 mm.

Type material. Holotype ♂, China: Yunnan Prov., Pingbian County, Daweishan, 7 August 2014, coll. Meina Guo (GUGC); paratypes, 2♂♂, same data as holotype except 4 August 2014, coll. Zhengxiang Zhou and 18 August 2017, coll. Yingjian Wang (GUGC).

Distribution. China (Yunnan).

Remarks. The new species is similar to *M. sinuatus* **sp. n.**, but can be distinguished by the characters noted in the key. See also Discussion.

Etymology. The new species name is derived from the Latin words "*multi*" and "*spinosus*", referring to the apical process of aedeagal shaft with many spines.

Mimotettix robustistylus Dai, Zhang & Webb, 2010

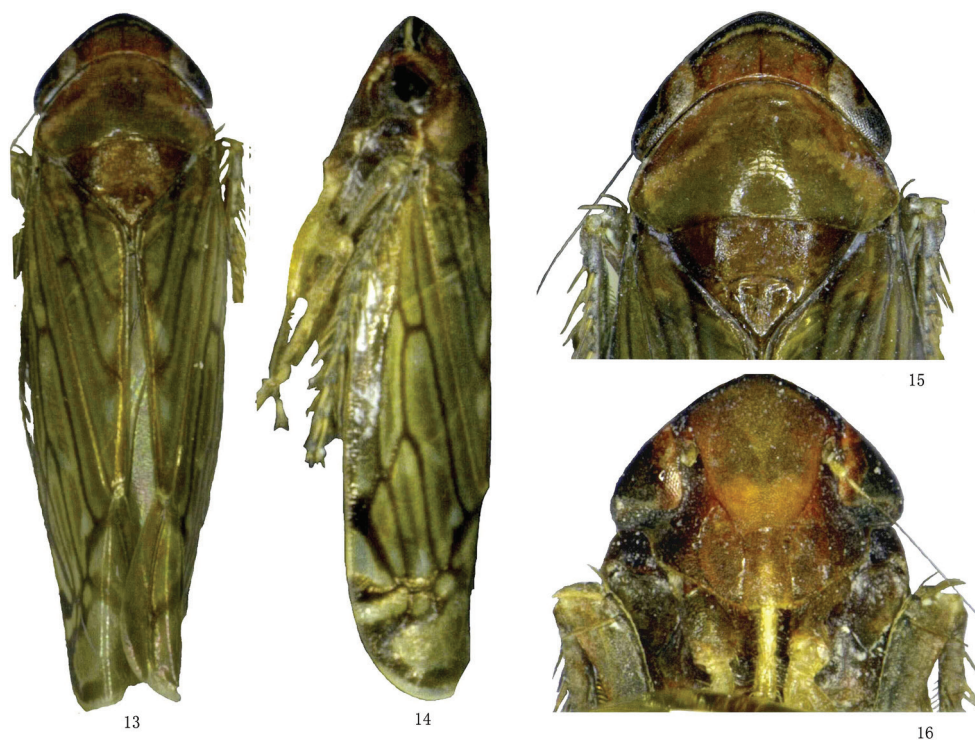*Mimotettix robustistylus* Dai, Zhang & Webb, 2010: 9, figs 13A-F.

Distribution. China (Yunnan).

Mimotettix sinuatus sp. n.

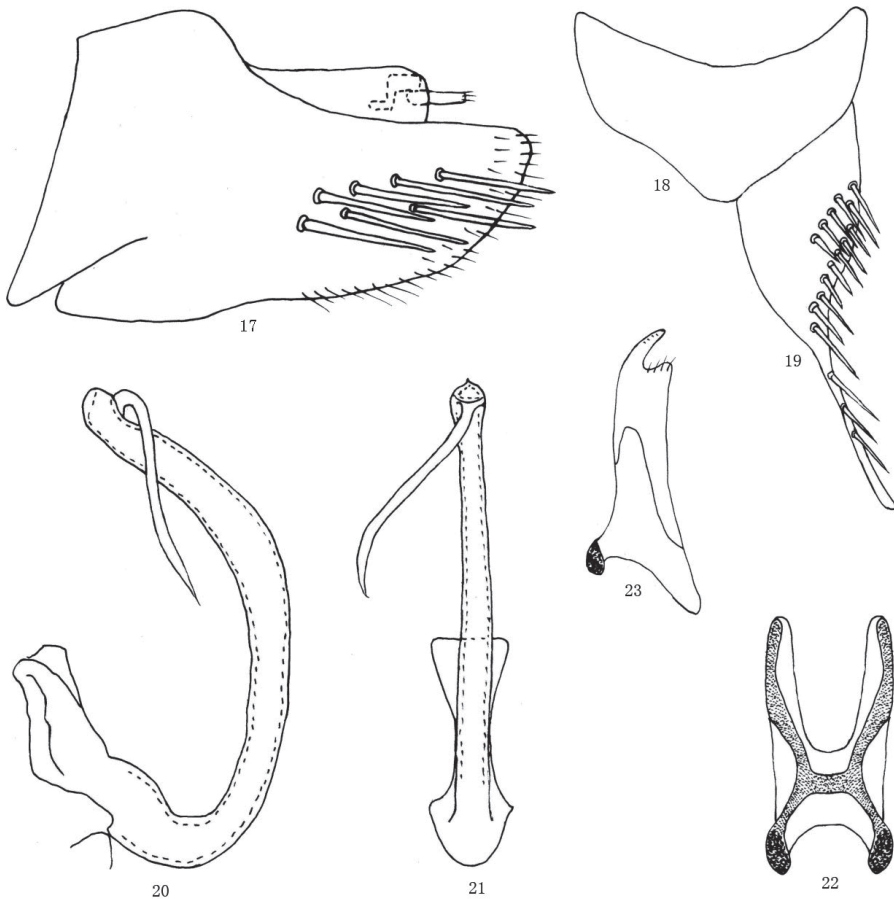http://zoobank.org/29D47664-D75C-4A1A-85F6-CACE788926FA
Figs 13–23

Description. External features as in *M. multispinosus* (see above), but spots on front wing are lighter. Mesonotum and genae appear to be darker.

Figures 13–16. *Mimotettix sinuatus* sp. n., **13** ♂, dorsal view **14** ♂, lateral view **15** ♂, head and thorax, dorsal view **16** ♂, face, ventral view.

Figures 17–23. *Mimotettix sinuatus* sp. n., **17** Pygophore, left lateral view **18** Valve, ventral view **19** Subgenital plate, ventral view **20** Aedeagus, lateral view **21** Aedeagus, ventral view **22** Connective, ventral view **23** Style, dorsal view.

Male genitalia: As in *M. multispinosus* (see above) but pygofer less elongate (Fig. 17) and aedeagal shaft distinctly broader distally in lateral view, with sinuate elongate apical process tapered to acute apex, half length of shaft (Figs 20, 21). Connective 'H' shaped with arms of stem short and not sinuate in lateral view, bracing base of aedeagus (Fig. 22).

Measurement. Length (including tegmen): ♂, 5.4–5.6 mm; ♀, 5.5–5.7 mm.

Type material. Holotype ♂, China: Yunnan Prov., Lvchun County, Huanglianshan, 14 August 2014, coll. Meina Guo (GUGC); paratypes, 1♂2♀♀, same data as holotype except 14 August 2014, coll. Zhengxiang Zhou (GUGC).

Distribution. China (Yunnan).

Remarks. The new species is similar to *M. multispinosus* sp. n. but can be distinguished by the characters noted in the key. See also Discussion.

Etymology. The new species name is derived from the Latin word "*sinuatus*", referring to the sinuate aedeagal process.

Mimotettix spinosus Li & Xing, 2010

Mimotettix spinosus Li & Xing, 2010: 378, figs 1a–g; Dai et al. 2010: 8, figs 12A–F; Li et al. 2011: 135, plates 5–127, figs 1–7.

Material examined. China: 1♂ (Holotype), Guizhou Prov., Libo County, Maolan, 21 October 1998, coll. Zizhong Li (GUGC).

Distribution. China (Guizhou, Yunnan, Shaanxi), Malaysia.

Discussion

Species of *Mimotettix* are distinctly marked leafhoppers, mainly brown with a series of cream and brown transverse bands on the anterior margin of the head and with hyaline spots on the forewings. In the male genitalia they can be distinguished by the simple aedeagus with the shaft bearing a single apical process directed ventrally. All are very similar in coloration and difficult to distinguish externally, but the structure of the male genitalia is markedly different and separates the genus into two groups: 1) subgenital plate apex extended and very narrow, connective 'H' shaped with arms of stem bracing aedeagus, aedeagus with the apical process strongly turned to left or right side of shaft, apex laterally compressed (*M. multispinosus* sp. n. and *M. sinuatus* sp. n.) and, 2) subgenital plate short triangular shaped, connective 'Y' shaped, aedeagus with apical process in line with shaft in ventral view or slightly curved to one side, apex not laterally compressed (other species).

Acknowledgements

References

Dai W, Zhang YL, Webb MD (2010) Review of the Old World leafhopper genus *Mimotettix* Matsumura (Hemiptera: Cicadellidae: Deltocephalinae) with description of new species. Zootaxa 2651: 1–26.

Distant WL (1908) Rhynchota-Homoptera. In: Bingham CT (Ed.) The Fauna of British India including Ceylon and Burma v.4. Published under the authority of the Secretary of State for India in Council, C.T.Bingham, 501pp.

Distant WL (1918) Rhynchota-Homoptera: Appendix. Heteroptera: Addenda. In: Shipley AE, Marshall AKG (Eds) The Fauna of British India, including Ceylon and Burma (vol. 7: i-viii). Published under the authority of the Secretary of State for India in Council, Taylor & Francis, London, 1–210.

Ishihara T (1953) Some species of the Deltocephalinae of Japan. Dobutsugaku Zasshi 63: 266–270.

Kwon YJ, Lee CE (1979) Some new genera and species of Cicadellidae of Korea (Homoptera: Auchenorrhyncha). Nature & Life 9(1): 49–61.

Li ZZ, Dai RH, Xing JC (2011) Deltocephalinae from China (Hemiptera: Cicadellidae). Popular Science Press, Beijing. [In Chinese with English summary]

Li ZZ, Wang LM (2005) Two new species of the genus *Mimotettix* from China (Hemiptera, Cicadellidae, Euscelinae). Acta Zootaxonomica Sinica 30: 798–800. [In Chinese with English summary]

Li ZZ, Xing JC (2010) A new species and two new combinations of *Mimotettix* Matsumura (Hemiptera: Cicadellidae: Deltocephalinae) from China. Journal of Mountain Agriculture and Biology 29(5): 377–380. [In Chinese with English summary]

Matsumura S (1914) Die Jassinen und einige neue Acocephalinen Japans. Journal of the College of Agriculture, Tohoku Imperial University, Sapporo 5: 165–240.

Melichar L (1903) Homopteren-Fauna von Ceylon. Verlag von Felix L. Damer, Berlin, 248pp.

Webb MD, Heller FR (1990) The leafhopper genus *Pseupalus* in the Old World Tropics, with a check-list of the Afrotropical and Oriental Paralimnini (Homoptera: Cicadellidae: Deltocephalinae). Stuttgarter Beitrage zur Naturkunde, Serie A (Biologie) 452: 1–10.

Xing JC, Li ZZ, Song QZ (2013) A new species of the genus *Mimotettix* Matsumura, 1914 (Hemiptera: Cicadellidae: Deltocephalinae) from China. Munis Entomology & Zoology 8(1): 4–8.

RESEARCH ARTICLE

Tosanoides annepatrice, a new basslet from deep coral reefs in Micronesia (Perciformes, Percoidei, Serranidae)

Richard L. Pyle[1], Brian D. Greene[2], Joshua M. Copus[3], John E. Randall[3]

1 *Bernice P. Bishop Museum, 1525 Bernice Street, Honolulu, Hawai'i 96817, USA* **2** *Association for Marine Exploration, 47-224 Kamehameha Hwy, Kaneohe, Hawai'i 96744, USA* **3** *Hawaii Institute of Marine Biology, 46-007 Lilipuna Rd, Kaneohe, Hawai'i 96744, USA*

Corresponding author: *Richard L. Pyle* (deepreef@bishopmuseum.org)

Citation: Pyle RL, Greene BD, Copus JM, Randall JE (2018) *Tosanoides annepatrice*, a new basslet from deep coral reefs in Micronesia (Perciformes, Percoidei, Serranidae). ZooKeys 786: 139–153. doi: 10.3897/zookeys.786.28421

Abstract

The new species *Tosanoides annepatrice* **sp. n.** is described from four specimens collected at depths of 115–148 m near Palau and Pohnpei in Micronesia. It differs from the other three species of this genus in life color and in certain morphological characters, such as body depth, snout length, anterior three dorsal-fin spine lengths, caudal-fin length, and other characters. There are also genetic differences from the other four species of *Tosanoides* (d ≈ 0.04–0.12 in mtDNA cytochrome oxidase I). This species is presently known only from Palau and Pohnpei within Micronesia, but it likely occurs elsewhere throughout the tropical western Pacific.

Keywords

closed-circuit rebreather, coral-reef twilight zone, mesophotic coral ecosystems, Micronesia

Introduction

The authors have explored mesophotic coral ecosystems (MCEs; coral-reef habitat at depths of 30–150 m; also referred to as the "coral-reef twilight zone") throughout Micronesia for decades, and have utilized advanced mixed-gas closed-circuit rebreather diving operations since 1997, which has led to the discovery of dozens of new species of fishes (Pyle 1996a, 1996b, 2000, Pyle and Copus in press). One such new species was first discovered in 2007 during an expedition to Micronesia to film the BBC documentary *Expedition Pacific Abyss* (British Broadcasting Corporation 2007), when the

second author collected a specimen of *Tosanoides* Kamohara, 1953 at a depth of 115 m off Ngaruangl Atoll, Kayangel State, Republic of Palau. Although the specimen differed substantially in color from the other two species of the genus known at the time, additional specimens were needed to ensure it was a distinct and previously undescribed species. During an expedition to Pohnpei, Federated States of Micronesia in 2015 (Rowley et al. in press), the first two authors observed additional individuals of this *Tosanoides* at a depth of 148 m off the west end of Ahnd (Ant) Atoll, outside the entrance to a small cave along a vertical reef drop-off. During a subsequent expedition to Pohnpei in 2016, the second author managed to collect one large adult male and two juvenile specimens.

The specimens represent an undescribed species of the serranid subfamily Anthiadinae Poey 1861 (commonly spelled Anthiinae), within the genus *Tosanoides*. The genus currently includes four nominal species: *Tosanoides filamentosus* Kamohara, 1953 (type species), *T. flavofasciatus* Katayama & Masuda, 1980, *T. obama* Pyle, Greene & Kosaki, 2016, and *T. aphrodite* Pinheiro, Rocha & Rocha, 2018. Herein we describe the fourth member of the genus, *Tosanoides annepatrice*, based on morphologic and genetic differences compared with the other known species. In addition, the species currently referred to as *Pseudanthias fucinus* (Randall & Ralston, 1985) from the Hawaiian Islands is likely a member of the genus *Tosanoides*, and is similar in many respects to *T. aphrodite*.

At least two other undescribed species of this genus have been reported; one from the Coral Sea (Gerald R. Allen pers. comm.) and one from Rapa Nui (Easter Island) (Easton et al. 2017).

Materials and methods

Specimens were collected with hand nets during deep dives using mixed-gas, closed-circuit rebreathers, and brought to the surface alive with the aid of a hypodermic needle to vent gas from the swim bladders. Methods for counts and measurements follow those described in Pyle et al. (2016). Gender of adult specimens based on examination of gonads. Description template and wording follow Pyle et al. (2016), modified from Katayama and Masuda (1980) for consistency.

The holotype has been deposited at the Bernice Pauahi Bishop Museum fish collection, Honolulu (**BPBM**), and paratypes have been deposited at the U.S. National Museum of Natural History, Washington, D.C. (**USNM**) and California Academy of Sciences, San Francisco (**CAS**).

Fresh tissue samples were obtained from the holotype and paratypes. DNA barcodes (cytochrome c oxidase I; COI) were sequenced following the protocol described in Copus et al. (2015). Barcode of Life Database (BOLD) identifiers for DNA sequences are presented along with museum catalog numbers for type material and non-type specimens. A neighbor-joining tree building method was used to reconstruct the phylogenetic tree using Geneious v.6.2 (Kearse et al. 2012) under the HKY model of sequence evolution, with a random seed of 920,582, 100,000 bootstrap replicates, and 50% support threshold. Estimates of genetic differences (d) were also calculated in Geneious.

Taxonomy

Tosanoides annepatrice sp. n.
http://zoobank.org/CACCF76F-744C-478E-B303-24674D1C433B
Figs 1–5

Type Locality. Republic of Palau, Kayangel State, Ngaruangl Atoll, 8.14733°N, 134.61763°E.

Material. Holotype. BPBM 40848, male, Barcode of Life TOSAN-001-18, 53.0 mm SL, Republic of Palau, Kayangel State, Ngaruangl Atoll, 8.14733°N, 134.61763°E, 115 m, 23 April 2007, B. D. Greene, aboard vessel *Big Blue Explorer*, hand nets, under rock on steep rocky slope. **Paratypes.** USNM 444916, male, Barcode of Life TOSAN-002-18, 68.7 mm SL, Federated States of Micronesia, Pohnpei, Ahnd (Ant) Atoll, W side, 6.75589°N, 157.91933°E, 148 m, 22 July 2016, B. D. Greene, hand nets, near entrance to cave on vertical drop-off.

BPBM 41354, immature, Barcode of Life TOSAN-003-18, 31.6 mm SL, same collection data as USNM 444916.

CAS 244531, immature, Barcode of Life TOSAN-004-18, 28.0 mm SL, same collection data as USNM 444916.

Diagnosis. A species of *Tosanoides* (*sensu* Katayama and Masuda 1980) distinguished by the following combination of characters: fourth or fifth dorsal spine the longest; dorsal-fin soft rays 16–17; anal-fin soft rays 8; pored lateral-line scales 33–34; head 2.3–2.9 in SL; body depth 2.6 in SL; color in life of males: head and body rose-pink, crossed by four bright yellow stripes, the third continuing as a bright red stripe

Figure 1. Holotype of *Tosanoides annepatrice* (BPBM 40848), 80.9 mm TL, collected at a depth of 115 m off Ngaruangl Atoll, Kayangel State, Republic of Palau. Photograph by RL Pyle.

with magenta edges along the middle of the body, becoming yellow centered on base of caudal fin; dorsal fin with a very broad middle yellow stripe with magenta margin; base of anal fin colored like body anteriorly, grading broadly to magenta posteriorly; pelvic fins yellow, except for magenta last two rays; eye magenta with an uneven ring of yellow around pupil; color of immature and presumed female yellow with irregular, near-vertical, wavy red lines following scale margins; anal fin magenta anteriorly, grading posteriorly to purple, with a greenish yellow streak; pelvic fins bright magenta.

Description. Dorsal fin X,16 (17), last soft ray branched to base; anal fin III,8, last soft ray branched to base; pectoral-fin rays 14; pelvic-fin rays I,5; principal branched caudal rays 14, upper procurrent unbranched caudal rays 6, lower procurrent unbranched caudal rays 4; pored lateral-line scales 33 (33–34); scale rows above lateral line to origin of dorsal fin 4; scale rows below lateral line to origin of anal fin 15 (14–15); gill rakers on upper limb 11, on lower limb 22 (22–23); vertebrae 26 (10+16).

Body ovoid, compressed, its greatest depth 2.62 (2.57–2.64) in SL, the width just posterior to gill opening 2.40 (2.22–2.56) in depth; head length 2.93 (2.35–2.77) in SL; snout short, its length 5.66 (4.28-7.00) in head; orbit diameter 2.41 (2.53–2.85) in head; interorbital convex, the least bony width 3.42 (3.45–5.41) in head; least depth of caudal peduncle 2.78 (2.99–3.40) in head.

Mouth large, oblique and protractile; lower jaw not projecting beyond the upper when mouth closed; maxilla 2.01 (1.92–2.20) in head, expanded distally, reaching below posterior border of pupil, slightly diagonal, the gape forming an angle of ca. 20° to the horizontal, supramaxilla absent. A pair of nostrils on either side of head, close together, directly in front of eye, anterior nostril in a membranous tube with an elevated posterior edge, posterior nostril with a slight rim anteriorly. Teeth in upper jaw villiform, forming a band broader anteriorly with a pair of canines on each side

Figure 2. Paratype of *Tosanoides annepatrice* (USNM 444916), 104.0 mm TL, adult male, collected at a depth of 148 m off Ahnd (Ant) Atoll, Pohnpei, Federated States of Micronesia. Photograph by BD Greene.

and another pair of canines slightly posteriorly and internally directed backward, an outer row of ca. ten slender canines on each side of jaw curved forward; lower jaw with a patch of villiform teeth anteriorly; one canine on each side anteriorly facing forward and a second canine on each side curved forward, an outer row of ca. 15 slender canines like those of the upper jaw, posterior ones pointing forward; small teeth on vomer and palatines, teeth on vomer in a triangular band; tongue pointed, smooth. Preopercle with a round angle, upper limb serrate with ca. 25 spinules, lower limb smooth; opercle with two flat spines, upper one longest and at apex; subopercle and interopercle smooth. Gill rakers long and numerous, with eleven rakers on the upper limb and 22 (22–23) on the lower limb, longest raker much longer than gill filament.

Dorsal fin very slightly notched, inserted slightly posterior to dorsal end of gill opening, its base 1.69 (1.65–1.73) in SL; first dorsal-fin spine the longest, 1.81 (1.97–2.32) in head, second dorsal-fin spine originating immediately posterior to first, its length 1.97 (2.00–2.48) in head, third dorsal-fin spine 2.13 (2.11–2.53) in head, fourth dorsal-fin spine, 2.29 (2.24–2.70) in head, fifth dorsal-fin spine 2.51 (2.33–2.76) in head, last dorsal-fin spine 2.83 (2.90–3.14) in head; membranes between dorsal-fin spines mildly incised; longest dorsal soft ray (seventh or eighth) 2.15 (2.58-2.78) in head. Anal fin originating below base of third or fourth dorsal soft ray; second anal spine slightly stronger than the third; length of first anal-fin spine 5.32 (5.17–6.00) in head, second anal-fin spine 2.13 (2.00–2.25) in head, third anal-fin spine 2.21 (2.19–2.59) in head; posterior margin of anal fin rounded; length of longest anal soft ray (fifth or sixth) 1.60 (1.77–2.38) in head. Pectoral fins subsymmetrical, longer than head, reaching a vertical at base of third or fourth anal soft ray, their length 2.31 (2.28–2.52) in SL; caudal fin deeply convex, upper and lower lobes each with two filamentous extensions on their outermost principle rays, its length 1.90 (1.95–2.26);

Figure 3. Adult male *Tosanoides annepatrice* alive in an aquarium, collected in Pohnpei. Photograph by LA Rocha.

Figure 4. Paratype of *Tosanoides annepatrice* (BPBM 41354), 46.8 mm TL, immature female, collected at a depth of 148 m off Ahnd (Ant) Atoll, Pohnpei, Federated States of Micronesia. Photograph by BD Greene.

pelvic spine 1.83 (1.66–2.15) in head; first soft ray of pelvic fin with a filamentous extension (broken in holotype), its length (3.07–4.08), in SL.

Scales moderately large, ctenoid; four in a series from origin of dorsal fin to lateral line, 15 (14–15) from origin of anal fin to lateral line; head closely scaled except for lips and tip of snout anterior to nostrils; dorsal and anal fins with small scales basally, a single row on spinous portion of dorsal fin, reaching distally ca. 1/5 of distance to outer margin posteriorly on soft portions of dorsal and anal fins; ca. seven or eight vertical scale rows on base of caudal fin; scales on pectoral fins basally, extending posteriorly on lower half of pectoral fin approximately one third distance to posterior margin. Lateral line with 33 (33–34) pored scales, high, concurrent with back, forming an angle below last several dorsal rays and extending along middle of caudal peduncle to base of caudal fin.

The two immature paratypes differ from the adult specimens in having a proportionally larger head (2.35–2.77 in SL, compared with 2.77–2.93), shorter snout (6.33–7.00 in head, compared with 4.28–5.66), longer dorsal-fin base (1.70–1.73 in SL, compared with 1.65–1.69) and anal-fin base (4.65–4.91 in SL, compared with 4.91–5.05), narrower caudal peduncle (3.17–3.40 in head, compared with 2.78–2.99), shorter pelvic spine (2.09–2.15 in head, compared with 1.66–1.83), longer pelvic fin (2.43–2.62 in head, compared with 3.07–4.08), shorter dorsal-fin rays (longest 2.77–2.78 in head, compared with 2.15–2.58) and anal-fin rays (longest 2.28–2.38 in head, compared with 1.60–1.77), shorter first anal-fin spine (5.95–6.00 in head, compared with 5.17–5.32), and shorter caudal-fin (2.08–2.26 in SL, compared with 1.90–1.95).

Figure 5. Adult female *Tosanoides annepatrice* alive in an aquarium, collected in Pohnpei. Photograph by LA Rocha.

Color in life as in Fig. 1–5. This species is sexually dichromatic. Male (holotype; Fig. 1–3): head and body rose-pink, the scale edges orange-red; head crossed by four bright yellow stripes, the upper three one-third to one-half eye diameter in width, the first high on nape, ending below base of third dorsal spine, second beginning on anterior profile at upper edge of eye, curving as it passes dorsally, and narrowing to a point nearly to origin of lateral line; third starts on upper lip, covers most of side of snout, reappears behind upper half of eye, continues slightly downward to a mixed orange-yellow spot just below opercular spine, and links to a short yellow band that ends at upper half of pectoral fin, continuing as a bright red stripe with magenta edges along the middle of the body, becoming a broad oblique yellow stripe centered on base of caudal fin; fourth stripe covers most of ventral part of head, leaving only a pink tip to the lower jaw and a mark like two tiny pink flags obliquely across upper lip and suborbital; yellow stripe continues ventrally on chest and abdomen, narrowing as it passes to origin of anal fin; dorsal fin with a very broad middle yellow stripe, colored like body basally, with a magenta margin that covers outer half of first dorsal spine; anal fin mainly yellow, continuous anteriorly with yellow band ventrally on abdomen; base of fin colored like body anteriorly, grading broadly to magenta posteriorly; an orange-red submarginal line on anteriorly half of soft portion of fin; pectoral fins with hyaline membranes and yellow rays that broaden ventrally to a triangular yellow spot; pelvic fins yellow, except for magenta last two rays, the two zones separated by an orange-red line; eye magenta with an uneven ring of yellow around pupil, and a large, white-edged, blue-green spot before pupil. Immature (Figure 4) and presumed female (Figure 5) fish: head and body bright yellow with irregular, near-vertical, wavy red lines

Figure 6. Holotype (upper; BPBM 41315) and paratype (lower; USNM 440451) of *Tosanoides obama* collected at depths of 90–92 m in the Northwestern Hawaiian Islands. Photographs by RL Pyle.

following scale margins, those above lateral line narrower, the 13 lines below soft portion of dorsal fin ending ventrally in a very irregular red stripe at level of lower edge of eye, reappearing reversely slanted ventrally; five short oblique thin red lines on side of nape; ca. nine progressively shorter and thinner broken lines on caudal peduncle and base of caudal fin, reversely slanted on lower half; lines ending in abdomen and above spinous portion of anal fin obscured by reddish violet pectoral fin; head bright yellow like body with two narrow mixed magenta-violet parallel bands, one horizontal from front of snout through upper part of eye, the second from lower lip through lower part of eye, both continuing obliquely downward across postorbital head; three bright magenta marks along upper margin of nape, the first as a spot above eye, the next two as

Figure 7. *Tosanoides flavofasciatus*, BPBM 40858, collected at a depth of 120 m off Ngemelis Island, Republic of Palau. Photograph by RL Pyle.

dashes at edge of nape, the latter ending at origin of dorsal fin; dorsal fin bright greenish yellow with a bright purple margin that narrows posteriorly on spinous portion of fin, then broadens on sort portion, again narrowing posteriorly; an obscure blackish red line basally on spines and rays of dorsal fin, in height ca. equal to maximum width of pupil, some branching to irregular Y-shape; anal fin magenta anteriorly, grading posteriorly to purple, with a greenish yellow streak from base of spinous portion of fin to outer fourth of fourth-from-last anal ray; caudal fin greenish yellow basally and out on upper and lower margins, progressively narrower posteriorly, rays in rest of fin gradually changing from yellow to bluish gray posteriorly; pelvic fins bright magenta; eye with a bluish purple pupil ruined by violet, the dorsal edge with an arc of dark purple.

Color in alcohol uniformly pale yellow except for eye, which is black.

Morphometric data for selected characters of type specimens are provided in Table 1.

Distribution. *Tosanoides annepatrice* is known on the basis of four specimens, one (the holotype) collected at a depth of 115 m in Palau, and three paratypes collected at a depth of 148 m near Pohnpei. Additional individuals have been observed at depths of ~120–150 m at Pohnpei. The species likely occurs at similar depths throughout much of Micronesia, and perhaps more broadly within the tropical western Pacific; but more exploration of habitat at appropriate depths throughout this region is necessary to determine its complete geographic range.

Habitat and Ecology. *Tosanoides annepatrice* has been observed and collected along steep limestone coral-reef drop-offs at depths from 115–150 m. The paratypes

Table 1. Morphometric and meristic data for selected characters of type specimens of *Tosanoides annepatrice*. Values of morphometric data (other than TL and SL) are represented as % of SL.

Measurements	Holotype BPBM 41315	Paratype USNM 444916	Paratype BPBM 41354	Paratype CAS 244531
Morphometrics				
Sex	Male	Male	Immature	Immature
Total length (TL) in mm	80.9	104.0	46.8	40.4
Standard length (SL) in mm	53.0	68.7	31.6	28.0
Head length	34.2	36.1	36.1	42.5
Body depth	38.1	38.7	38.9	37.9
Body width	41.6	45.1	39.0	43.4
Snout length	17.7	23.4	15.8	14.3
Predorsal length	38.3	38.1	37.3	39.3
Preanal length	68.1	63.2	61.7	65.7
Base of dorsal fin	59.2	60.7	57.9	58.9
Base of anal fin	19.8	20.4	21.5	20.4
Orbit diameter	41.4	35.1	39.5	36.1
Interorbital width	29.3	27.4	28.9	18.5
Caudal peduncle depth	35.9	33.5	31.6	29.4
Pelvic spine	54.7	60.1	46.5	47.9
Pelvic fin	24.5	32.6	41.1	38.2
First dorsal spine length	55.2	43.1	50.9	43.7
Second dorsal spine length	50.8	43.1	50.0	40.3
Third dorsal spine length	47.0	42.3	47.4	39.5
Fourth dorsal spine length	43.6	37.1	44.7	38.7
Fifth dorsal spine length	39.8	36.3	43.0	37.8
Last dorsal spine length	35.4	31.9	34.2	34.5
Longest dorsal ray length	46.4	38.7	36.0	36.1
First anal spine length	18.8	19.4	16.7	16.8
Second anal spine length	47.0	45.2	50.0	44.5
Third anal spine length	45.3	40.7	45.6	38.7
Longest anal ray length	62.4	56.5	43.9	42.0
Caudal fin length	52.6	51.4	48.1	44.3
Pectoral fin length	43.2	39.7	42.4	43.9
Meristics				
Dorsal spines	X	X	X	X
Dorsal rays	16	17	17	17
Anal spines	III	III	III	III
Anal rays	8	8	8	8
Pectoral rays	14	14	14	14
Pored lateral line scales	33	33	33	34
Dorsal scale rows	4	4	4	4
Ventral scale rows	15	14	15	14
Gill rakers	11+22	11+22	11+23	11+22

were collected along a small rocky crevice near the entrance to a cave, but other individuals have been seen in similar habitats not in association with caves. Most individuals of this species have been observed in groups consisting of one apparent male and several apparent females and juveniles.

Etymology. We name this species *annepatrice* (a noun in apposition) in honor of Anne Patrice Greene, mother of Brian D. Greene who collected all known specimens of this new species, in recognition of the support and encouragement she has consistently provided to Brian's exploration of the deep coral reefs of Micronesia.

Morphological comparisons. The morphology of this species is consistent with the diagnosis for the genus *Tosanoides* as presented by Katayama & Masuda 1980. Compared with *Pseudanthias* Bleeker, 1871 (the only other genus it resembles), *T. annepatrice* shares with the other three species of *Tosanoides* fewer pored lateral-line scales (30–34, compared with 35–52) number of anal soft rays (8, compared with 6–7), and unbranched pectoral fin rays. Morphological comparisons with other species of *Tosanoides* are as follows, and only compare values for adult specimens of *T. annepatrice*.

Tosanoides annepatrice is more similar morphologically to *T. filamentosus* than to *T. obama* (Figure 6) or *T. flavofasciatus* (Figure 7), primarily on the basis of proportional dorsal-fin spine lengths (first dorsal spine the longest, compared with third or fourth dorsal spine the longest in *flavofasciatus*), body depth (2.6 in SL, compared with 2.5 for *T. flavofasciatus* and 2.8–2.9 for *T. obama*), and snout length (4.3–5.7 in head, compared with 2.3–2.9 for *T. flavofasciatus* and 6.4 – 7.1 for *T. obama*). It is also similar to *T. obama* in number of pored lateral line scales (33–34, compared with 30–32 for *T. flavofasciatus* and 35 for *T. filamentosus*) and number of pectoral-fin rays (14, compared with 13 for *T. flavofasciatus* and *T. filamentosus*). The dorsal-fin profile of *T. annepatrice* differs considerably from both *T. flavofasciatus* and *T. obama*, in having much longer spines (2.6 in head, compared with 2.7–3.0). Another unique feature of *T. annepatrice* is that in both adult specimens, the second dorsal-fin spine is immediately adjacent to the first spine. This feature is not evident in the two immature paratypes, so it is uncertain whether this character is typical of all adults, only adult males, or is peculiar to these two specimens.

All four species of *Tosanoides* can also be easily distinguished from each other on the basis of life color.

Genetic comparisons. Vertebrate mtDNA barcode (cytochrome oxidase I) sequences obtained from *T. annepatrice* reveal genetic differences of 3.9–4.0% when compared with *T. filamentosus*, and 9.9–12% pairwise genetic distances when compared with the other two described species of *Tosanoides* (Figure 8). The difference from *T. filamentosus* is consistent with many species-level divergences in other fish taxa (e.g., Johns and Avise 1998, Bellwood et al. 2004, Fessler and Westneat 2007, Randall and Rocha 2009, Rocha 2004, Rocha et al. 2008, Pyle and Kosaki 2016), and considerably more so for the other two species. Based on a preliminary genetic analysis, all four species of *Tosanoides* have closer genetic affinities to each other than to representatives of other Indo-Pacific anthiadine genera analyzed (Figure 8). On this basis, as well as morphological comparisons, we are confident in assigning the new species to the
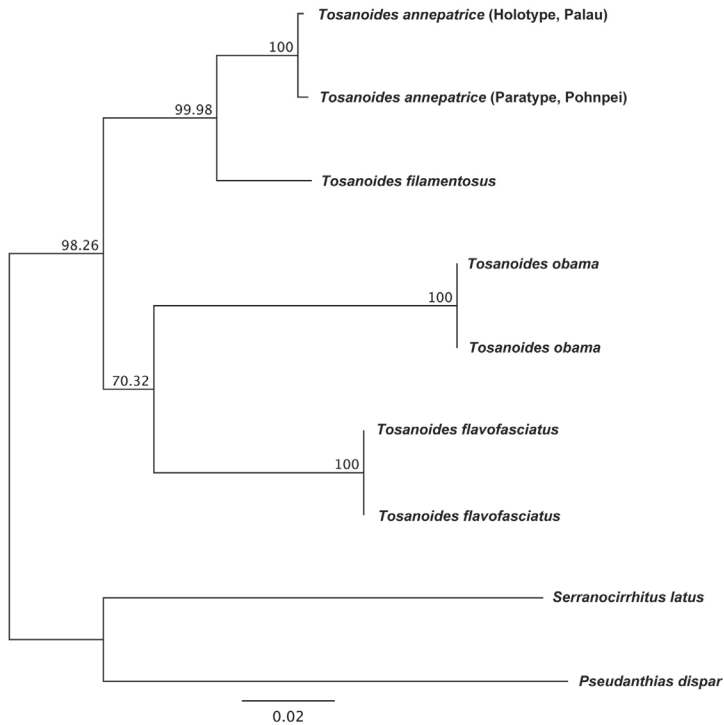
Figure 8. Neighbor-joining phylogenetic reconstruction of *Tosanoides* rooted with outgroups *Serrano-cirrhitys latus* and *Pseudanthias dispar*. Node labels represent percent consensus support for each node. Compiled by Joshua M Copus.

genus *Tosanoides* until a more exhaustive investigation of phylogenetic relationships among the species in this subfamily is completed.

Discussion. *Tosanoides annepatrice* is yet another example of several new fish species that have been discovered on deep coral reefs over the past several decades, mostly involving the use of modern mixed-gas closed-circuit rebreather diving technology (Pyle 1996a, 1996b, 2000, in press). In recent years there has been increased attention focused on mesophotic coral ecosystems (MCEs), coral-reef habitat at depths of approximately 30–150 m in tropical regions worldwide (Hinderstein et al. 2010, Baker et al. 2016, Loya et al. in press). Many more new species of fishes and other reef-associated marine organisms are likely to be discovered as a result of continued exploratory work in this poorly documented environment (Pyle and Copus in press, Pyle et al. in press), and particularly throughout Micronesia (Rowley et al. in press).

Acknowledgements

References

Baker EK, Puglise KA, Harris PT (Eds) (2016) Mesophotic coral ecosystems – A lifeboat for coral reefs? The United Nations Environment Programme and GRID-Arendal, Nairobi and Arendal, 98 pp. http://apps.unep.org/publications/pmtdocuments/-Mesophotic_Coral_Ecosystems__A_lifeboat_for_coral_reefs_-2016Mesoreport_finaldraft.pdf.pdf

Bellwood DR, van Herwerden L, Konow N (2004) Evolution and biogeography of marine angelfishes (Pisces: Pomacanthidae). Molecular Phylogenetics and Evolution 33: 140–155. http://doi.org/10.1016/j.ympev.2004.04.015

Bleeker P (1871) Atlas ichthyologique des Indes Orientales Néêrlandaises, publié sous les auspices du Gouvernement colonial néêrlandais. Tome VII. Percoides I, Priacanthiformes, Serraniformes, Grammisteiformes, Percaeformes, Datniaeformes. 7: Pls. 287–288. http://biodiversitylibrary.org/page/50234768

Bowen BW, Bass AL, Rocha LA, Grant WS, Robertson DR (2001) Phylogeography of the trumpetfish (*Aulostomus* spp.): ring species complex on a global scale. Evolution 55: 1029–1039. http://doi.org/10.1554/0014-3820(2001)055[1029:POTTAR]2.0.CO;2

British Broadcasting Corporation (BBC) (2007) Expedition Pacific Abyss. Discovery Channel/BBC. 14 October 2007. https://www.bbc.co.uk/programmes/b00d55lm

Copus JM, Pyle RL, Earle JL (2015) *Neoniphon pencei*, a new species of holocentrid (Teleostei: Beryciformes) from Rarotonga, Cook Islands. Biodiversity Data Journal 2015(3): e4180. http://doi.org/10.3897/BDJ.3.e4180

Easton EE, Sellanes J, Gaymer CF, Morales N, Gorny M, Berkenpas E (2017) Diversity of deep-sea fishes of the Easter Island Ecoregion. Deep Sea Research Part II: Topical Studies in Oceanography 137: 78–88. http://doi.org/10.1016/j.dsr2.2016.12.006

Fessler JL, Westneat MW (2007) Molecular phylogenetics of the butterflyfishes (Chaetodontidae): Taxonomy and biogeography of a global coral reef fish family. Molecular Phylogenetics and Evolution 45: 50–68. http://doi.org/10.1016/j.ympev.2007.05.018

Hinderstein LM, Marr JCA, Martinez FA, Dowgiallo MJ, Puglise KA, Pyle RL, Zawada DG, Appeldoorn R (2010) Mesophotic coral ecosystems: characterization, ecology, and management. Coral Reefs 29: 247–251. http://doi.org/10.1007/s00338-010-0614-5

Johns GC, Avise JC (1998) A comparative summary of genetic distances in the vertebrates from the mitochondrial cytochrome *b* gene. Molecular Biology and Evolution 15: 1481–1490. http://mbe.oxfordjournals.org/content/15/11/1481.short

Kamohara T (1953) Marine fishes newly found in Prov. Tosa, Japan, with descriptions of a new genus and species. Research Reports of Kôchi University 2(11): 1–10. https://ir.jimu. kochi-u.ac.jp/dspace/bitstream/10126/2566/1/002-11.pdf

Katayama M, Masuda H (1980) *Tosanoides flavofasciatus*, a new anthiine fish from Sagami Bay, Japan, and the Tonga Ridge, Melanesia. Japanese Journal of Ichthyology 27(1): 51–55. https://www.jstage.jst.go.jp/article/jji1950/27/1/27_1_51/_pdf

Kearse M, Moir R, Wilson A, Stones-Havas S, Cheung M, Sturrock S, Buxton S, Cooper A, Markowitz S, Duran C, Thierer T, Ashton B, Mentjies P, Drummond A (2012). Geneious Basic: an integrated and extendable desktop software platform for the organization and analysis of sequence data. Bioinformatics 28: 1647–1649.

Loya Y, Puglise KA, Bridge TCL (in press) Mesophotic Coral Ecosystems. Springer, New York.

Pinheiro HT, Rocha C, Rocha LA (2018) *Tosanoides aphrodite*, a new species from mesophotic coral ecosystems of St. Paul's Rocks, Mid Atlantic Ridge (Perciformes, Serranidae, Anthiadinae). ZooKeys 786: 105–115. https://doi.org/10.3897/zookeys.786.27382

Pyle RL (1996a) The Twilight Zone. Natural History 105(11): 59–62.

Pyle RL (1996b) Exploring deep coral reefs: How much coral reef biodiversity are we missing? Global Biodiversity 6: 3–7.

Pyle RL (2000) Assessing undiscovered fish biodiversity on deep coral reefs using advanced self-contained diving technology. Marine Technology Society Journal 34: 82–91. http://doi.org/10.4031/MTSJ.34.4.11

Pyle RL (in press) Advanced technical diving. In: Loya Y, Puglise KA, Bridge TCL (Eds) Mesophotic coral ecosystems. Springer, New York.

Pyle RL, Copus JM (in press) Mesophotic coral ecosystems: Introduction and overview. In: Loya Y, Puglise KA, Bridge T (Eds) Mesophotic coral ecosystems. Springer, New York.

Pyle RL, Kosaki RK (2016) *Prognathodes basabei*, a new species of butterflyfish (Perciformes, Chaetodontidae) from the Hawaiian Archipelago. ZooKeys 2016(614): 137–152. http://doi.org/10.3897/zookeys.614.10200

Pyle RL, Greene BD, Kosaki RK (2016) *Tosanoides obama*, a new basslet (Perciformes, Percoidei, Serranidae) from deep coral reefs in the Northwestern Hawaiian Islands. ZooKeys 2016(641): 165. http://doi.org/10.3897/zookeys.641.11500

Pyle RL, Kosaki RK, Copus JM, Whitton RK, Pinheiro HT, Rocha LA (in press) Fishes: biodiversity. In: Loya Y, Puglise KA, Bridge TCL (Eds) Mesophotic coral ecosystems. Springer, New York.

Randall JE, Ralston S (1985) A new species of serranid fish of the genus Anthias from the Hawaiian Islands and Johnston Island. Pacific Science 38(3): 220–227

Randall JE, Rocha LA (2009) *Chaetodontoplus poliourus*, A new angelfish (Perciformes: Pomacanthidae) from the tropical western Atlantic. The Raffles Bulletin of Zoology 57(2): 511–

520. http://lkcnhm.nus.edu.sg/nus/pdf/PUBLICATION/Raffles%20Bulletin%20of%20
Zoology/Past%20Volumes/RBZ%2057(2)/57rbz511-520.pdf

Rowley SJ, Roberts TE, Coleman RR, Joseph E, Spalding HL, Dorricott MKI (in press) Pohn-
pei, Federated States of Micronesia. In: Loya Y, Puglise KA, Bridge TCL (Eds) Mesophotic
coral ecosystems. Springer, New York.

Reece JS, Bowen BW, Smith DG, Larson AF (2010) Molecular phylogenetics of moray eels
(Murenidae) demonstrates multiple origins of a shell-crushing jaw (*Gymnomuraena*, *Echid-
na*) and multiple colonizations of the Atlantic Ocean. Molecular Phylogenetics and Evolu-
tion 57: 829–835. http://doi.org/10.1016/j.ympev.2010.07.013

Rocha LA (2004) Mitochondrial DNA and color pattern variation in three western Atlantic
Halichoeres (Labridae), with the revalidation of two species. Copeia 4: 770–782. http://doi.
org/10.1643/CG-04-106

Rocha LA, Lindeman KC, Rocha CR, Lessios HA (2008) Historical biogeography and specia-
tion in the reef fish genus *Haemulon* (Teleostei: Haemulidae). Molecular Phylogenetics
and Evolution 48: 91–928. http://doi.org/10.1016/j.ympev.2008.05.024